

Phytosulfokine signaling positively regulates shoot growth by controlling ABA homeostasis under osmotic stress

Dissertation

zur Erlangung des Doktorgrades der

Mathematisch-Naturwissenschaftlichen Fakultät

der Christian-Albrechts-Universität

zu Kiel

vorgelegt von

Komathy Rajamanickam

Kiel, 2022

First examiner: Prof. Dr. Jennifer Selinski

Second examiner: Prof. Dr. Frank Kempken

Date of the oral examination: 19.04.2022

To my father

Table of Contents

LIST OF ABBREVIATIONS	1
SUMMARY	3
ZUSAMMENFASSUNG	4
1 GENERAL INTRODUCTION	6
1.1 Phytosulfokine	6
1.2 The PSK receptors.....	7
1.3 PSK signaling under osmotic stress	10
1.4 Accumulation of Absciscic acid	12
2 OBJECTIVES OF THIS THESIS	15
3 PSK signaling controls ABA homeostasis and signaling genes and maintains shoot growth under osmotic stress	16
3.1 ABSTRACT	17
3.2 INTRODUCTION	18
3.3 MATERIALS AND METHODS	20
3.3.1 Plant material and growth conditions	20
3.3.2 Drought experiment and plant analysis	21
3.3.3 Histochemical GUS analysis	22
3.3.4 RNA isolation, RT-PCR and quantitative real time PCR	22
3.3.5 ABA measurement	23
3.3.6 Statistical analysis	24
3.4 RESULTS	25
3.4.1 PSKR1 promotes shoot growth under osmotic stress.....	25
3.4.2 PSKR signaling in the root is not required for osmotic stress signaling to the shoot	28
3.4.3 Osmotic stress and ABA promote expression of <i>PSKR</i> and <i>PSK</i> genes.....	34
3.4.4 PSKR signaling regulates ABA levels and ABA responsiveness	37
3.5 DISCUSSION	42
3.5.1 PSK receptor signaling mediates osmotic stress-induced inhibition of cotyledon development	42
3.5.2 PSKRs support shoot growth during osmotic stress.....	43
3.5.3 PSK precursor and receptor genes are induced in the shoot by mannitol and ABA to promote growth	44
3.5.4 ABA homeostasis in osmotically stressed leaves is controlled by PSKR signaling	44
3.6 ACKNOWLEDGEMENTS	46

3.7 AUTHOR CONTRIBUTIONS.....	46
3.8 SUPPLEMENTARY MATERIAL.....	47
4 Functional analysis of receptor domains of phytosulfokine receptors PSKR1 and PSKR2.....	58
4.1 ABSTRACT	59
4.2 INTRODUCTION	60
4.3 MATERIALS AND METHODS	63
4.3.1 Plant material and growth conditions	63
4.3.2 Cloning strategy for developing domain swapping constructs.....	63
4.3.3 Shoot growth and root elongation assay.....	64
4.3.4 Total RNA isolation and expression analysis	64
4.3.5 Cloning, protein expression and purification	65
4.3.6 Biolayer interferometry	66
4.3.7 Databases and prediction tools.....	67
4.3.8 Statistical analysis	67
4.3.9 Accession numbers	67
4.4 Results	68
4.4.1 PSKR1 but not PSKR2 is important for shoot growth under mild osmotic stress	68
4.4.2 Functional analysis of PSK receptor chimeras reveal that the promoter, LRR and kinase domain of <i>PSKR1</i> are collectively important for an effective PSK signaling under osmotic and pathogen stress conditions.....	70
4.4.3 <i>PSKR1</i> is transcriptionally regulated upon osmotic and MAMP stress while <i>PSKR2</i> remains unaltered	81
4.4.4 The <i>PSKR1</i> promoter contains regulatory regions that influence both dehydration and elicitor responses.....	85
4.4.5 Potential differences in LRR2 contrastive to LRR1 determined through computational analysis.....	90
4.5 DISCUSSION	98
4.5.1 Transcriptional control of <i>PSKR1</i> by putative osmotic- and PTI-responsive CAREs is absent in the promoter region of <i>PSKR2</i>.....	98
4.5.2 Computational analysis identified a residue that differed between the LRRs which is crucial for a functional ligand binding domain.....	100
4.6 CONCLUSION	101
4.7 AUTHOR CONTRIBUTIONS.....	102
4.8 SUPPLEMENTARY MATERIAL.....	103
5 CONCLUSIVE DISCUSSION AND PERSPECTIVES	107
5.1 PSK/PSKR is associated with ABA signaling	107
5.2 PSK/PSKR signaling maintains shoot growth upon osmotic stress by regulating ABA levels....	108

5.3 PSKR does not mediate long-distance drought signaling.....	109
5.4 PSKR1 is the main transducer of PSK signaling	109
5.5 PSK interaction at the LRR of PSKRs	110
6 REFERENCES	111
ACKNOWLEDGEMENTS.....	122
DECLARATION.....	124

LIST OF ABBREVIATIONS

AAO	abscisic aldehyde oxidase
ABA	abscisic acid
ABA-GE	ABA-glucosyl ester
ABI	ABA-insensitive
ACT2	ACTIN2
AHA	Arabidopsis H ⁺ -ATPase
BAK1	BRI1-ASSOCIATED KINASE 1
BAM	BARELY ANY MERISTEM
BG	β-glucosidase
BLI	bio-layer interferometry
BRI1	BRASSINOSTEROID INSENSITIVE 1
CaM	calmodulin
CARE	<i>cis</i> -acting regulatory element
CEP	C-terminally encoded peptide
CEPR	CEP receptor
cGMP	cyclic guanosine monophosphate
CLE	CLAVATA/EMBRYO SURROUNDING REGION-RELATED
CLV	CLAVATA
CNGC17	CYCLIC NUCLEOTIDE GATED CHANNEL 17
CYP	cytochrome P450
D _{post}	fluorescence intensity of the donor after acceptor photobleaching
D _{pre}	fluorescence intensity of the donor before acceptor photobleaching
ED	extracellular domain
EF-Tu	elongation factor thermo unstable
elf18	18 amino acid fragment of EF-Tu
flg22	22 amino acid fragment of flagellin
FLS2	flagellin insensitive 2
F_m	maximum fluorescence
F_o	minimum fluorescence
FRET	Förster resonance energy transfer
FRET _{eff}	FRET efficiency

F_v	variable fluorescence
GAPC	GLYCERALDEHYDE-3-PHOSPHATE DEHYDROGENASE C
GC	guanylate cyclase
GUS	β -glucuronidase
HAE	HAESA
His1K	Anti-Penta-HIS sensor
HSL2	HAESA-like 2
ID	island domain
IDA	INFLORESCENCE DEFICIENT IN ABSCISSION
IPTG	isopropyl- β -D-thiogalactopyranoside
JMD	juxtamembrane domain
KD	kinase domain
LC-ESI-MS/MS	liquid chromatography electrospray ionization –tandem mass spectrometry
LRR	leucine rich repeat
MAMP	microbe-associated molecular pattern
MBP	maltose binding protein
NCED	nine <i>cis</i> -epoxycarotenoid dioxygenases
NHS	<i>N</i> -hydroxysuccinimide
PM	plasma membrane
PP2C	PROTEIN PHOSPHATASE TYPE 2C
PS II	photosystem II
PSK	phytosulfokine
PSKR	phytosulfokine receptor
PTI	pattern-triggered immunity
PYR1	PYRABACTIN RESISTANCE1
PYL1	PYR1-like
RCAR	REGULATORY COMPONENTS OF ABA RECEPTORS
RLK	receptor like kinase
SA	streptavidin-coated sensor
SBT	SUBTILASE
SERK	SOMATIC EMBRYOGENESIS RECEPTOR KINASE
SnRK	SUCROSE NON-FERMENTING 1-RELATED PROTEIN KINASE
TMH	transmembrane helix
TPST	TYROSYLPROTEIN SULFOTRANSFERASE

SUMMARY

As sessile organisms, plants are constantly exposed to a wide range of abiotic stresses, particularly water stress that negatively affects plant growth and development. To counteract such conditions, plants have developed signaling mechanisms that sense and respond to environmental cues by effective cell-to-cell communication facilitated predominantly by phytohormones. Among them, peptide hormones have recently emerged as key signaling molecules of stress responses. Phytosulfokine (PSK) is a peptide growth hormone that is perceived by two plasma membrane-bound leucine-rich repeat receptor-like kinases (LRR-RLKs), named PSK receptor 1 and 2 (PSKR1 and PSKR2) in *Arabidopsis thaliana*. Considering the growth promoting effects of PSK, we hypothesized that it could regulate plant growth under drought stress conditions and used the PSKR null mutant *pskr1-3 pskr2-1* to test our hypothesis. Our study shows that PSKR signaling enhanced drought tolerance by maintaining shoot growth and photosynthetic efficiency. Hydroponic and grafting analyses revealed that PSKR signaling was not required for long-distance signaling of osmotic stress from the root to the shoot. And, accumulation of abscisic acid (ABA), an important drought stress hormone, was dependent on PSKR signaling as ABA levels increased in wild type shoots but not in *pskr1-3 pskr2-1*. Furthermore, exogenous application of ABA partially improved growth of *pskr1-3 pskr2-1* shoots under osmotic stress. Additionally, transcriptome analysis showed misregulation of ABA synthesis genes and induced expression of *ABI1* and *ABI2*, which are both repressors of ABA signalling, in *pskr1-3 pskr2-1* shoots. Our data also revealed that PSK signaling is mainly modulated by PSKR1 rather than PSKR2 under water-deficit conditions. To elucidate functional differences between PSKR1 and PSKR2, we generated chimeras of PSKRs in which we switched the promoters, the LRR and the kinase domain of *PSKR1* and *PSKR2* and expressed the hybrid receptor genes in the receptor-deficient *pskr1-3 pskr2-1* background. Functional analysis of hybrid receptors revealed that the promoter of *PSKR1* is the main driver of PSKR activity and the LRR and kinase domain of *PSKR1* slightly improved PSKR activity compared to *PSKR2* receptor components. Altogether, these results reveal an important role of PSKR signaling in response to water-deficit conditions in an ABA-dependent manner and that PSKR1 functions as the major receptor rather than PSKR2.

ZUSAMMENFASSUNG

Als sessile Organismen sind Pflanzen ständig einer Vielfalt von abiotischen Stressfaktoren ausgesetzt. Insbesondere Wasserstress wirkt sich negativ auf Wachstum und Entwicklung von Pflanzen aus. Um solche Bedingungen zu überdauern, haben Pflanzen Signalmechanismen entwickelt, welche Umweltreize wahrnehmen und diese mit Hilfe einer effizienten Zell-zu-Zell-Kommunikation weiterleiten. Diese werden überwiegend durch Phytohormone vermittelt. Unter diesen wurden kürzlich Peptidhormone als Schlüsselmoleküle der Signaltransduktion von Stressantworten identifiziert. Phytosulfokin (PSK) ist ein Peptidhormon, welches in Arabidopsis von zwei Plasmamembran-gebundenen leucine-rich repeat receptor-like kinases (LRR-RLKs), PSK Rezeptor 1 und 2 (PSKR1 und PSKR2) wahrgenommen wird. In Anbetracht der wachstumsfördernden Wirkung von PSK, stellten wir die Hypothese auf, dass es das Pflanzenwachstum bei Trockenstress regulieren könnte und untersuchten die PSKR null Mutante *pskr1-3 pskr2-1*, um diese Hypothese zu testen. Unsere Studie zeigt, dass die PSKR-Signaltransduktion die Toleranz gegen Trockenstress erhöht, in dem Sprosswachstum sowie eine effiziente Photosyntheserate aufrechterhalten werden. In hydroponischen und Pfropfungsanalysen zeigte sich, dass die Signalweiterleitung über die PSK-Rezeptoren nicht essenziell für die Übertragung von osmotischen Stresssignalen aus der Wurzel zum Spross ist. Allerdings wurde eine Akkumulation des Trockenstresshormons Abscisinsäure (ABA) in Sprossen des Wildtyps aber nicht in *pskr1-3 pskr2-1* beobachtet, was auf eine Abhängigkeit von der PSKR-Signaltransduktion hindeutet. Zudem wurde durch exogene Zugabe von ABA das Wachstum von *pskr1-3 pskr2-1* Sprossen unter osmotischem Stress gefördert. Transkriptomanalysen zeigten eine Fehlregulierung von ABA-Synthesegenen sowie eine Induktion von *ABI1* und *ABI2*, Repressoren des ABA-Signals, in *pskr1-3 pskr2-1* Sprossen. Des Weiteren zeigten unsere Daten, dass die PSK-Signaltransduktion bei Wassermangel hauptsächlich durch PSKR1 und weniger durch PSKR2 reguliert wird. Um funktionale Unterschiede zwischen PSKR1 und PSKR2 aufzuklären, generierten wir chimärische PSKRs, bei denen Promotoren, LRR und Kinasedomänen von *PSKR1* und *PSKR2* ausgetauscht wurden. Diese hybriden Rezeptorgene wurden in dem rezeptordefizienten *pskr1-3 pskr2-1* Hintergrund exprimiert. Die funktionale Analyse der hybriden Rezeptoren zeigte, dass der *PSKR1*-Promotor der wesentliche Antrieb der PSKR-Aktivität ist, und zusätzlich,

dass PSKR1-LRR und -Kinase die PSRK-Aktivität leicht erhöhten, verglichen mit den PSKR2-Komponenten. Zusammen deuten unsere Ergebnisse auf eine wichtige Rolle der PSKR-Signaltransduktion in der Antwort auf Wasserknappheit abhängig von ABA hin und offenbaren, dass PSKR1 als Hauptrezeptor dient.

1 GENERAL INTRODUCTION

Cell-to-cell communication is indispensable and in animals, many peptide signals are known to be involved in cell-to-cell interactions. For many years, the phytohormones – auxin, cytokinin, abscisic acid, gibberellin, brassinosteroids, jasmonic acid, salicylic acid, ethylene and strigolactones were thought to be crucial signaling molecules that coordinate plant growth, development, and defense (Lindsey et al., 2002; Vanstraelen et al., 2012). However, research over the last two decades has identified secreted peptides as important signaling molecules that act as phytohormones which are also involved in processes of plant regulation including growth, development, and responses to biotic and abiotic stress factors (Matsubayashi, 2014; Tavormina et al., 2015; Oh et al., 2018; Olsson et al., 2019; Fletcher, 2020; Jeon et al., 2021; Kim et al., 2021). Secreted signaling peptides are categorized into two classes: small post-translationally modified peptides and cysteine-rich peptides. Post-translationally modified peptides are processed and modified in the secretory pathway before secretion, with typical modifications such as tyrosine sulfation, proline hydroxylation and hydroxyproline arabinosylation (Tavormina et al., 2015; Matsubayashi et al., 2018). And among them, Phytosulfokine (PSK) was the first tyrosine-sulfated peptide that has been discovered in plants (Matsubayashi et al., 1996).

1.1 Phytosulfokine

PSKs are disulfated pentapeptides (Tyr(SO₃H)-Ile-Tyr(SO₃H)-Thr-Gln) and were initially discovered as a mitogenic factor stimulating proliferation in *Asparagus officinalis* cell cultures (Matsubayashi and Sakagami, 1996). PSKs have been found to be conserved in 53 species from both dicots as well as monocots and belong to the group of plant peptide growth factors. PSK is derived from a 75-123 amino-acid preproprotein that is encoded in the nucleus (Lorbiecke and Sauter, 2002). Each preproPSK has a secretory signal sequence at the N-terminus and a canonical PSK sequence near the C-terminus flanked by dibasic amino acid residues implying proteolytic processing similar to that of animal peptide hormones (Yang et al., 2001; Lorbiecke and Sauter, 2002; Igarashi et al., 2003). ProPSK undergoes tyrosine-sulfation catalyzed by tyrosylprotein sulfotransferase (TPST) in the Golgi apparatus

(Hanai et al., 2000; Komori et al., 2009) and the disulfated ProPSK is secreted into the apoplast where proteolytic processing occurs to yield bioactive PSK. Information on the enzymes involved in precursor processing of PSK is still limited. To date, proteolytic processing of ProPSK4 in the apoplast by the subtilase SBT1.1 (Srivastava et al., 2008) and ProPSK1 by SBT3.8 (Stührwohldt et al., 2021) has been demonstrated while evidence as such is lacking for other proPSKs.

Seven *Arabidopsis* loci encode putative PSK precursor genes (Kaufmann and Sauter, 2019). PSK precursor genes are ubiquitously present in higher plants. *AtPSK1-5* contain the canonical YIYTQ sequence and are expressed in all tissues and developmental stages (Stührwohldt et al., 2011; Chen et al., 2017). *AtPSK6* is a pseudogene containing a PSK-like YIYTH sequence and the locus *At2g22942* contains two canonical PSK sequences which have been identified as putative PSK precursors. RNA-seq data of *AtPSK6* and *At2g22942* show very low expression levels (Chen et al., 2017) and their biological role is yet to be resolved.

1.2 The PSK receptors

Identification of a PSK-receptor pair helped to understand the molecular mechanisms underlying signal transduction. DcPSKR, a PSK receptor, was first isolated as a PSK binding protein in microsomal fractions from carrot (*Daucus carota*) cell cultures by a ligand-based affinity chromatography approach (Matsubayashi et al., 2002). *DcPSKR* is conserved among plants and in *Arabidopsis* its two orthologous genes were identified to be *PSKR1* and *PSKR2* (Matsubayashi et al., 2006; Amano et al., 2007). DcPSKR and AtPSKR1/2 receptors belong to subgroup X of the leucine-rich repeat receptor-like kinases (LRR-RLKs), a protein family with more than 223 members in *Arabidopsis* (Torii et al., 2004; Morillo and Tax, 2006; Gou et al., 2010).

In *Arabidopsis*, PSK/PSKR1-mediated signaling was shown to promote root growth and hypocotyl elongation while PSK/PSKR2-mediated signaling contributed only to growth of roots but not hypocotyls (Matsubayashi et al., 2006; Kutschmar et al., 2009; Stührwohldt et al., 2011). Plants lacking both PSKR1 and PSKR2 showed lower yield (seeds) (Stührwohldt et al., 2014) and impaired root and shoot growth (Kutschmar et al., 2009; Stührwohldt et al., 2011). PSK-dependent plant growth is rendered mainly via cell

expansion rather than cell proliferation (Kutschmar et al., 2009; Stührwoldt et al., 2011). Binding of PSK to PSKR1 stimulates allosteric changes resulting in heterodimerization with the co-receptor BRI1-associated kinase1 (BAK1)/SERK3, a somatic embryogenesis receptor-like kinase (SERK) family member. Also, PSKR1 interacts directly with the Arabidopsis H⁺-ATPases (AHAs), AHA1 and AHA2 and this complex associates with the cyclic nucleotide-gated cation channel 17 (CNGC17), although PSKR1 does not directly bind to it (Ladwig et al., 2015; Wang et al., 2015). These plasma-membrane bound proteins form a functional core complex that mediates cell expansion (Fig. 1). PSK/PSKR1 induced protoplast expansion through CNGC17 activation that in turn led to cell wall acidification, osmotic adjustment, water influx and subsequent expansion of cells (Ladwig et al., 2015).

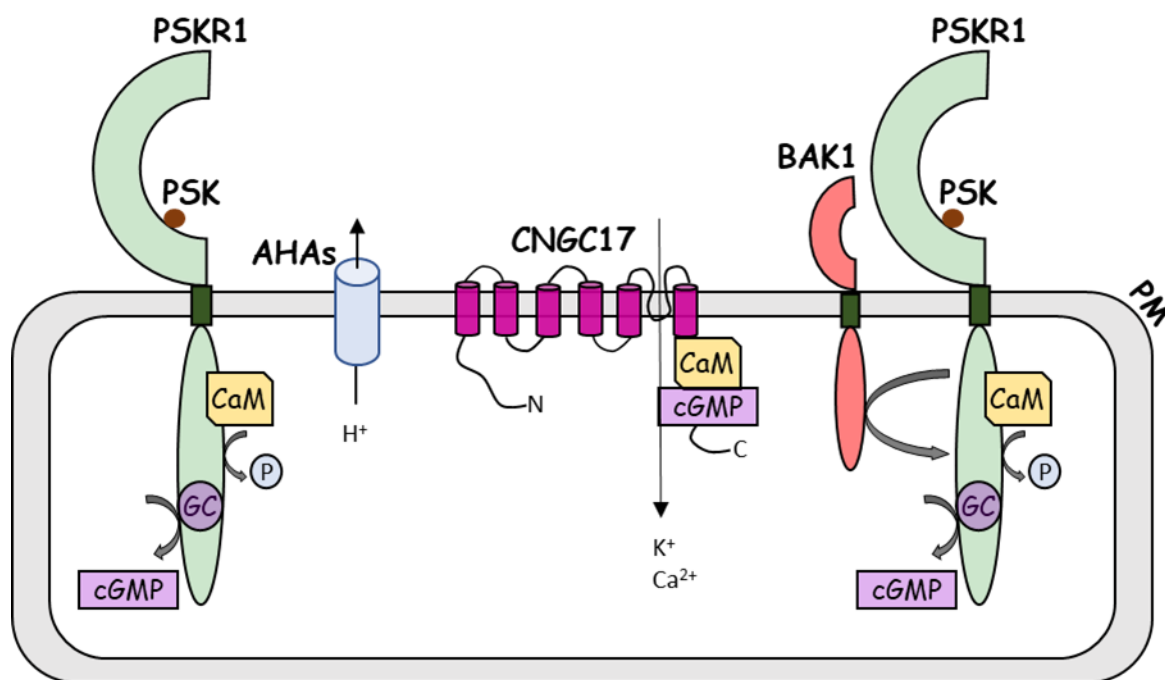


Figure 1. Model of PSK/PSKR1 associated protein nanoclusters at the plasma membrane (based on Ladwig et al., 2015).

PSK is perceived by PSKR1 at the plasma membrane (PM). PSKR1 is an active kinase with a binding site for calmodulin (CaM) and a guanylate cyclase (GC) centre that synthesizes cGMP (Kwezi et al., 2011; Hartmann et al., 2014). PSKR1 directly interacts with the co-receptor BAK1 and with the H⁺-ATPases AHA1 and AHA2 (AHAs). BAK1 and AHAs in turn bind to the cyclic nucleotide-gated cation channel 17 (CNGC17) that is subject to regulation by cGMP and CaM. AHAs, CNGC17 and BAK1 are assumed to form a functional core complex that connects H⁺ efflux to cation (K⁺, Ca²⁺) influx across the PM. PSKR1 is predicted to bind this complex to mediate cell expansion (Ladwig et al., 2015).

PSKRs are characterized by functional domains like ectodomain containing LRRs with an island domain, a single transmembrane helix, a juxtamembrane domain and an intracellular kinase domain (Matsubayashi et al., 2006) (Fig. 2). The ectodomain (ED) region is N-glycosylated and the PSKR1 ED contains 21 tandem copies of LRRs (Matsubayashi et al., 2002). The island domain (ID) of ~35 amino acids is a spacer region between two tandemly arranged LRRs and provides an interface for PSK interaction. Wang et al. (2015) solved the crystal structure of the PSK/PSKR1 ectodomain. PSK adopts an anti-parallel β -sheet conformation while interacting with PSKR1 ID. The two sulfate moieties of PSK directly interact with the PSKR1 ED via non-covalent interactions such as hydrogen bonds and van der Waals forces. A single α -helix consisting of a 21-amino-acid transmembrane domain anchors the PSKR into the plasma membrane connecting the ED in the apoplast with the juxtamembrane and subsequently the kinase domain in the cytoplasm (Matsubayashi et al., 2002; Sauter, 2015). The intracellular domain is a serine/threonine kinase with 12 conserved subdomains (Kwezi et al., 2011). A guanylate cyclase (GC) center and a calmodulin (CaM) binding site were identified within the functional kinase domain (Kwezi et al., 2011; Hartmann et al., 2014).

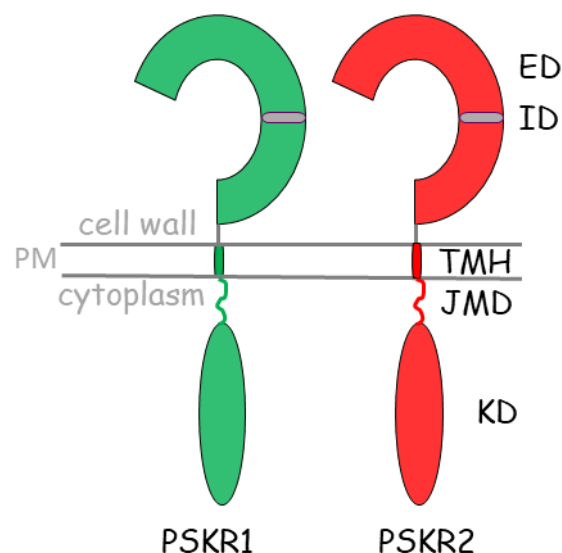


Figure 2. Schematic representation of the domains present in PSKR1 and PSKR2 .

PSKRs are structurally similar with defined domains. ED, ectodomain; ID, island domain; TMH, transmembrane helix; JMD, juxtamembrane domain; KD, kinase domain.

Although PSK is perceived by both PSKRs, the contribution to known PSK responses, for instance, shoot growth (Stührwohldt et al., 2011), root elongation (Hartmann et al., 2013) and immune responses (Igarashi et al., 2012; Zhang et al., 2018) are mainly conveyed through PSKR1, but not PSKR2. Until today, PSKR2 has not been extensively investigated compared to PSKR1 and its role, particularly in stress signaling is still less clear. So far it is known that both PSKRs are structurally similar and that PSKR2 serves as an alternative PSK receptor (Amano et al., 2007).

In the past, several studies have shown that PSK/PSKR-mediated signalling plays an important role in plant growth and development. For instance, it promotes adventitious root formation (Yamakawa et al., 1998), root growth (Kutschmar et al., 2009), hypocotyl elongation (Stührwohldt et al., 2011), cell growth and differentiation (Matsubayashi et al., 1999; Matsubayashi et al., 2006), gametogenesis, pollen germination (Chen et al., 2000) and fertilization (Lorbiecke et al., 2005), somatic embryogenesis as well as the maintenance of procambial cell identity (Holzwardt et al., 2018). In addition, a crucial role of PSK/PSKR-mediated signaling in plant immunity has been confirmed (Yamakawa et al., 1999; Loivamäki et al., 2010; Igarashi et al., 2012; Mosher et al., 2013; Rodiuc et al., 2015; Zhang et al., 2018; Yang et al., 2019). However, a comprehensive analysis of its role in response to abiotic stress is limited and almost unknown.

1.3 PSK signaling under osmotic stress

Among others, drought or high salinity are the two major adverse environmental factors that frequently limit plant growth and productivity (Comas et al., 2013; Chandrasekaran et al., 2014; Augé et al., 2015). These abiotic factors impose osmotic stress on plants by reducing the water potential of the environment and plant cells experience it when the solute concentrations in their apoplast change. To experimentally mimic such conditions, mannitol, a sugar alcohol, is widely applied to stimulate osmotic stress in vitro and study plant responses in a controlled environment (Slama et al., 2007; Darko et al., 2019; Kalve et al., 2020).

Plant responses to water-deficit conditions involve numerous regulatory mechanisms primarily aiming to (i) prevent water loss through transpiration via stomatal closure

mediated by the classical phytohormone, abscisic acid (ABA) (Nakashima et al., 2014; Takahashi et al., 2018) and (ii) maintain optimal plant growth by controlling cell expansion (Maggio et al., 2006; Zonia and Munnik, 2007; Osakabe et al., 2013). Since PSK is a growth promoting peptide-hormone and PSK-dependent plant growth is mainly mediated through cell expansion caused by water influx which depends on the availability of water, it is intriguing to know that under water-deficit conditions can PSK contribute to plant growth? If so, does it involve or is independent of the central regulator of abiotic stress, the ABA (Finkelstein, 2013; Wani and Kumar, 2015).

Plant peptides are now emerging as key signaling molecules that are able to act locally and systemically at extremely low concentrations (nM) to regulate abiotic stress responses (Segonzac and Monaghan, 2019; Wang and Irving, 2011). Recently, several studies revealed that peptide hormones and their respective receptor-like kinases play important roles in modulating adaptation and tolerance mechanisms under water-deficit conditions. For instance, CLAVATA3(CLV)/EMBRYO-SURROUNDING REGION-RELATED (CLE) peptides, particularly CLE25 perceived by BARELY ANY MERISTEM1 (BAM1) and BAM2 receptors act as mobile drought signals from root to shoot that induce ABA-dependent stomatal closure in *Arabidopsis thaliana* (Takahashi et al., 2018; Zhang et al., 2019), INFLORESCENCE DEFICIENT IN ABSCISSION (IDA) recognized by HAESA (HAE) and HAESA-LIKE 2 (HSL2) receptors is involved in drought-induced cauline leaf abscission (Patharkar and Walker, 2016) and C-terminally encoded peptide 5 (CEP5) through CEP receptors, CEPR1/2 confers drought stress tolerance in *Arabidopsis* (Smith et al., 2020). Likewise, a recent study identified that PSK precursor processing is necessary to promote root growth providing first evidence of an important role for PSK in drought stress response (Stührwohldt et al., 2021).

At the same time, when water availability is limited, plants first reduce shoot growth and then root growth, depending on the constraint, extent, and duration (Comas et al., 2013; Pierik and Testerink, 2014; Koevoets et al., 2016). It is also known, that shoot growth is a more sensitive indicator of stress that is highly-dose dependent (Claeys et al., 2014). However, there is a big gap in our knowledge about PSK/PSKR signaling and its involvement in shoot growth.

1.4 Accumulation of Absciscic acid

Plants exposed to osmotic stress conditions, sense water limitations in roots first and subsequently transmit the stress signal from roots to shoots to induce stomatal closure. Indeed, an important response to osmotic stress is the accumulation of ABA for regulating stomatal closure (Munemasa et al., 2015). Furthermore, ABA is predominantly present in the vasculature of leaves as well as all ABA synthesis-associated enzymes that are expressed in vascular tissues (Kuromori et al., 2018). Accumulated ABA then spreads to all tissues and elicits many adaptive responses in plants (Zhu, 2002; Raghavendra et al., 2010; Roychoudhury et al., 2013) such as activation of gene expression and stomatal closure as a means to provide resistance against osmotic stress (Shinozaki et al., 2003; Finkelstein, 2013).

ABA accumulation is dependent on synthesis, degradation, activation, and conjugation (Fig. 3). The transcriptional regulation of genes involved in either ABA production or ABA inactivation is of great importance in homeostasis (Ma et al., 2018). De novo ABA synthesis is the main mechanism responsible for the accumulation of ABA in response to water deficiency (Christmann et al., 2005). In this pathway, nine *cis*-epoxycarotenoid dioxygenases (NCEDs) cleave neoxanthin to form xanthoxin (Fig. 3) (Luchi et al., 2001; Schwartz et al., 2003). Xanthoxin is then exported from plastids to the cytosol and is converted into abscisic aldehyde, which is finally oxidized to ABA by abscisic aldehyde oxidase (AAO) (Fig. 3) (Seo et al., 2000).

An alternative pathway for ABA synthesis occurs via hydrolysis of ABA-glucosyl ester (ABA-GE), which is an inactive form of ABA (Fig. 3). ABA-GE can be hydrolysed by β -glucosidase (BG) homologs BG1 and BG2 in Arabidopsis (Lee et al., 2006; Xu et al., 2012). BG1 is localized to the endoplasmic reticulum and BG2 in the vacuole. This is an ideal and important way to rapidly increase ABA levels since it is a single-step reaction (Fig. 3) (Xu et al., 2012).

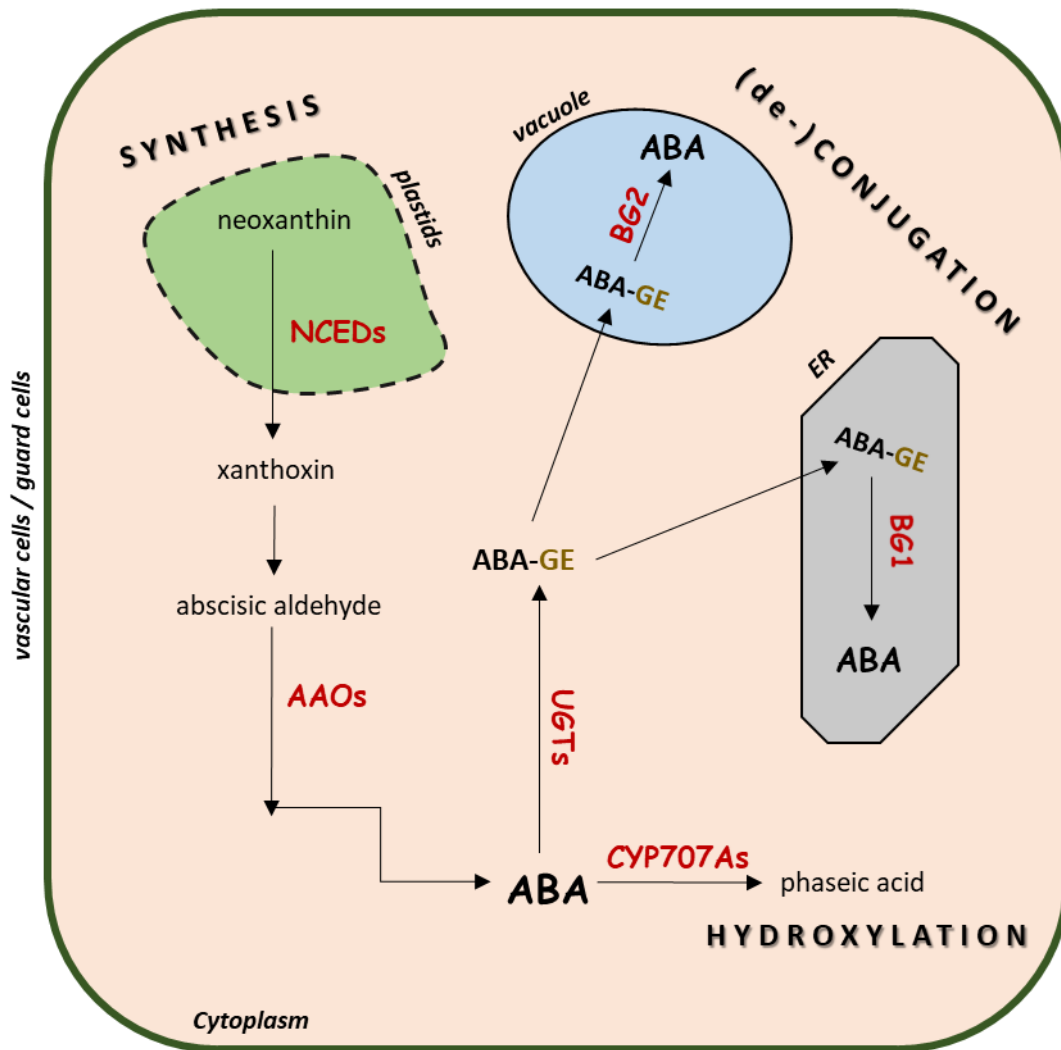


Figure 3. Schematic representation of ABA homeostasis and important players under osmotic stress.

ABA de novo biosynthesis is catalyzed by nine *cis*-epoxycarotenoid dioxygenases (NCEDs) and abscisic aldehyde oxidases (AAOs), while ABA degradation is mainly catalyzed by CYP707As leading to the generation of phaseic acid. The UDP-glucosyltransferases (UGTs) modify ABA to inactive ABA-glucosyl ester (ABA-GE), while the glucosyl hydrolase (BG1 and BG2) convert ABA-GE to active ABA. Enzymes are denoted in red.

ABA catabolism is also a mechanism for regulating ABA levels and proceeds via two pathways, namely ABA 8'-hydroxylation catalyzed by ABA 8'-hydroxylase, an enzyme that belongs to the cytochrome P450 (CYP) 707A family (Saito et al., 2004) and conjugation of ABA with glucose catalysed by ABA-uridine diphosphate (UDP) glucosyltransferases (UGTs) (Fig. 3) (Priest et al., 2006; Dong et al., 2014).

Accumulated ABA is then transported to sites of action, such as guard cells (Merilo et al., 2015; Kuromori et al., 2018). In guard cells, ABA molecules bind to the pyrabactin resistance 1/PYR1-like/regulatory component of the ABA receptor (PYR/PYL/RCAR) in the nucleus and the cytosol, thereby activating the sucrose non-fermenting 1-related protein kinases (SnRKs) (Umezawa et al., 2010; Joshi-saha et al., 2011) which in turn phosphorylate a number of transcription factors that activate stress responsive genes (Fig. 4). Inversely, the protein phosphatase type 2C (PP2C) proteins, ABA-insensitive 1 (ABI1) and ABI2, which are the main components of ABA signaling under osmotic stress, inhibit the activity of SnRKs via dephosphorylation, exerting negative regulation of ABA signaling (Rodriguez et al., 1998; Gosti et al., 1999; Kuhn et al., 2006; Saez et al., 2006; Yoshida et al., 2006; Fujii et al., 2009; Nishimura et al., 2010; Cutler et al., 2010; Raghavendra et al., 2010) (Fig. 4).

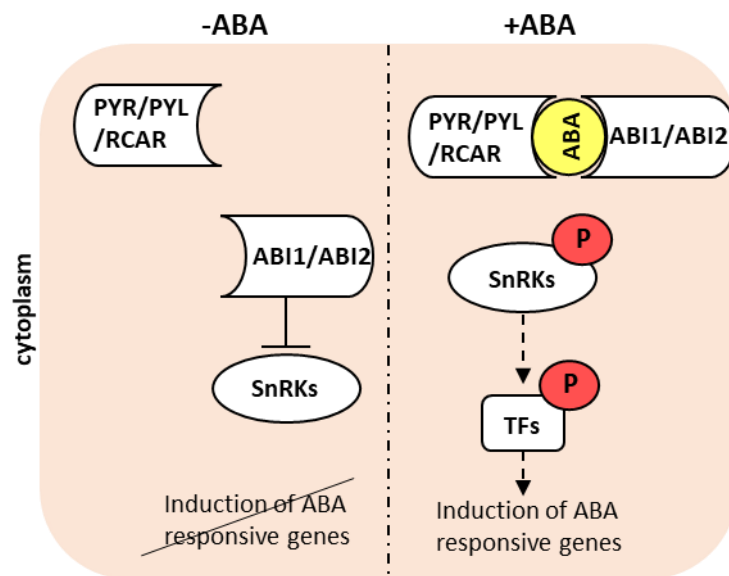


Figure 4. Model of repression and activation of the ABA-signaling pathway in guard cells.

In the absence of ABA, the negative regulators of ABA signaling, ABI1 and ABI2, physically interact with the sucrose non-fermenting 1-related protein kinases (SnRKs) to abolish kinase activity via dephosphorylation. This inhibits the activation of stress-related genes. Under osmotic stress conditions, ABA molecules bind to the ABA receptors, PYR/PYL/RCAR, leading to conformational changes that allow for interaction with ABIs, thereby suppressing their phosphatase activity. Free SnRKs phosphorylate downstream transcription factors that in turn trigger the activation of ABA-responsive genes.

2 OBJECTIVES OF THIS THESIS

The aim of this work is to extend the understanding of PSK/PSKR signaling in response to osmotic stress. To that end, PSKR signaling was found to be essentially important to maintain shoot growth and photosynthetic activity under osmotic stress by balancing water stress responses.

This thesis includes two chapters that address the following questions:

Chapter 1:

- Does PSKR modulate long-distance root-shoot signaling under osmotic stress?
- Is ABA accumulation mediated by PSKR signaling upon osmotic stress?
- Are both PSK receptors functional under osmotic stress?

Chapter 2:

- Between the two PSK receptors, why are PSKR2 functions largely inactive in response to osmotic stress?
- Can the functional component of PSKR2 be detected using a chimeric receptor design approach?

3

PSK signaling controls ABA homeostasis and signaling genes and maintains shoot growth under osmotic stress

Komathy Rajamanickam¹, Martina D. Schönhof¹, Bettina Hause²,
Margret Sauter¹

¹Plant Developmental Biology and Plant Physiology, University of Kiel,
Kiel, Germany

²Department of Cell and Metabolic Biology, Leibniz Institute of Plant
Biochemistry, Halle (Saale), Germany

3.1 ABSTRACT

Water deficit impairs growth and survival of plants. Many water stress responses are under control of abscisic acid (ABA), but little is known about growth control under osmotic stress. Based on the previously described growth-promoting activity of the peptide hormone phytosulfokine (PSK), we hypothesized that it may contribute to growth regulation under water stress conditions. To test this hypothesis, we analyzed the *Arabidopsis thaliana* PSK receptor (PSKR) null mutant *pskr1-3 pskr2-1* under mannitol and drought stress. In particular under mild water stress, fresh weight and photosynthetic efficiency were more reduced in *pskr1-3 pskr2-1* than in wild type. Hydroponic and grafting experiments showed that PSKR signaling was not required for long-distance signaling from mannitol-stressed roots to shoot but rather for cell growth promotion in the shoot. Unlike wild type, *pskr1-3 pskr2-1* shoots did not accumulate ABA in response to mannitol, showed misregulation of ABA synthesis genes and elevated expression of *ABI1* and *ABI2*, repressors of ABA signaling whereas application of ABA partially reversed shoot growth inhibition by mannitol in *pskr1-3 pskr2-1*. In turn, mannitol, and ABA induced expression of *PSK3* and *PSKR1*, and ABA promoted expression of *PSK2* and *PSK4* revealing feedback regulatory loops between PSKR and osmotic stress signaling.

Key words

Peptide signaling, PSK receptor, drought stress, mannitol, grafting, growth, photosynthesis, leaf growth, abscisic acid, osmotic stress

3.2 INTRODUCTION

Water deficit is a major challenge for plants as it impairs growth and ultimately survival. It is a result of osmotic stress brought about by drought or high salinity. The non-ionic osmolyte mannitol is frequently used in osmotic stress and plant growth research (Nikonorova et al., 2018; Kalve et al., 2020). Osmotic stress induces responses to ameliorate the stress conditions such as a reduction of water loss through stomatal closure (Munemasa et al., 2015). The plant hormone abscisic acid (ABA) accumulates in plant shoots following drought or osmotic stress and controls stoma closure and transcriptional changes (Bartels and Sunkar, 2005; Yamaguchi-Shinozaki and Shinozaki, 2006; Finkelstein, 2013, Takahashi et al., 2020). In addition, ABA-independent pathways of osmotic stress resistance exist.

Active ABA levels are determined by synthesis, degradation, inactivation and remobilization. ABA is synthesized from xanthophylls. Nine-*cis*-epoxycarotenoid dioxygenase (NCED) catalyze a key regulated step (Luchi et al., 2001; Schwartz et al., 2003) and aldehyde oxidases (AO) catalyze the conversion of abscisic aldehyde to ABA (Seo et al., 2000). Degradation of ABA is initiated by ABA 8'-hydroxylase, an enzyme that is encoded by four members of the cytochrome P450 CYP707A family in *Arabidopsis* (Kushiro et al., 2004; Saito et al., 2004). ABA hydroxylation has been identified as the key step in ABA catabolism (Dejonghe et al., 2018). However, inactivation of ABA also occurs through conjugation to glucose by ABA UDP-glucosyltransferase (UGT) encoded by *UGT71B6-B8*, in *Arabidopsis* (Dong et al., 2014). ABA-glucose ester is a storage form of ABA that can be remobilized by ABA glucosidases BG1 and BG2 (Lee et al., 2006). Thus, ABA homeostasis depends on synthesis and inactivation pathways whereby many of the genes involved are regulated in response to dehydration and other stresses (Xu et al., 2013).

Water deficit is first perceived in the root and from there communicated to the shoot. Among other drought-induced signals that move from root to shoot is the signaling peptide CLAVATA3/EMBRYO-SURROUNDING REGION-RELATED 25 (CLE25) that moves through the vasculature to leaves where it is perceived by BAM receptor-like kinases (Takahashi et al., 2018; Takahashi et al., 2019). CLE25/BAM signaling activates NCED3, a key gene in ABA biosynthesis and thereby contributes

to ABA-dependent drought adaptation. The study revealed a crucial role of signaling peptides and receptor-like kinases in plant adaptation to water deficit.

Phytosulfokine (PSK) belongs to the group of secreted signaling peptides (Sauter, 2015; Kaufmann and Sauter, 2018). PSK is perceived by PSK receptors at the plasma membrane that belong to the leucine-rich repeat receptor-like kinase family encoded by two genes, PSKR1 and PSKR2, in *Arabidopsis thaliana* (Matsubayashi et al., 2006). Knockout of both receptor genes impairs root elongation and shoot growth whereas exposure of wild-type seedlings to PSK promotes growth by enhancing cell expansion (Kutschmar et al., 2009; Stührwohltdt et al., 2011). At the molecular level, PSKR1 interacts with the co-receptor Brassinosteroid-insensitive (BAK1) and the H⁺-ATPases AHA1 and AHA2, and indirectly through BAK1 and AHAs with the Cyclic nucleotide-gated channel 17 (CNGC17). These proteins assemble in a nanocluster at the plasma membrane and were proposed to form a functional unit that drives cell expansion (Ladwig et al., 2015). PSKR signaling promotes protoplast expansion in a CNGC17-dependent manner and was proposed to lead to cell wall acidification, water uptake, accompanied by osmotic adjustment, and consequently to expansion of cells.

Low water potential prevents water uptake and limits cell expansion resulting in reduced growth rates under drought conditions. While physiological responses to water-deficit, foremost stoma closure, have been well studied, the question, if growth inhibition by osmotic constraint is balanced by a growth-promoting pathway to prevent an extreme stress response resulting in growth arrest, has not been resolved. It is clear however that an, albeit reduced, growth rate is maintained in plants despite of osmotic constraints. In support of the hypothesis that PSK signaling maintains plant growth under osmotic stress a recent study demonstrated that PSK precursor processing is required to promote root growth in response to the osmolyte mannitol in *Arabidopsis* (Stührwohltdt et al., 2021).

Shoot growth is a more sensitive indicator to stress (Claeys et al., 2014) and was studied here to further investigate the role of PSKR signaling in response to osmotic stress. Our results show that PSKR signaling in the shoot is required to maintain shoot growth under mild osmotic stress, in part through altered ABA synthesis and signaling.

3.3 MATERIALS AND METHODS

3.3.1 Plant material and growth conditions

All experiments were performed with *Arabidopsis thaliana* (L.) Heynh. ecotype Columbia (Col-0) and mutants in the Col-0 background. The lines used were described previously as indicated: *pskr1-3* (Kutschmar et al., 2009; Stührwohldt et al., 2011), *pskr2-1* (Amano et al., 2007; Stührwohldt et al., 2011), *pskr1-2 pskr2-1* (Stührwohldt et al., 2011; Hartmann et al., 2013), *PSKR1ox2* and *PSKR1ox12* (Hartmann et al., 2013), *35S:PSKR1-GFP* (Hartmann et al., 2015). For GUS analyses of PSK receptors the lines *PSKR1:GUS-4* (Kutschmar et al., 2009; Stührwohldt et al., 2011) and *PSKR2:GUS-3* were used. For growth on plates, seeds were surface-sterilized for 25 min with 2% (w/v) sodium hypochlorite (NaOCl) followed by four washing steps with autoclaved water and placed on square plates containing half-strength MS medium (Murashige & Skoog, 1962; basal salt mixture, Duchefa Biochemie) and 1% (w/v) sucrose, solidified with 0.4% Gelrite (Duchefa Biochemie). After two days of stratification at 4°C in the dark, plates were transferred to long day conditions with a 16 h light (70 μM photons $\text{m}^{-2} \text{s}^{-1}$) and 8 h dark cycle at 22°C and 60% humidity.

For germination and greening assays, wild type and mutant parental plants were grown and harvested at the same time to ensure equal seed quality. Seeds were placed on medium supplemented with or without 1 μM (+)-*cis*, *trans*-abscisic acid (ABA) (Duchefa Biochemie), 350 μM mannitol and/or 1 μM PSK (Pepscan). PSK and ABA were always added freshly. ABA was diluted right before use. The penetration of the endosperm or testa by the embryo radicle was counted as successful germination event. Three independent experiments were performed with 100 seeds each per genotype per treatment.

To analyze shoot growth under stress conditions, seedlings were pregrown vertically under sterile conditions for 4 days to complete germination and cotyledon greening (Supplemental Fig. S6) and subsequently transferred to new plates supplemented with mannitol, sorbitol and/or ABA as indicated and grown for the times indicated. Growth was quantified with a fine scale as shoot fresh weight or shoot dry weight. Plant pictures are shown on a black background for better visualization. Primary root lengths were determined 7 days after transfer of 4-day-old seedlings to

mannitol because the roots reached the bottom of the plate after longer times making it impossible to measure root lengths later on.

For grafting, 6-day-old seedlings were grown on agar plates (0.5X MS pH 5.8; 0.5% (w/v) sucrose; 1% (w/v) agar) at short-day conditions (8 h light and 16 h dark). Grafting was performed as described (Marsch-Martínez et al., 2013). The rootstock and scion were prepared under sterile conditions by excising the hypocotyl of the seedlings. Cotyledons were also excised to improve healing. Adventitious roots were removed immediately when they appeared. The grafted plants were allowed to recover for 14 days, and successful grafts were chosen for osmotic stress experiments with mannitol. Plants were grown on mannitol or mannitol-free medium as indicated for another 14 days prior to analysis.

3.3.2 Drought experiment and plant analysis

Plants were grown in square pots (7x7x8 cm) on soil for three weeks under well-watered conditions with 50 ml of water every third day. After three weeks, the soil was water-saturated for 3 days and, subsequently, plants were watered every 3 days with 5 ml for another 3 weeks. Pots with control plants remained well-watered as before. Drought experiments were repeated three times and growth was quantified as shoot fresh weight.

For chlorophyll fluorescence measurements, an IMAGING-PAM chlorophyll fluorometer (Maxi version with blue measuring light, Walz, Effeltrich, Germany) was used. Plants were dark-adapted for 30 minutes prior to image capture. The maximum quantum yield of photosystem II (PS II) was measured as the ratio of $F_v/F_m = (F_m - F_o)/F_m$, where F_o is the minimum fluorescence measured using a weak excitation beam (setting 1 with 1 Hz), F_m is the maximum fluorescence measured by applying a saturated light pulse ($2,500 \mu\text{mol photons m}^{-2} \text{s}^{-1}$) and F_v is the variable fluorescence ($F_m - F_o$). Subsequently, plants were exposed to saturating pulses with background illumination and $\Delta F/F_m'$ measurement was done under steady state conditions. $\Delta F/F_m'$ was calculated using the formula $(F_m' - F)/F_m'$, where the prime (') denotes actinic light. Images and measurements were obtained using Imaging Win V2.41a software (Walz).

3.3.3 Histochemical GUS analysis

To analyze spatial distribution of *PSKR* and *PSK* expression, β -glucuronidase (GUS) assays were performed as described (Weigel & Glazebrook, 2002) with minor changes. Seedlings were collected in 90% (v/v) isopropanol, incubated for 10 minutes and washed with 50 mM sodium phosphate buffer (pH 7.2). Staining was performed for 15 h and stopped by transferring the seedlings to 70% (v/v) ethanol. Tissues were cleared with a chloral hydrate:deionized water:glycerol 6:2:1 (g/ml/ml) mixture that was added on microscopy slides instead of water. Seedlings were visualized under bright-field illumination with a Nikon SMZ18 binocular (Nikon) and photographed with a DIGITAL SIGHT-Ri1 camera (Olympus).

3.3.4 RNA isolation, RT-PCR and quantitative real time PCR

Total RNA was isolated from true leaves using TRI Reagent (Merck) following manufacturer's protocol. cDNA was synthesized from 1 μ g DNase I-treated (Thermo Fisher Scientific) total RNA by oligo(dT)-primed reverse transcription using RevertAid Reverse Transcriptase (Thermo Fisher Scientific). To avoid gDNA contamination and to ensure an equal amount of RNA input, cDNA was tested by PCR for *ACTIN2* (At3g18780) transcripts prior to qPCR analysis with the primers ACT2for 5'-CAAAGACCAGCTCTTCCATCG-3' and ACT2rev 5'-CTGTGAACGATTCCTGGACCT 3'. qPCR was used to examine the expression of *PSKR1*, *PSKR2*, *PSK1*, *PSK2*, *PSK3*, *PSK4*, *PSK5*, *NCED3*, *NCED5*, *NCED9*, *CYP707A1*, *CYP707A2*, *CYP77A3*, *CYP707A4*, *UGT71B6*, *UGT71B7*, *UGT71B8*, *BG1*, *BG2*, *AAO1*, *AAO2*, *ABI1* and *ABI2* with primers listed in Supplemental Table 1 using the Rotor Gene SYBR Green PCR Kit (Qiagen) according to manufacturers' protocol in a Rotor gene Q cycler (Qiagen). Ten ng cDNA per sample were applied in a total volume of 15 μ l. Estimation of raw data was done with the Rotor-Gene Q 2.3.1.49 (Qiagen) program.

The relative transcript abundance was calculated based on the $\Delta\Delta\text{CP}$ method including primer efficiency to normalize the data with two reference genes (Pfaffl, 2001; Van Desompele et al., 2007). In relation to each reference gene (*ACT2* and GLYCERALDEHYDE-3-PHOSPHATE DEHYDROGENASE 1 (*GAPC1*)) (Supplemental Table 1) values were averaged from three independent biological replicates with two technical replicates each. The expression of wild type under control conditions was set to 1 and all other values were calculated as fold change of that.

3.3.5 ABA measurement

Four-day-old seedlings were transferred to medium containing mannitol as indicated and grown for additional 7 days. Roots and shoots were harvested separately and immediately frozen in liquid nitrogen. About 50 mg of homogenized, frozen material was extracted with 500 μl of methanol containing isotope-labelled internal standard $^2\text{H}_6\text{-ABA}$ ($0.1 \text{ ng } \mu\text{l}^{-1}$) followed by centrifugation. The supernatant was diluted with 4.5 ml water and subjected to solid-phase extraction on HR-XC (Chromabond, Macherey-Nagel, Düren, Germany) column. Fractions containing ABA were eluted with acetonitrile and separated using the ACQUITY UPLC System (Waters, Eschborn, Germany) (Balcke et al. 2012). Detection of ABA and $^2\text{H}_6\text{-ABA}$ was done by ESI-tandem mass spectrometry (MS/MS) using a 3200 Q TRAP® LC/MS/MS mass spectrometer (Waters) (Balcke et al., 2012). ABA content per sample was calculated using the ratio of ABA and $^2\text{H}_6\text{-ABA}$ peak heights. Data were obtained from 5 biological replicates each.

To an alternative method to measure changes in ABA levels in response to mannitol, we obtained the *ABAleon2.1* line and the plasmid *barII-UT-ABAleon2.1* from Rainer Waadt (Waadt et al., 2014) that we used to generate a homozygous *pskr1-3 pskr2-1 ABAleon2.1* line. Plants were transformed with *Agrobacterium tumefaciens EHA105*, containing the *barII-UT-ABAleon2.1* construct with the floral dip method (Clough and Bent, 1998). The progeny was selected with BASTA®. In the T2 generation the seedlings were additionally screened with the FastGene® Blue/Green LED Flashlight (Nippon Genetics Europe GmbH) with an orange/blue filter to exclude silencing of the transgene. Acceptor photobleaching Förster resonance energy transfer (FRET) was used to measure relative differences in ABA levels in each genotype using

a Leica SP5 CLSM. Cells were excited sequentially at 458 and 514 nm and emission recorded with adequate filter sets. Post-bleach images were captured at 458 nm excitation (Supplemental Fig. S8). FRET is visualized as an increase in mTurquoise fluorescence following cpVenus173 photobleaching (Supplemental Figure S8). FRET efficiency was calculated according to the formula $FRET_{eff} = (D_{post} - D_{pre}) / D_{post}$ with D_{post} = fluorescence intensity of the donor after acceptor photobleaching and D_{pre} = fluorescence intensity of the donor before acceptor photobleaching.

3.3.6 Statistical analysis

Statistical analyses were done using Minitab® 16.1. Data that were not distributed normally were evaluated using a Kruskal-Wallis or Mann-Whitney test for pairwise comparison. Normally distributed data were tested for equal variance. In the case of equal variance, ANOVA, otherwise a t-test for pairwise comparison was chosen.

3.4 RESULTS

3.4.1 PSKR1 promotes shoot growth under osmotic stress

PSK signaling is known to promote root and shoot growth (Sauter, 2015). A recent report demonstrated that PSK precursor synthesis and precursor processing by subtilisin serine proteases enhance root growth under mannitol stress conditions revealing a role of PSK signaling of growth under osmotic stress (Stührwohldt et al., 2021). To better understand PSK signaling of growth under osmotic stress, we employed the PSK receptor null line *pskr1-3 pskr2-1* (Stührwohldt et al., 2011; Hartmann et al., 2013) and focussed on shoot growth of seedlings exposed to mannitol. Seedlings were grown for 4 days without mannitol, then transferred to plates containing 0 mM, 25 mM, 50 mM, 100 mM or 200 mM mannitol. Shoot growth was analyzed after an additional 2 weeks (Fig. 1). Wild type seedlings displayed inhibition of shoot size, shoot fresh weight and shoot dry weight by mannitol in a dose-dependent manner, a phenotype that was exacerbated in *pskr1-3 pskr2-1* seedlings (Fig. 1A, B, C and D). The strongest growth inhibition of *pskr1-3 pskr2-1* seedlings compared to wild type was observed at low concentrations of 25 mM and 50 mM mannitol suggesting that PSKR signaling maintains shoot growth particularly well during mild osmotic stress. Growth reduction induced by mannitol was largely due to reduced leaf size (Fig. 1B). To see if cell expansion was dependent on PSK signaling under mannitol stress as reported for unstressed conditions (Matsubayashi et al., 2006; Kutschmar et al., 2009; Stührwohldt et al., 2011; Ladwig et al., 2015) we analyzed epidermal cell sizes of wild type and *pskr1-3 pskr2-1* first true leaves (Fig. 1E and F). The average epidermal cell size was smaller in *pskr1-3 pskr2-1* compared to wild type at control conditions (Fig. 1E, F). When exposed to 50 mM mannitol, cells became even smaller in both genotypes with a more severe effect observed in *pskr1-3 pskr2-1* seedlings indicating that PSK receptor signaling promotes cell expansion under osmotic stress conditions but cannot fully overcome the stress. As of note, reduction in cell size went along with reduced lobing of the epidermal cells under mannitol (Fig. 1E). The osmotic compound sorbitol that was used for comparison also exacerbated growth inhibition in *pskr1-3 pskr2-1* seedlings compared to wild type in a dose-dependent manner (Supplemental Fig. S1).

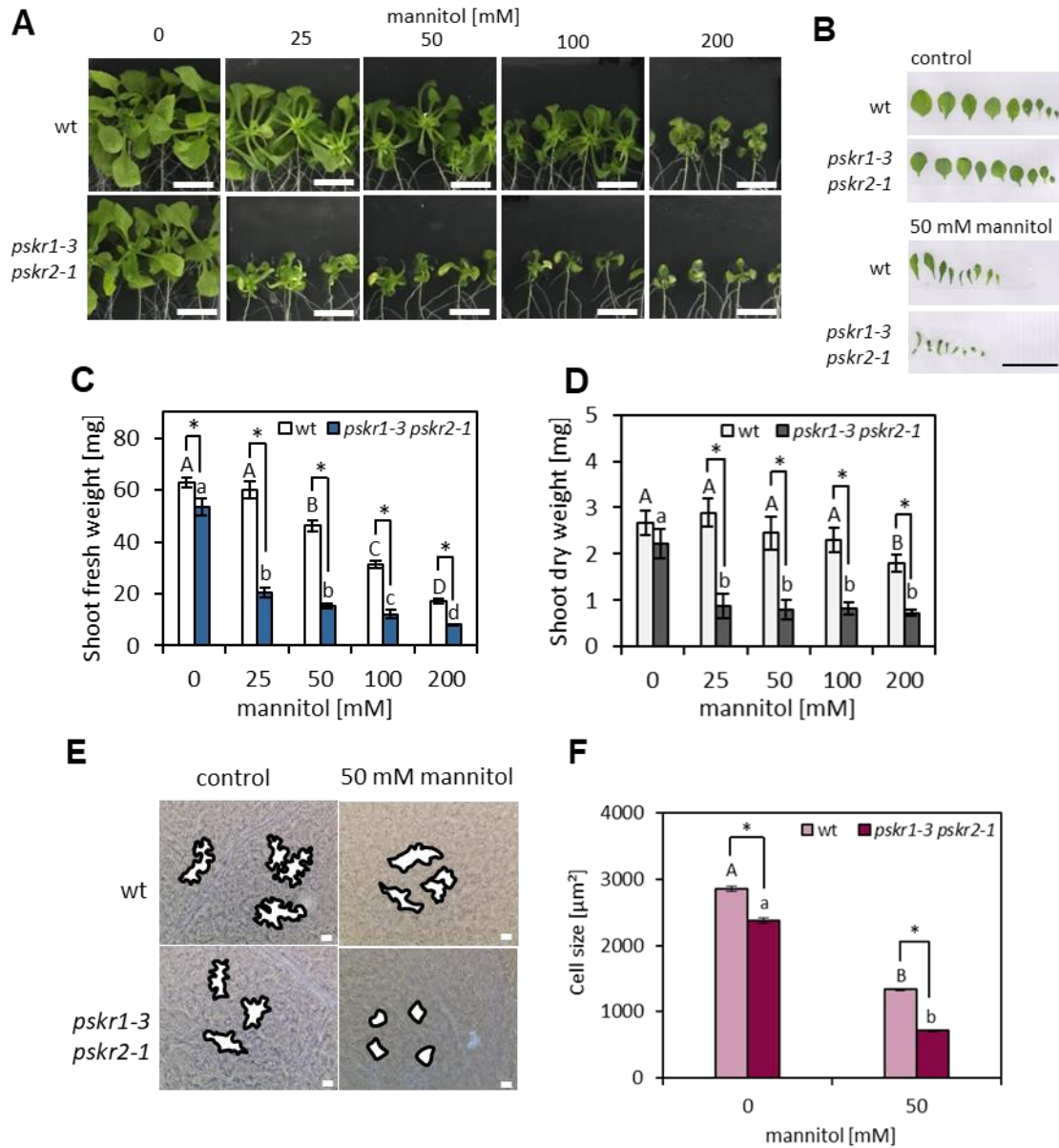


Figure 1. PSK receptor signaling promotes shoot growth under mannitol stress.

Four-day-old wild type and *pskr1-3 pskr2-1* seedlings were transferred to media containing mannitol as indicated.

(A) Shoot phenotypes of wild type (wt) and *pskr1-3 pskr2-1* plants grown for 2 weeks. Scale bars = 10 mm. **(B)** Leaf numbers, sizes and morphology of wild type and *pskr1-3 pskr2-1* plants grown on mannitol-free medium or on 50 mM mannitol for 2 weeks. Scale bar = 10 mm. **(C)** Shoot fresh weights of wt and *pskr1-3 pskr2-1* plants grown as in A. **(D)** Shoot dry weights of wt and *pskr1-3 pskr2-1* plants grown as in A. Significantly different values within a genotype are denoted by different letters (Kruskal-Wallis, Tukey's test, $p < 0.05$, $n \geq 36$, 3 independent experiments). Asterisks indicate significant differences between genotypes (Mann-Whitney test, $p < 0.05$). **(E, F)** Epidermal cell phenotypes and sizes of plants grown as in A-D. Photographs of the abaxial epidermis. Single cell outlines are highlighted in bold black lines (scale bar = 10 nm). Average cell sizes of the first true leaf were analyzed from 12 seedlings with 40-50 cells measured per seedling. Significant differences between treatments

are indicated by different letters. Asterisks indicate significant differences between genotypes (Mann-Whitney test, $P < 0.05$, $n \geq 1500$, 3 independent experiments).

Primary root growth was inhibited at 200 mM mannitol in both genotypes with a significantly stronger inhibition in *pskr1-3 pskr2-1* than wild type confirming previously reported results (Stührwohltd et al., 2021) whereas root elongation was unaffected by mannitol up to 100 mM in both genotypes (Supplemental Fig. S2) indicating that PSKR signaling was important to maintain shoot growth at mild osmotic stress conditions.

To pinpoint which of the two PSK receptors mediated resistance to osmotic stress-induced growth inhibition of the shoot, we used single PSK receptor gene knock out lines (Kutschmar et al., 2009). Growth inhibition by 50 mM mannitol was comparable in the single knockout line *pskr1-3* and the double knockout line *pskr1-3 pskr2-1* whereas *pskr2-1* plants showed wild-type shoot growth indicating that PSKR1 promotes growth of plant shoots exposed to mild osmotic stress (Fig. 2).

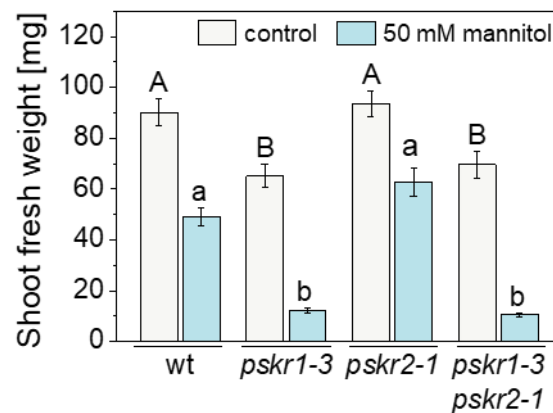


Figure 2. PSKR1 is crucial for shoot growth promotion under mannitol stress.

Four-day-old wild type, *pskr1-3*, *pskr2-1*, and *pskr1-3 pskr2-1* seedlings were transferred to media with or without 50 mM mannitol. Mean (\pm SE) shoot fresh weights of seedlings after 3 weeks. Different letters indicate significant differences (Kruskal-Wallis, Tukey's test, $p < 0.05$, $n \geq 36$, 3 independent experiments).

For shoot growth experiments, we grew seedlings for 4 days on medium without osmoticum prior to osmotic stress treatment. However, osmotic stress resistance may also be important at earlier developmental stages during germination. To close this knowledge gap, we investigated seed germination and cotyledon greening in wild type and *pskr1-3 pskr2-1* exposed to mannitol, PSK and ABA. ABA is known as a drought hormone and mediates osmotic stress responses (Zhao et al., 2018). While seed germination was delayed by ABA and mannitol, no significant differences in germination rate were observed between wild type and *pskr1-3 pskr2-1* at any of the treatments indicating that inhibition of seed germination by ABA or mannitol was not controlled by PSK/PSKR signaling (Supplemental Figs. S3 and S4). On the other hand, cotyledon greening that is known to be delayed under unfavourable conditions such as under ABA or mannitol treatment (Guan et al., 2014) was delayed in wild type but not *pskr1-3 pskr2-1* seedlings (Supplemental Figs. S5 and S6) suggesting that PSK/PSKR signaling contributes to stress acclimation during very early seedling development. Application of mannitol to four-day-old seedlings was hence a useful approach to circumvent these early developmental processes when studying shoot growth regulation.

3.4.2 PSKR signaling in the root is not required for osmotic stress signaling to the shoot

Water deficit is perceived in roots and the stress signal is transmitted to the shoot via the vasculature (Takahashi and Shinozaki, 2019; Takahashi et al., 2020). We next clarified whether PSKR signaling was required for stress perception in the root or for a root-derived stress signal in the shoot. Osmotic stress was routinely applied by transferring seedlings to plates containing mannitol. In order to test whether PSKR signaling of growth was induced through direct contact of leaves with mannitol or as part of the water deficit response signaled by roots, we compared growth on plates where the whole seedling had access to media to growth on plates where only roots were in contact with media (Fig. 3A, B). Stronger inhibition of shoot growth was observed in *pskr1-3 pskr2-1* compared to wild type in both setups but shoots that were not in contact with media began to dry out after eight days (Fig. 3A and B). To

overcome this problem, a hydroponic system was established (Fig. 3C) where seedlings were grown on a mesh separating the shoot from the medium.

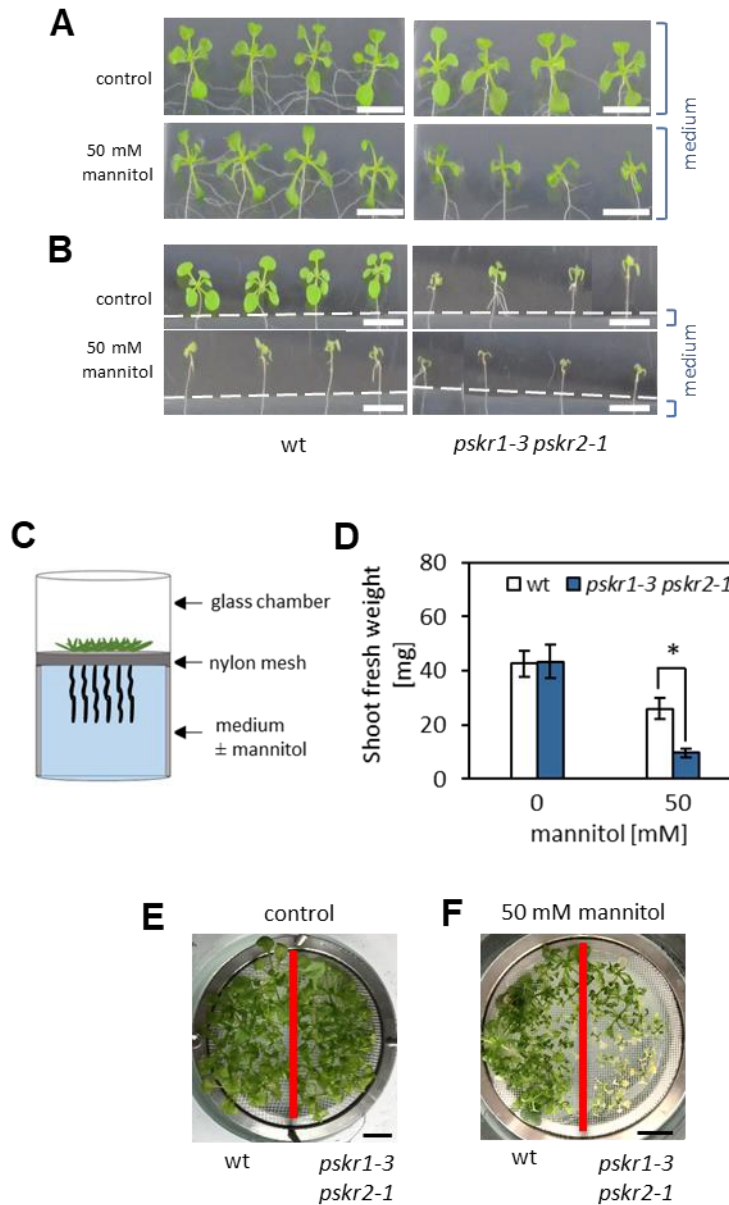


Figure 3. Mannitol stress is sensed by roots.

(A) Seedlings were pre-grown for 4 days and then transferred to medium supplemented with or without 50 mM mannitol. Phenotypes of shoots grown on plates with media for 8 days. (B) Seedlings were grown on plates with excised media at the height of the shoot to prevent direct contact of the shoot with mannitol (A,B: scale bar = 10 mm). (C) Scheme of the hydroponic system used to apply mannitol to roots. (D) Seedlings were pre-grown for 10 days as shown in C and then transferred to fresh medium supplemented with or without 50 mM mannitol. Shoot fresh weight was determined after two weeks. Results are averages of three independent experiments (Mann-Whitney test, $P < 0.05$, $n \leq 45$). (E, F)

Shoot phenotypes of wt and *pskr1-3 pskr2-1* plants grown on medium (E) without or (F) with 50 mM mannitol (scale bar = 10 mm).

After 10 days, seedlings were transferred to media containing 50 mM mannitol and grown for another 14 days. Shoot growth of *pskr1-3 pskr2-1* seedlings was significantly impaired compared to wild type (Fig. 3D-F) indicating that osmotic stress sensed by the roots led to PSKR-dependent shoot growth promotion.

To find out if PSKR signaling was required for osmotic stress perception in roots and participated to signal water deficit to the shoot, we performed grafting experiments as a widely used technique to investigate long-distance signaling in plants (Chen et al., 2006; Corbesier et al., 2007; Molnar et al., 2010; Liang et al., 2012). Wild type and *pskr1-3 pskr2-1* shoot scions and root stocks were grafted as indicated schematically in Figure 4A. Cotyledons were removed before grafting to prevent formation of adventitious roots which lower grafting efficiency. Ungrafted seedlings, also with cotyledons removed for better comparison, and within-genotype self-grafts were included as controls. Grafted wild type and *pskr1-3 pskr2-1* seedlings showed the same growth phenotypes as ungrafted seedlings indicating that the setup worked properly (Fig. 4C-E). Seedlings with a wild type shoot and a *pskr1-3 pskr2-1* root had the same shoot growth phenotype as wild type seedlings at control and stress conditions whereas seedlings with a *pskr1-3 pskr2-1* shoot and a wild type root had a *pskr1-3 pskr2-1* phenotype (Fig. 4C-E). These observations indicated that PSKR signaling does not contribute to root-shoot communication of osmotic stress but is required for growth promotion in the shoot during the stress. Excision of cotyledons inhibited shoot growth of *pskr1-3 pskr2-1* but not wild type seedlings even in the absence of osmotic stress (compare Fig. 1A, C and Fig. 4A, E) suggestive of a crosstalk between cotyledons and true leaves that is dependent on PSKR signaling. Taken together, the results showed that PSKR acts downstream of a mobile root-derived signal in the shoot to maintain growth under osmotic stress.

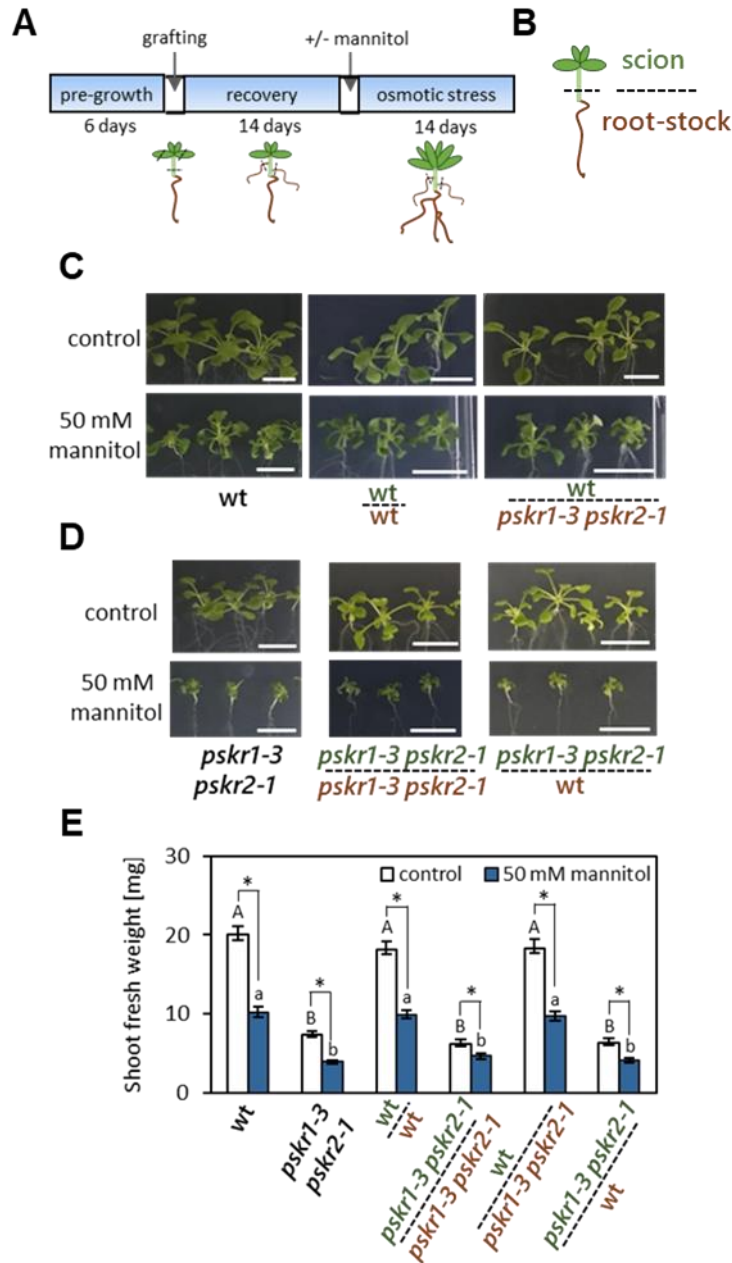


Figure 4. PSKR signalling in the shoot promotes growth in response to mannitol.

Wild type shoots were grafted with double receptor knockout roots (wt + *pskr1-3 pskr2-1*) and vice versa (*pskr1-3 pskr2-1* + wt) under short day conditions. Successful grafts were analyzed for shoot fresh weight grown under long day conditions. **(A)** A scheme representing the grafting procedure. **(B)** Model to represent labelling. **(C, D)** Shoot phenotypes of successful grafts on (\pm) 50 mM mannitol plates. Cotyledons of wt and *pskr1-3 pskr2-1* were cut and included as controls (scale bar = 10mm). **(E)** Fresh weight of the shoots supplemented with/without 50 mM mannitol were measured on the fourteenth day. Results are averages obtained from three independent experiments. The capital and minor letters indicate significant differences between genotypes upon control and mannitol treatments respectively (Kruskal-Wallis test $P < 0.05$, $n \geq 24$) and asterisks indicate significant differences within treatments for a particular genotype (Mann-Whitney test, $P < 0.05$).

To confirm that the PSKR-dependent maintenance of shoot growth under mild mannitol stress was a response to low water potential, we exposed wild type and *pskr1-3 pskr2-1* seedlings to mild drought stress (Fig. 5A). Plants were grown for 3 weeks under well-watered conditions and subsequently watered with one tenth the water supplied before. Shoot fresh weight after 3 weeks of growth under water-limiting conditions was reduced by about 50% in *pskr1-3 pskr2-1* seedlings compared to wild type (Fig. 5B). Enhanced drought symptoms in the knock-out mutant were further revealed by reduced photosynthetic efficiency of PSII (Fig. 5C, D). Using IMAGING-PAM, two parameters in dark-adapted and steady-state light conditions, F_v/F_m and $\Delta F/F_m'$, were measured that reveal a response to abiotic stress (Zhang and Sharkey 2009; Kalaji et al., 2016), including drought (Yao et al., 2018). From the false colour images (Fig. 5C) the average F_v/F_m and $\Delta F/F_m'$ ratios of rosettes were determined in both genotypes under control and drought conditions. The F_v/F_m ratio was close to 0.8 in both genotypes in well-watered conditions and decreased more under drought in *pskr1-3 pskr2-1* than wild type (Fig. 5D). The $\Delta F/F_m'$ ratio indicates steady-state quantum yield of PSII in light-adapted conditions and is an accurate indicator of operational PSII efficiency (Murchie and Lawson 2013). This ratio was also significantly lower in drought-exposed *pskr1-3 pskr2-1* plants compared to wild type (Fig. 5E) revealing that plants lacking PSKR signaling are more sensitive to low water potential.

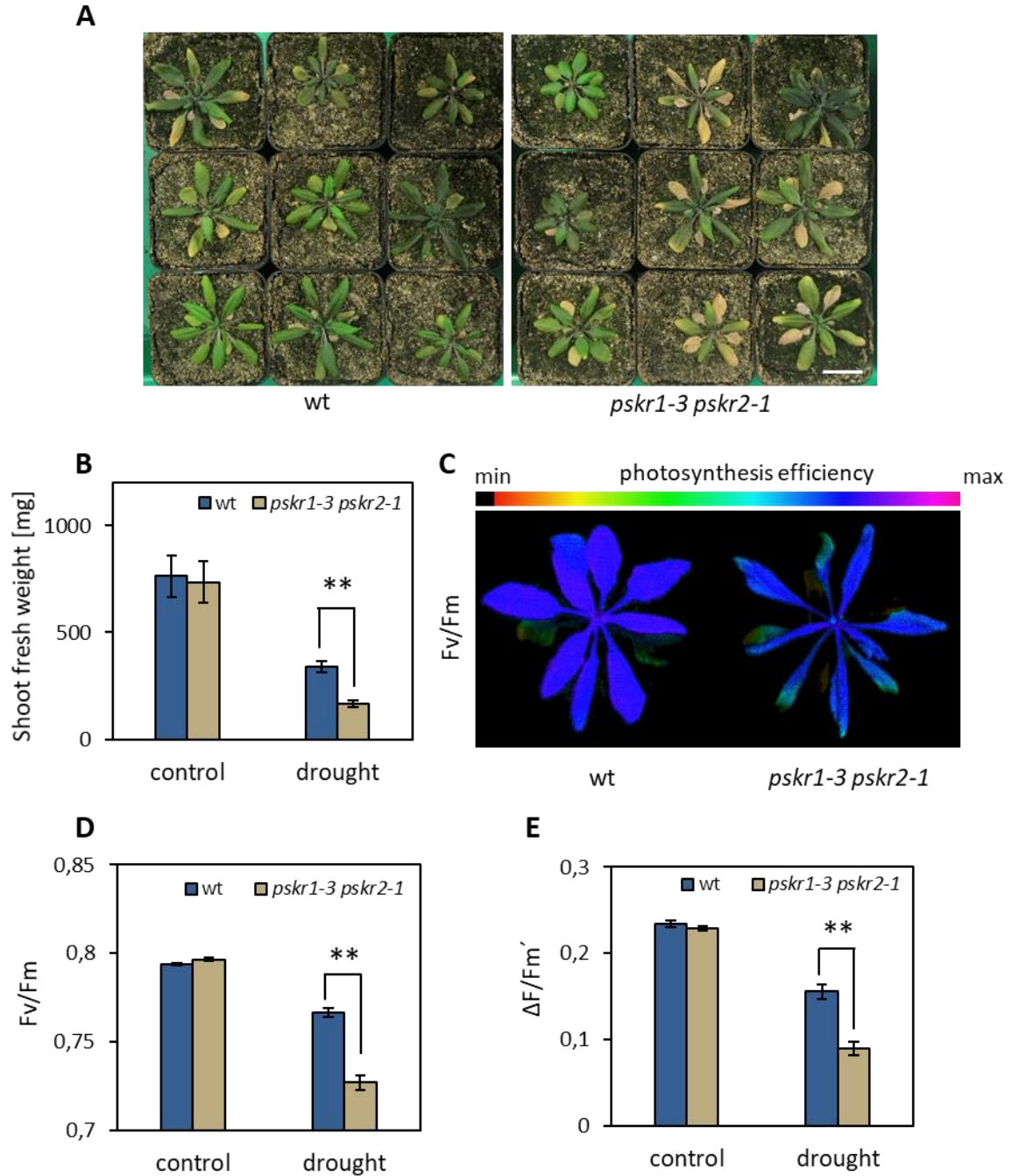


Figure 5: PSK receptor signaling provides drought stress tolerance.

Plants were watered with 50 ml every three days for three weeks, soil water-saturated for three days and subsequently watered with 5 ml every three days for another three weeks or with 50 ml as a control. **(A)** Phenotypes of plants exposed to mild drought stress (scale bar = 3 cm). **(B)** Average (\pm SE) shoot fresh weights of wild type and *pskr1-3 pskr2-1* plants obtained from three independent experiments (Mann-Whitney test, $P < 0.01$, $n \geq 36$). **(C)** Representative chlorophyll fluorescence images of drought exposed plants displaying the maximum quantum yield of PS II, Fv/Fm. **(D)** Fv/Fm ratio (\pm SE) of control

and drought-stressed wild type and mutant plants (Mann-Whitney test, $**P < 0.01$, $n \geq 36$). (E) $\Delta F/F_m'$ ratio (Mann-Whitney test, $**P < 0.01$, $n \geq 36$).

3.4.3 Osmotic stress and ABA promote expression of *PSKR* and *PSK* genes

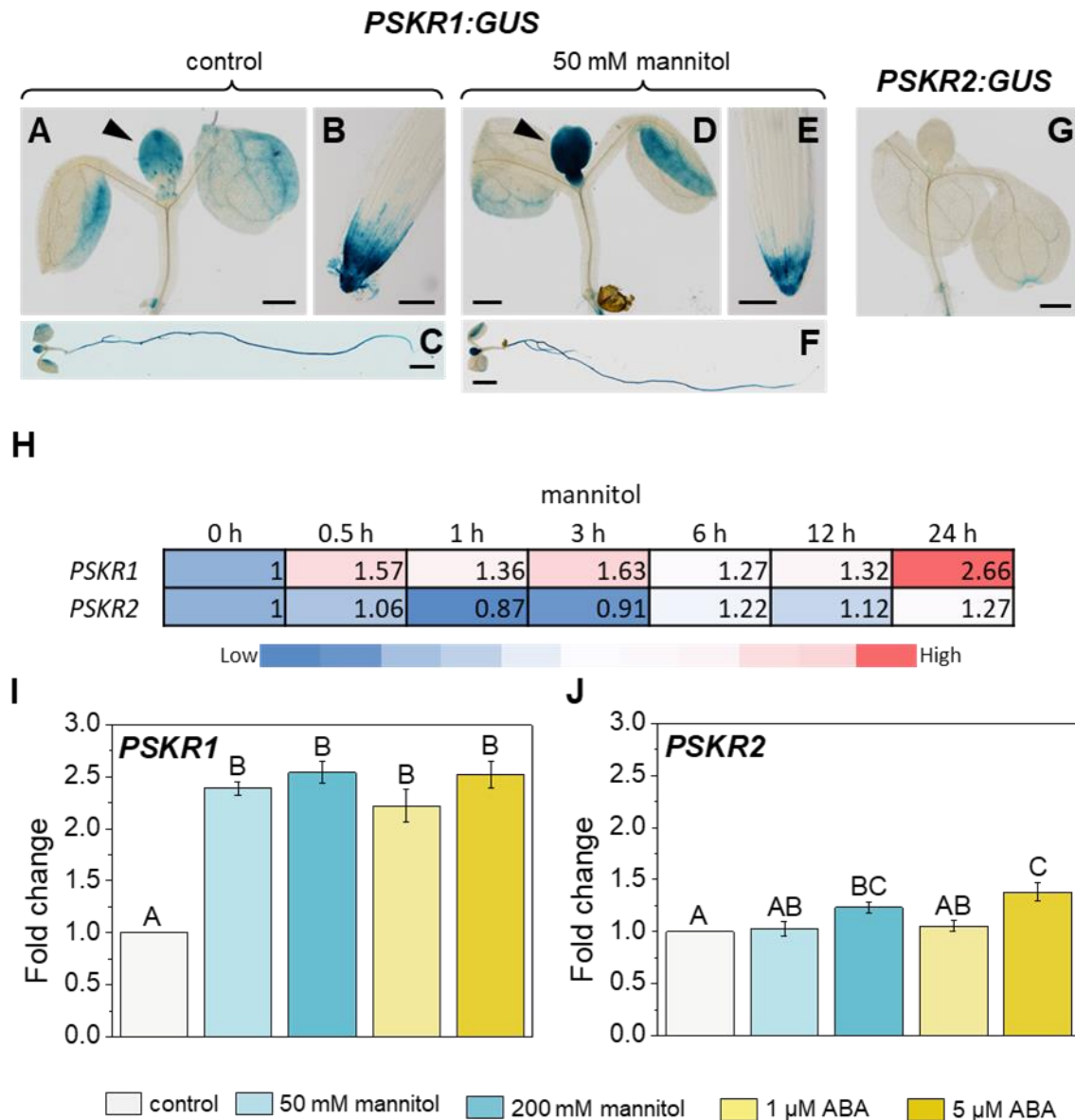


Figure 6. *PSKR1* expression is induced by mannitol and ABA.

(A-F) *PSKR1:GUS-4* activity in seven-day-old seedlings treated with 50 mM mannitol for one day or left untreated as a control. (A-C) Expression in shoot, and root under control conditions. (D-F) Expression in shoot, and root under mannitol. Arrowheads point at true leaves; scale bar = 0.5 mm (A, D), = 0.1 mm (B, E), = 2 mm (C, F). (G) *PSKR2:GUS-3* activity in the shoot; scale bar = 0.5 mm. (H) Shoot tissue samples of 18-day-old plants analyzed for the expression of *PSKR1* and *PSKR2* under 300 mM mannitol treatment. Microarray data obtained from Arabidopsis efp browser 2.0 database available online (<http://www.bar.utoronto.ca/>) (Kilian et al., 2007). (I, J) Seven-day-old seedlings exposed to 50 mM, 200

mM mannitol, 1 μ M or 5 μ M ABA for one day or left untreated as a control. Relative transcript levels of (H) *PSKR1* and (I) *PSKR2* were analyzed by RT-qPCR in true leaves. Values are means (\pm SE); different letters indicate significant differences (one-way ANOVA, Tukey's test, $P < 0.05$, 3 biological replicates).

We next analyzed expression of *PSK* and *PSKR* genes in response to mannitol and ABA as a drought stress-induced hormone. *Promoter:GUS* lines (Kutschmar *et al.*, 2009; Stührwohldt *et al.*, 2011) were used to obtain spatial resolution and microarray and qRT-PCR data were used to quantify changes in gene expression.

PSKR1:GUS activity was detected in cotyledons, true leaves and in the root and appeared to be induced in true leaves by mannitol (Fig. 6A-F). Microarray data showed induction of *PSKR1* in shoots after one day of treatment with 300 mM mannitol (Fig. 6H). RT-qPCR data confirmed elevated *PSKR1* transcript levels in true leaves after one day of exposure to 50 mM or 200 mM mannitol as well as by 1 μ M and 5 μ M ABA (Fig. 6I). By contrast, *PSKR2:GUS* activity was present in the cotyledon hydathode region (Fig. 6G) and *PSKR2* was induced at 200 mM mannitol and 5 μ M ABA but not at lower concentrations (Fig. 6J) in accordance with the finding that shoot growth promotion under mild osmotic stress was dependent on *PSKR1* (Fig. 2).

Of the five *PSK* precursor genes, *PSK2*, *PSK3*, *PSK4* and *PSK5* but not *PSK1* were expressed in the shoot in accordance with the previous finding that *PSK1* is root-specific (Kutschmar *et al.*, 2009) (Fig. 7A). *PSK3:GUS* activity was particularly high in young, expanding leaves. Analysis of *PSK* precursor gene expression by RT-qPCR showed significant induction of *PSK3* by 200 mM mannitol and 5 μ M ABA in wild type while *PSK2* and *PSK4* expression was induced by ABA (Fig. 7B-F). Knockout of *PSK* signaling in *pskr1-3 pskr2-1* resulted in elevated *PSK2* and *PSK4* expression at control conditions suggestive of feedback inhibition by *PSKR* signaling. Mannitol but not ABA resulted in hyperinduced *PSK1*, *PSK2*, *PSK3* and *PSK5* transcript levels in *pskr1-3 pskr2-1* compared to wild type. Taken together, the data revealed common and differential induction of *PSK* genes in response to mannitol and ABA and a negative feedback loop between *PSKR* signaling and *PSK* expression.

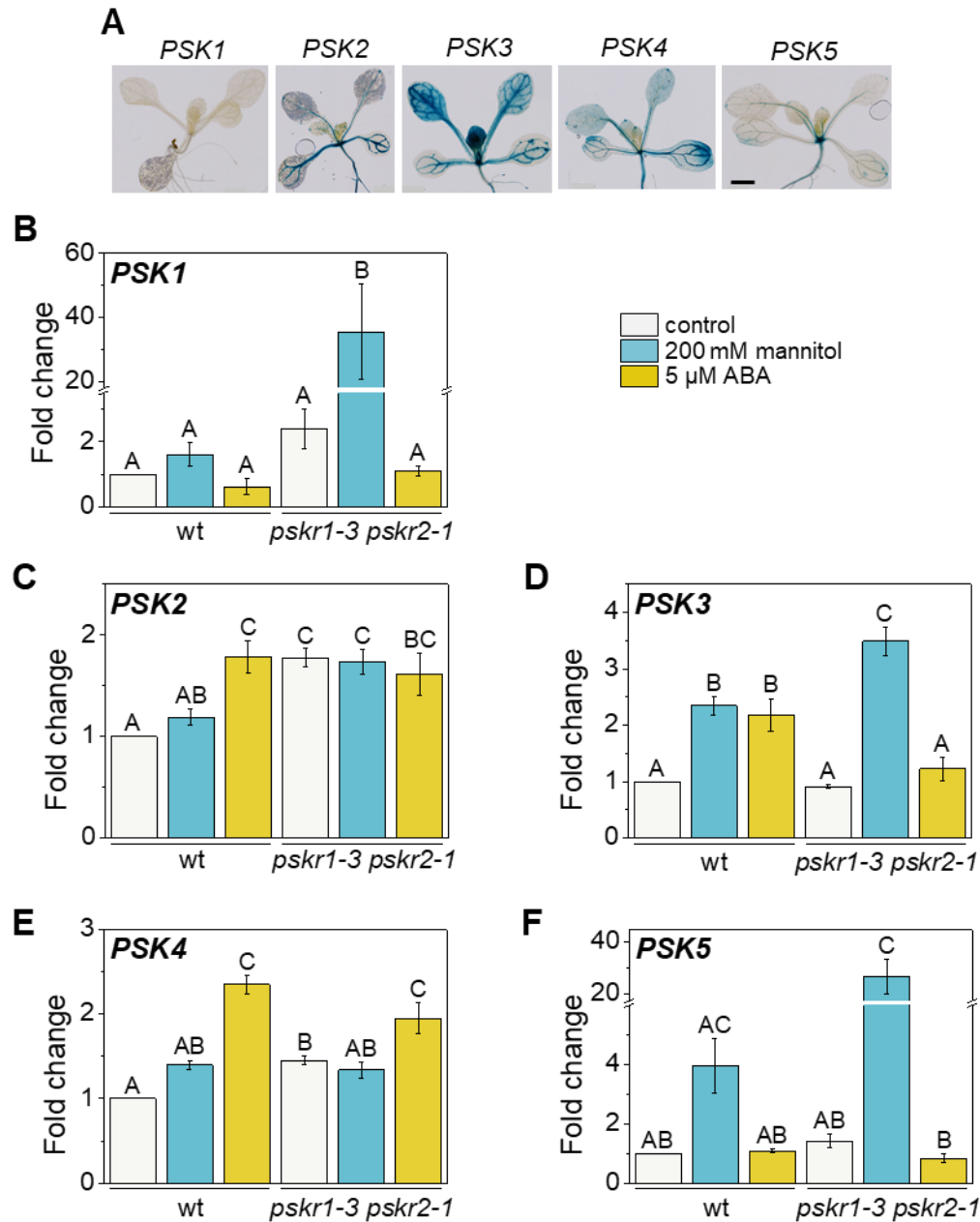


Figure 7. *PSK* genes are differentially regulated by mannitol, ABA and *PSKR* signaling.

(A) GUS staining of *PSK1::GUS-3*, *PSK2::GUS-2*, *PSK3::GUS-3*, *PSK4::GUS-4* and *PSK5::GUS-1* seedlings; scale bar = 2 mm. (B-F) Seven-day-old seedlings were exposed to 200 mM mannitol or 5 μ M ABA for one day for qPCR analyses in first true leaves. Results (\pm SE) are averages from three biological replicates with two technical repeats each. Different letters indicate significant differences. (B) Transcript levels of *PSK* genes relative to *PSK3* that was set to 1. (C-F) Relative transcript levels of *PSK1-5* in wild type and in *pskr1-3 pskr2-1* seedlings treated with mannitol or ABA as indicated (B, F: Kruskal-Wallis, Tukey's test, $P < 0.05$; C-E: one-way ANOVA, Tukey's test, $P < 0.05$).

3.4.4 PSKR signaling regulates ABA levels and ABA responsiveness

Responses to osmotic stress are regulated by ABA-dependent and ABA-independent pathways. *PSK3* and *PSKR1* were regulated by both, mannitol and ABA suggesting that PSK/PSKR-ABA crosstalk occurs under osmotic stress. Since ABA is predominantly synthesized in leaves upon drought (Cardoso et al., 2020) we asked whether ABA levels were regulated by PSKR signaling. Analysis of ABA levels in wild type seedling shoots by mass spectrometry revealed a dose-dependent increase in ABA in response to mannitol (Fig. 8A). A similar increase was observed in roots (Supplemental Fig. S7). By contrast, ABA levels did not increase in *pskr1-3 pskr2-1* shoots in response to mannitol whereas in roots, ABA levels increased in *pskr1-3 pskr2-1* seedlings at 200 mM mannitol albeit overall levels were lower than in wild type (Supplemental Fig. S7).

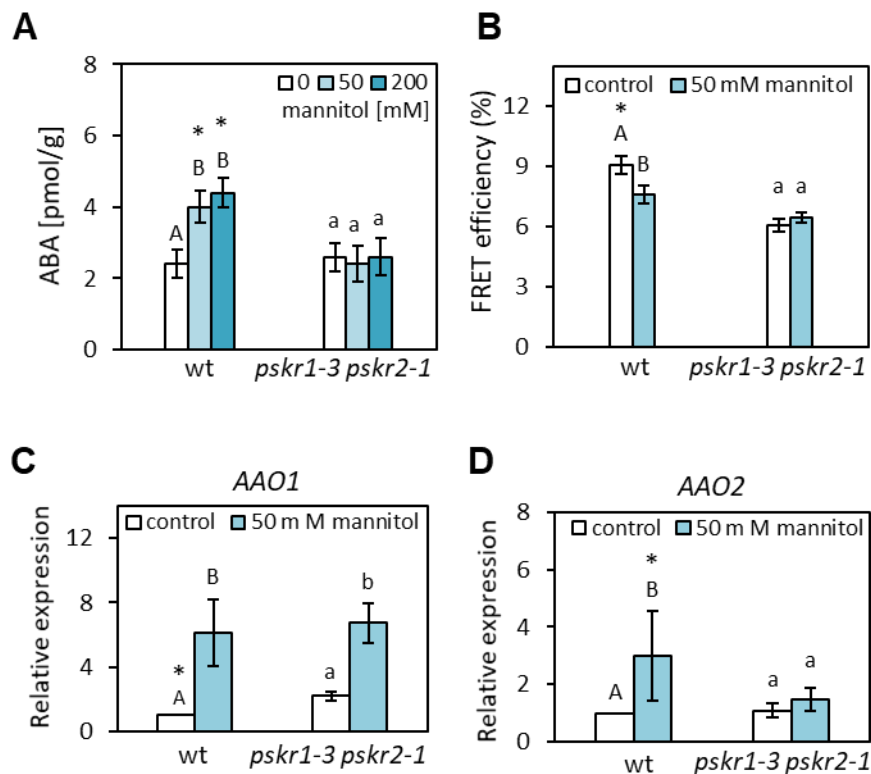


Figure 8. Mannitol-induced ABA accumulation in the shoot is PSKR-dependent.

(A) Four-day-old wild type and *pskr1-3 pskr2-1* seedlings were transferred to 0 mM, 50 mM or 200 mM mannitol and ABA levels in the shoot were determined after seven days. Different capital and minor letters indicate statistically significant differences between treatments (Kruskal-Wallis, Tukey's test, $P < 0.05$, 5 biological replicates). Asterisks indicate significant differences between genotypes per

treatment (Mann-Whitney test, $P < 0.05$, $n = 6$). **(B)** ABA levels in the first true leaf were compared by photobleaching-based FRET analysis in wild type and *pskr1-3 pskr2-1* seedlings treated as in **A**. Decreased FRET efficiency indicates elevated ABA levels. Different capital and minor letters indicate significantly different values between treatments and asterisk indicate significant differences between genotypes for a specific treatment (Mann-Whitney test, $P < 0.05$, $n \geq 142$, 3 independent experiments). **(C, D)** Transcript of the ABA synthesis genes *AAO1* and *AAO2* were determined by RT-qPCR in true leaves of 4-day-old seedlings transferred to mannitol for another 3 days as indicated. Significantly different values for wt and *pskr1-3 pskr2-1* are represented by capital (one-way ANOVA with Tukey's test, $P < 0.05$, $n = 6$) and minor letters (Mann-Whitney test, $P < 0.05$, $n = 6$). Asterisks indicate significant differences between genotypes at given treatment (Mann-Whitney test, $P < 0.05$, $n = 6$).

To verify a PSKR-dependent ABA accumulation in the shoot, we introduced the ABA sensor ABAleon2.1 (Waadt et al. 2014) into the *pskr1-3 pskr2-1* background. Photobleaching-based FRET analysis (Supplemental Fig. S8) revealed a decreased FRET efficiency, reporting elevated ABA in wild type but not in *pskr1-3 pskr2-1* in response to mannitol (Fig. 8B). The difference in absolute FRET efficiency between genotypes may be owed to the fact that the lines were transformed rather than introgressed.

NCED3 is an ABA-biosynthetic enzyme that is upregulated in water-stressed leaves (Iuchi et al., 2001; Endo et al., 2008). We analyzed expression of *NCED3*, *NCED5* and *NCED9*, but found no significant differences in shoots of wild type and *pskr1-3 pskr2-1* seedlings exposed to mannitol (Supplemental Fig. S9). We next analyzed *AAO1* and *AAO2*. *AAO1* and *AAO2* enzymes catalyze the conversion of abscisic aldehyde to ABA. *AAO1* transcript levels were significantly higher in *pskr1-3 pskr2-1* than wild type and were upregulated in both genotypes by mannitol to the same level (Fig. 8C). By contrast, *AAO2* was upregulated significantly by mannitol in wild type but not *pskr1-3 pskr2-1* (Fig. 8D) which may contribute to the lower ABA level observed under osmotic stress.

Apart from synthesis, ABA levels depend on transient in-/activation and on degradation. ABA is inactivated to ABA-glucosyl ester (ABA-GE) by glucosyl transferases UGT71B6-B8 (Priest et al., 2006) (Supplemental Figure S9A). Of these, *UGT71B6* is induced by mannitol in wild type and hyperinduced by mannitol in *pskr1-3 pskr2-1*, suggesting that loss of PSKR signaling favors ABA inactivation under

mannitol stress. No genotype-dependent differences were observed in response to ABA.

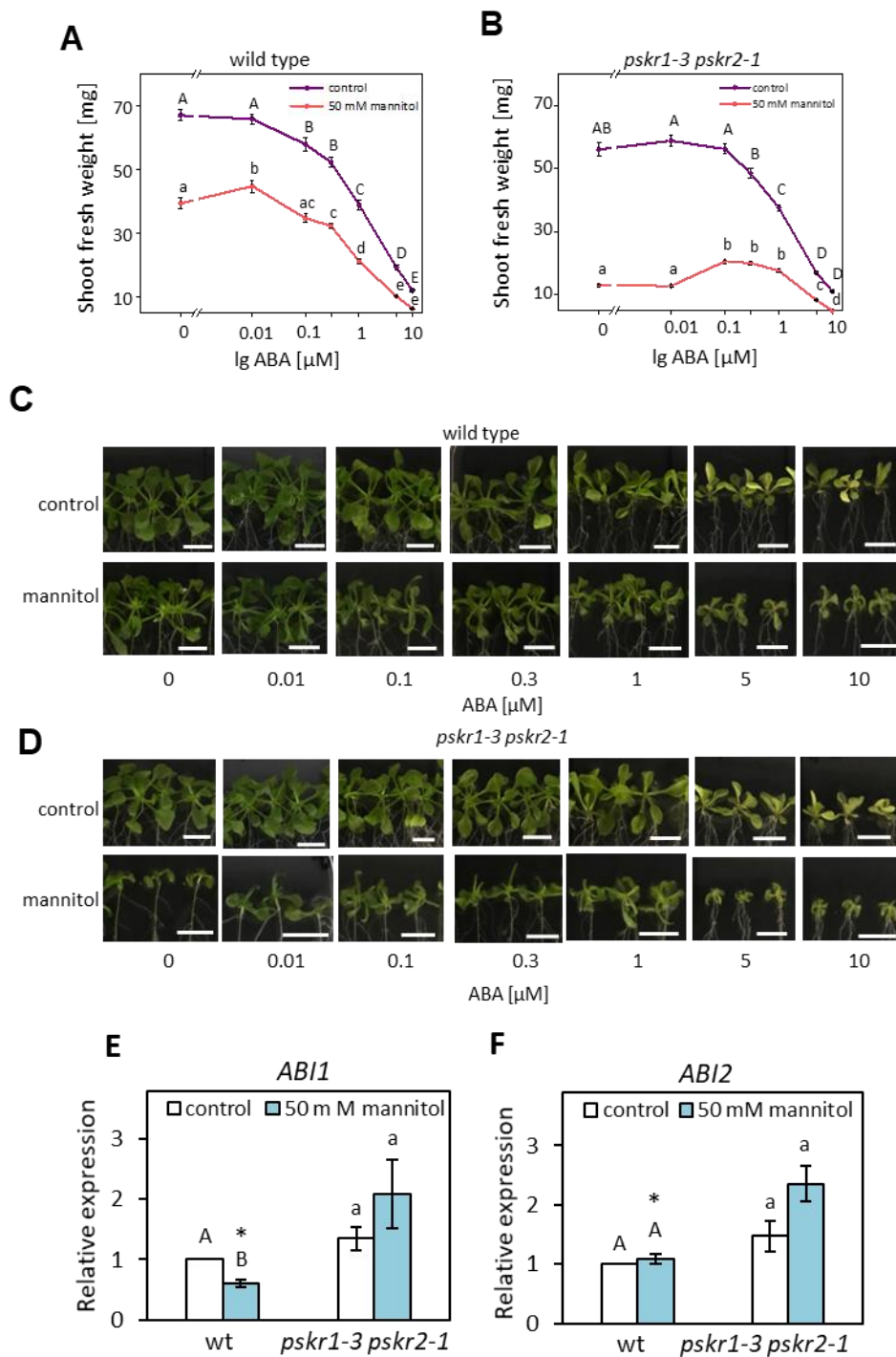


Figure 9. PSKR and ABA pathways partially interact.

(A, B) Shoot fresh weights of wild type and *pskr1-3 pskr2-1* seedlings that were transferred after four days to plates containing ABA and mannitol as indicated were determined after two weeks (Kruskal-Wallis, Tukey's test, $P < 0.05$; $n = 36$). (C, D) Phenotypes of seedlings analyzed in A, B. (E, F) RT-qPCR

analysis of the ABA signalling genes *ABI1* and *ABI2* in true leaves of four-day-old seedlings grown on mannitol for another three days. Significantly different values for wild type and *pskr1-3 pskr2-1* are represented by capital and minor letters (Mann-Whitney test, $P < 0.05$, $n = 6$). Asterisks indicate significant differences between genotypes at a given treatment (Mann-Whitney test, $P < 0.05$, $n = 6$).

Release of ABA from ABA-GE is catalyzed by two ABA glucosidases, BG1 and BG2 (Xu et al., 2012). Transcripts of *BG1* were induced by ABA but not mannitol whereas *BG2* was not regulated. No differences in response to mannitol or ABA were observed between wild type and *pskr1-3 pskr2-1* (Supplemental Figure S10). *CYP707A1-4* genes code for ABA 8'-hydroxylases that degrade ABA to phaseic acid (Kushiro et al., 2004; Saito et al., 2004; Okamoto et al., 2006). *CYP707A1* transcript levels were higher in *pskr1-3 pskr2-1* than in wild type exposed to mannitol possibly indicating enhanced ABA degradation in the mutant under osmotic stress (Supplemental Figure S11). In conclusion, the findings revealed crosstalk between PSKR signaling and ABA metabolism and suggest that PSKR signaling promotes expression of genes that favor ABA accumulation. These observations are in accordance with the finding that PSKR signaling is needed to enhance ABA levels in response to mannitol.

We next explored whether the inability of *pskr1-3 pskr2-1* seedling shoots to accumulate ABA under osmotic stress could be complemented by exogenous ABA. A dose-response analysis showed that ABA at 0.1 μM and higher inhibited shoot growth in wild type under control conditions whereas *pskr1-3 pskr2-1* seedling growth was inhibited at 0.3 μM ABA and higher (Fig. 9A, B, C and D). In the presence of mannitol, shoot growth was promoted at 0.01 μM ABA in wild type and at 0.1 and 1 μM ABA in *pskr1-3 pskr2-1* seedlings indicating that low levels of ABA promote shoot growth under osmotic stress. The need for higher ABA required to promote shoot growth in *pskr1-3 pskr2-1* seedlings may be explained by a lower endogenous ABA content fostering the idea that PSKR promotes growth in part by increasing ABA in response to mannitol. It should be noted, however, that growth inhibition by mannitol was only partially alleviated by ABA in *pskr1-3 pskr2-1* suggesting that other levels of regulation exist.

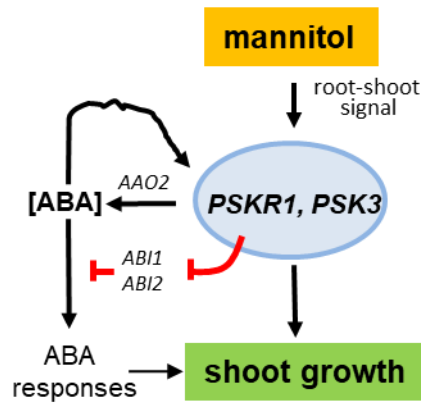


Figure 10. Model of shoot growth control during mannitol stress by PSKR1 and ABA.

Mannitol induces *PSKR1* and *PSK3* gene expression and PSKR signaling promotes ABA synthesis, through upregulation of the ABA synthesis gene *AAO2*, and ABA signaling, through repression of *ABI1* and *ABI2*. In mutants that lack PSKRs, reduced ABA in mannitol-stressed shoots contributes to shoot growth inhibition. Growth under mannitol stress is further promoted by ABA-independent PSKR signaling.

Finally, we analyzed a possible interaction between PSKR signaling and ABA signaling by using two marker genes of ABA signaling, ABA-INSENSITIVE 1 (*ABI1*) and *ABI2*, that act as negative regulators of ABA signaling and have been implicated in stress acclimation (Ludwików, 2015). Under mannitol, *pskr1-3 pskr2-1* seedlings accumulated higher *ABI1* and *ABI2* transcript levels than wild type whereas no difference was observed at unstressed conditions (Fig. 9E, F) indicating that ABA signaling under osmotic stress may be repressed in *pskr1-3 pskr2-1*. In conclusion, several lines of evidence suggest a role for PSKR signaling in plant acclimation to osmotic stress through crosstalk with ABA metabolism and signaling at the transcriptional level (Figure 10).

3.5 DISCUSSION

3.5.1 PSK receptor signaling mediates osmotic stress-induced inhibition of cotyledon development

Seed germination and seedling establishment are stringently controlled by environmental conditions to ensure seedling survival. In particular, water availability is a requirement for seedling establishment. Under water-limited conditions, ABA acts as a hormonal signal that prevents germination and inhibits seedling growth. PSK signaling was previously shown to promote organ growth through cell expansion (Kutschmar et al., 2009; Hartmann et al., 2013). Under osmotic stress imposed by mannitol treatment, PSK receptor signaling inhibited postgermination seedling development while the PSK receptor null mutant *pskr1-3 pskr2-1* showed enhanced cotyledon greening and seedling growth. Seedling development is likewise inhibited by ABA. Both, mannitol and ABA-dependent inhibition are, to a large part, dependent on PSKR signaling. More so, seedlings overexpressing PSKR1 were hypersensitive to ABA and to mannitol suggesting that PSKRs mediate growth adaptation in response to osmotic stress. Inhibition of cotyledon greening by PSKR signaling is a novel finding as PSKRs were previously described as growth-promoting receptors. The current observation thus extends our view on growth regulation by PSKRs and reveals that PSKR signaling inhibits early seedling growth under unfavorable environmental conditions. By contrast, postgermination shoot growth under water-limiting conditions was promoted by PSKR1 signaling. PSKR-dependent inhibition of growth at the early seedling stage and promotion of postgermination shoot growth under water-limiting conditions suggests that developmental arrest of seedlings and maintenance of vegetative growth of plants are best choices to cope with water shortage and that PSKR signaling can be wired accordingly.

3.5.2 PSKRs support shoot growth during osmotic stress

A recent report showed that PSK precursor processing via SBT3.8 subtilase improves root growth and drought stress resistance in *Arabidopsis* (Stührwohldt et al., 2021). Drought stress experiments described here revealed that PSKR signaling is required to maintain postgermination shoot growth, and photosynthetic efficiency to counteract drought-induced senescence. It was previously reported that PSKR1 delays senescence after bolting and provides cellular longevity and potential for growth (Matsubayashi et al., 2006). This ability appears particularly important during water limiting conditions. A crucial role of PSKR1 in promoting osmotic stress resistance of the shoot was revealed in single receptor gene knockout lines. *pskr1-3* seedlings displayed the same growth retardation as seedlings of the double receptor knock out line *pskr1-3 pskr2-1* whereas *pskr2-1* seedlings had a wild type phenotype.

Grafting experiments and osmotic stress application to the root showed that shoot growth requires PSKR signaling in the leaves likely induced by a long-distance stress signal transmitted from the roots via the vasculature (Takahashi and Shinozaki, 2019; Takahashi et al., 2020). Whether the peptide PSK participates in long distance signaling cannot be excluded but, clearly, PSKR signaling is neither required for signal synthesis in the root nor for the transmission of the signal from root to shoot. In the leaves, cells communicate via the extracellular signal PSK and the plasma membrane-bound PSKR1 receptor despite of a continuous network of plasmodesmata that enable cell-cell communication. It has been suggested that apoplastic signals allow for signal integration and output coordination (Chivasa and Goodman, 2020). In that light, PSK/PSKR1 signaling appears highly suitable to coordinate leaf growth.

Plants adjust shoot and root growth to limited soil water availability with different sensitivities dependent on the degree and duration of the stress (Deak and Malamy, 2005; Comas et al., 2013; Pierik and Testerink, 2014; Koevoets et al., 2016). Root growth was inhibited at 200 mM mannitol and higher (this study; Stührwohldt et al., 2021) whereas shoot growth was reduced already at 50 mM mannitol supporting the finding that shoot growth is more sensitive to the stress (Claeys et al., 2014). In accordance with a well-adjusted stress management, shoot growth maintenance via PSKR1 signaling was most efficient at low mannitol concentrations providing particularly good protection against mild water stress to the highly sensitive shoot.

3.5.3 PSK precursor and receptor genes are induced in the shoot by mannitol and ABA to promote growth

Plant shoots exposed to mannitol displayed elevated transcript levels of *PSKR1* and of the PSK precursor gene *PSK3*, that were also induced by ABA suggesting that the PSK signal pathway is promoted by osmotic stress signaling through ABA to actively maintain shoot growth. Mannitol and ABA exerted common but also differential control of PSK signaling genes pointing to a fine-tuned regulatory network rather than a linear pathway of growth control. *PSK2* and *PSK4* were induced by ABA but not by mannitol revealing ABA regulation of PSK signaling in a pathway that is unrelated to mannitol-induced osmotic stress. Intricate regulatory loops were revealed by hyperinduction of *PSK1*, *PSK3* and *PSK5* by mannitol in the PSK receptor null background compared to wild type which suggested that PSK signaling feedback-inhibits expression of ligand precursor genes under osmotic stress possibly to balance growth under water-limited conditions. The regulated signaling genes *PSK3* and *PSKR1* were expressed most prominently in young expanding leaves in accordance with their role in driving cell expansion (Hartmann et al., 2013; Ladwig et al., 2015).

3.5.4 ABA homeostasis in osmotically stressed leaves is controlled by PSKR signaling

Mannitol-induced osmotic stress led to an increase of ABA in leaves. The elevation of ABA levels was dependent on PSKR signaling raising the question how PSK signaling controls ABA homeostasis at the molecular level. The steady-state level of active ABA is determined by ABA synthesis, catabolism, inactivation, and remobilization (Cutler and Krochko, 1999; Nambara and Marion-Poll, 2005). NCEDs are key enzymes of ABA synthesis that cleave 9-*cis*-xanthophylls to xanthoxin, a precursor of ABA. Arabidopsis NCED3 was previously described as the major stress-induced *NCED* gene in leaves with *NCED5* and *NCED9* being induced to a minor degree in response to water-deficit (Tan et al., 2003). In our study, *NCED3* was induced by mannitol in wild type and hyperinduced in the *PSKR* null mutant whereas *NCED5* was induced by ABA which favors elevated ABA synthesis in drought-stressed shoots in both genotypes. The final

step in ABA synthesis is catalyzed by AAO that is encoded by two genes in Arabidopsis, *AAO1* and *AAO2* (Seo et al., 2000). *AAO1* was induced by mannitol in wild type and *pskr1-3 pskr2-1* shoots, whereas *AAO2* was induced in wild type but not *pskr1-3 pskr2-1* indicating that at least some of the capacity to synthesize ABA in response to osmotic stress is controlled by *PSKRs*. Similarly, *pskr1-3 pskr2-1* shoots showed hyperinduction of the ABA-conjugating gene *UGT71B6* and downregulation of the ABA-glucose β -glucosidase gene *BG1* in shoots when exposed to mannitol. BGs were previously described as key regulators of osmotic stress resistance (Xu et al., 2012). *BG1* is regulated by miR165/166 and downregulation of miR165/166 resulted in elevated *BG1* expression and in elevated ABA levels (Yan et al., 2016). Taken together, the data show that PSKR signaling impacts expression of genes related to ABA metabolism in response to mannitol. The changes in gene expression suggest that ABA synthesis and release from ABA-glucose may be reduced in the PSK receptor null mutant whereas conjugation of ABA may be favored. This would explain why ABA levels do not increase in osmotically stressed *pskr1-3 pskr2-1* shoots.

In addition to ABA synthesis, ABA signaling may be controlled by *PSKRs*. ABA is perceived by Pyrabactin Resistance/Pyrabactin Resistance-Like/Regulatory Components of ABA Receptor (PYR/PYL/RCAR) receptors. The protein phosphatases 2C (PP2Cs) ABI1 and ABI2 act as PYR/PYL/RCAR-coreceptors that keep downstream SnRK2s in an inactive state in the absence of ABA (Joshi-Saha et al., 2011; Mitula et al., 2015). When PYR/PYL/RCAR receptors bind ABA, the PP2Cs are inactivated leading to the activation of SnRKs that are critical for osmotic stress responses (Boudsocq et al., 2004; Fujii et al., 2011). Expression analysis revealed higher transcript levels of the negative ABA regulator genes *ABI1* and *ABI2* in *pskr1-3 pskr2-1* compared to wild type following mannitol treatment suggesting that *PSKRs* promote not only synthesis but also ABA signaling during osmotic stress.

A particular role of ABA in growth maintenance under water stress conditions was revealed by exogenous ABA. In wild type, ABA promoted growth at 0.01 μ M whereas the growth-promoting concentrations were shifted to 0.1-1 μ M ABA in *pskr1-3 pskr2-1* in seedlings. A requirement for a higher concentration of ABA needed to promote growth is in accordance with lower endogenous ABA levels in the mutant. The relative growth promoting effect of ABA under mannitol stress was higher in the mutant than in wild type but ABA did not fully restore the dwarf phenotype of the mutant at any

concentration indicating that additional pathways are misregulated in *pskr1-3 pskr2-1* seedlings that ensure growth under water-limiting conditions.

In summary, PSKR signaling controls adaptation of the shoot to drought stress by maintaining growth under water-limiting conditions and by maintaining photosynthetic activity. PSKR signaling is not required for long-distance signaling of osmotic stress from the root to the shoot but rather promotes ABA levels and possibly ABA signaling in the shoot. Our study reveals a role of PSKR signaling in balancing shoot growth and water-stress responses.

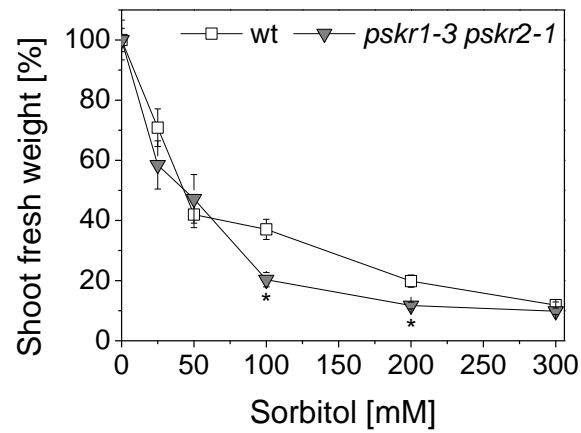
3.6 ACKNOWLEDGEMENTS

Hagen Stellmach (IPB Halle) is acknowledged for helping in ABA measurements and we thank Prof. Wolfgang Bilger (University of Kiel) for help with PAM imaging. We are grateful to Rainer Waadt and Prof. Karin Schumacher (University Heidelberg) for providing the *ABAleon2.1* line and the plasmid *barII-UT-ABAleon2.1*. This work was funded by the Deutsche Forschungsgemeinschaft through grants SA495/8-1 and SA495/8-2.

3.7 AUTHOR CONTRIBUTIONS

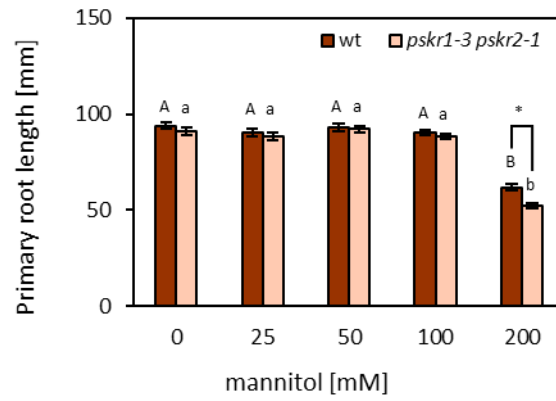
The present study was designed by Margret Sauter, Martina Schönhof and me. Bettina Hause performed ABA measurements and I analysed the data. GUS, germination, and cotyledon greening assays were carried out and analysed by Martina Schönhof. qPCR experiments were performed by me and Martina Schönhof. The rest of the experiments were performed and analysed by me. Margret Sauter conceived and wrote the manuscript along with me with contributions from Bettina Hause.

3.8 SUPPLEMENTARY MATERIAL



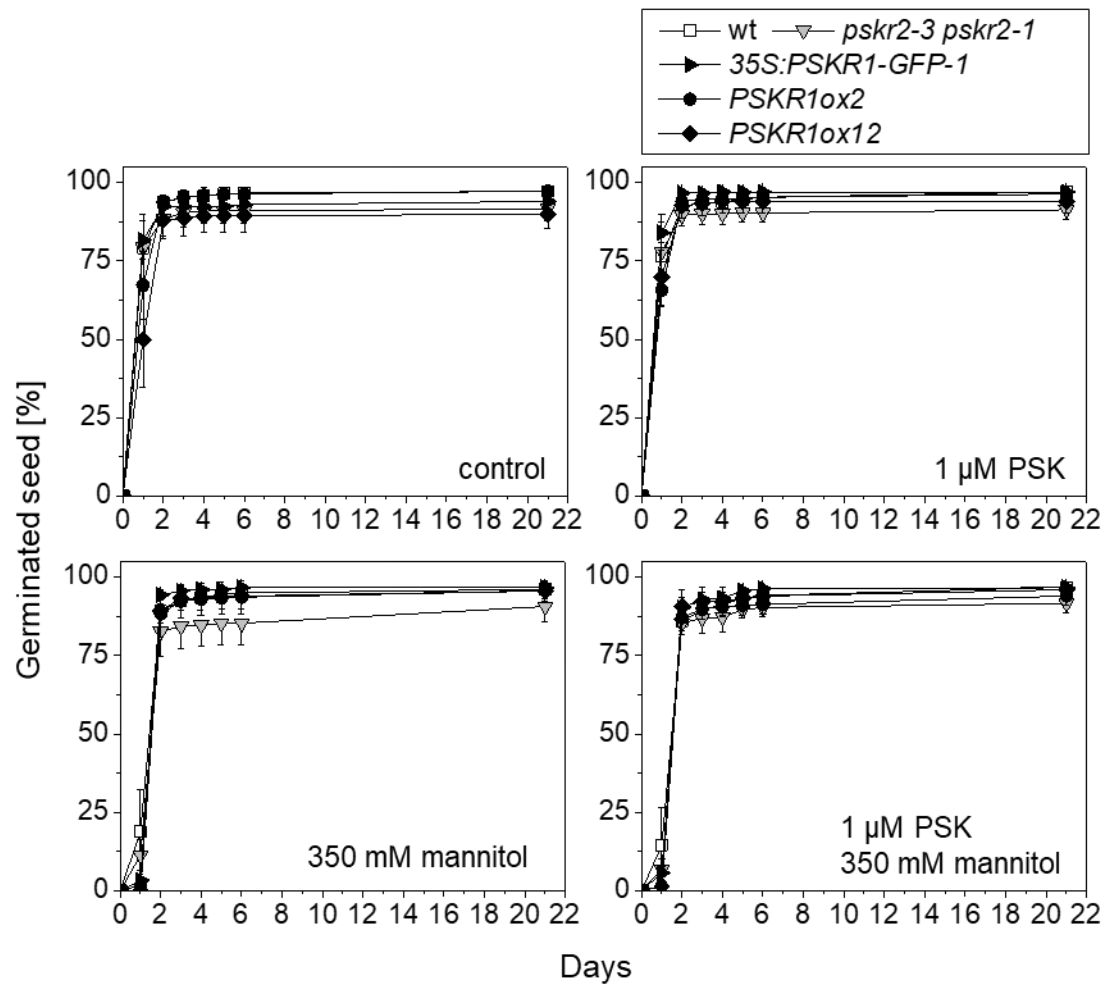
Supplemental Figure S1. PSKRs confer enhanced resistance to sorbitol.

Four-day-old seedlings were transferred to medium supplemented with different sorbitol concentrations and analyzed after another 3 weeks. Mean \pm SE of shoot fresh weight of PSK receptor double knockout mutants on sorbitol are given in percent with values under control conditions set to 100%. Asterisks indicate significant differences between genotypes (Mann-Whitney test, $p < 0.05$, $n \geq 18$, 3 independent experiments).



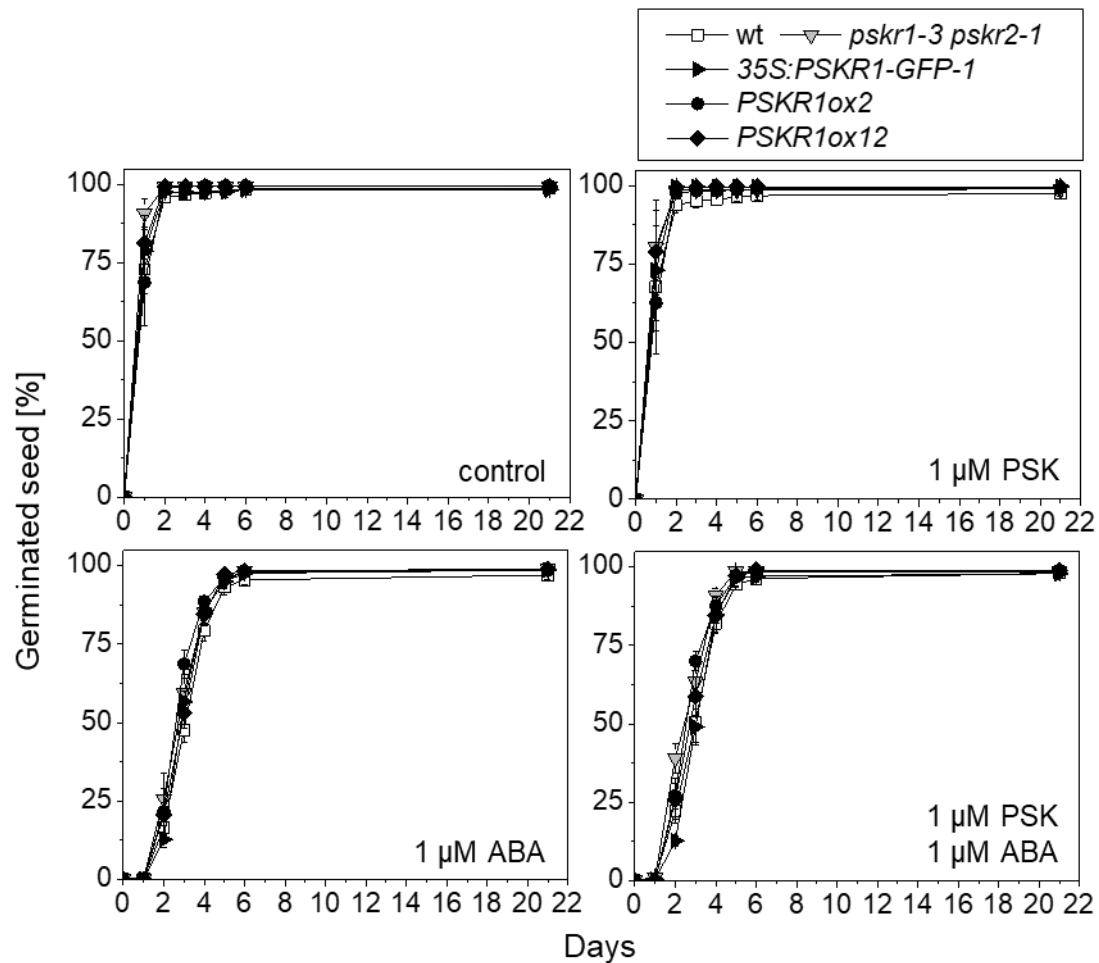
Supplemental Figure S2. PSK receptor signaling is required to maintain root growth under severe osmotic stress.

Four-day-old wild type and *pskr1-3 pskr2-1* seedlings were transferred to media containing mannitol as indicated. Primary root lengths of seedlings grown for 7 days after transfer. Significantly different values within a genotype are denoted by different letters (Kruskal-Wallis, Tukey's, test, $p < 0.05$, $n \geq 36$, 3 independent experiments). Asterisk indicates significant differences between genotypes (Mann-Whitney test, $p < 0.05$).



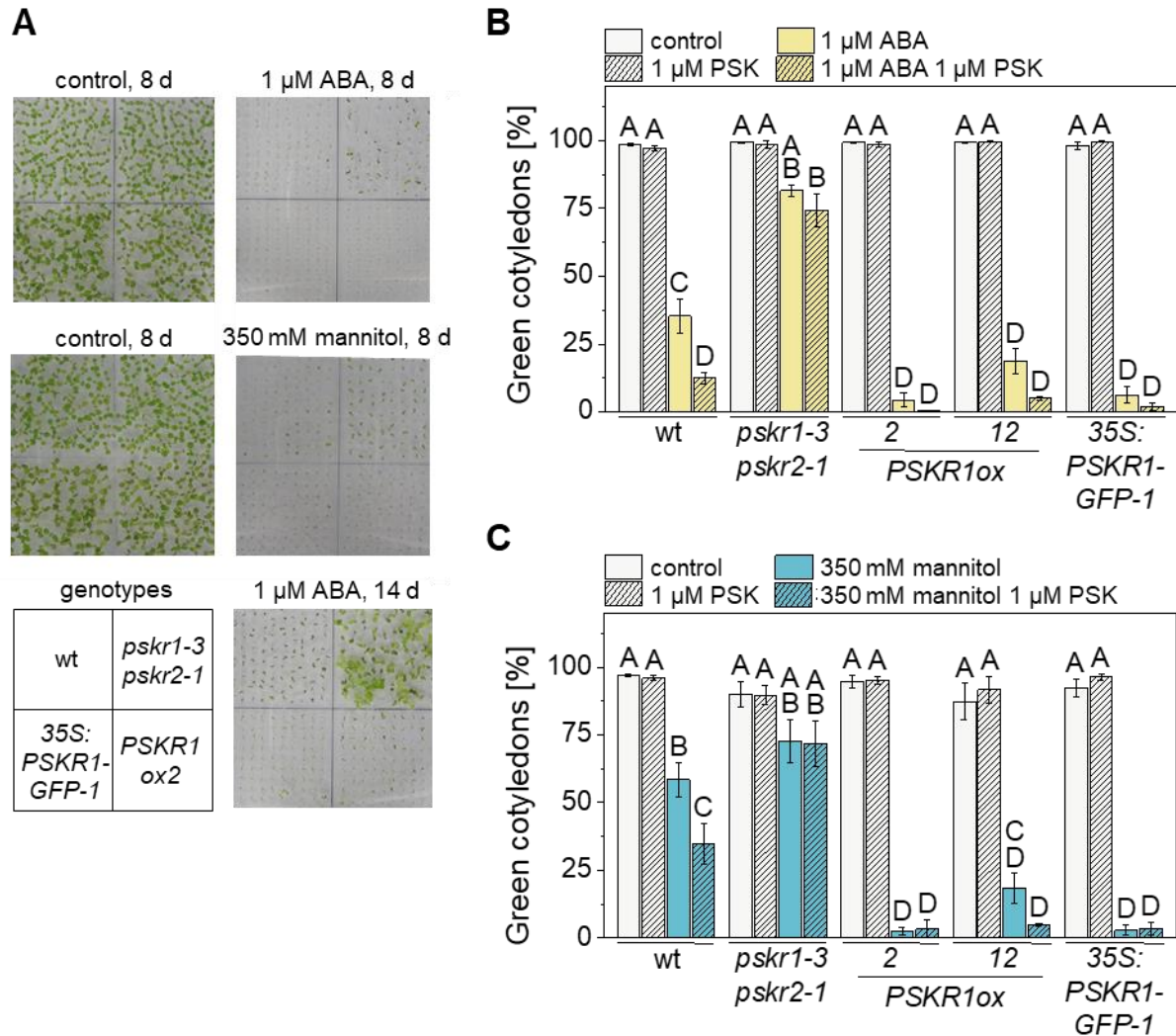
Supplemental Figure S3. Inhibition of seed germination by mannitol is not dependent on PSK receptor signaling.

Germination rates were determined in response to 1 μ M PSK and 350 mM mannitol. Values are means (\pm SE) from three independent biological experiments each with 100 seeds analyzed. Seeds with a visible radicle were scored as germinated.



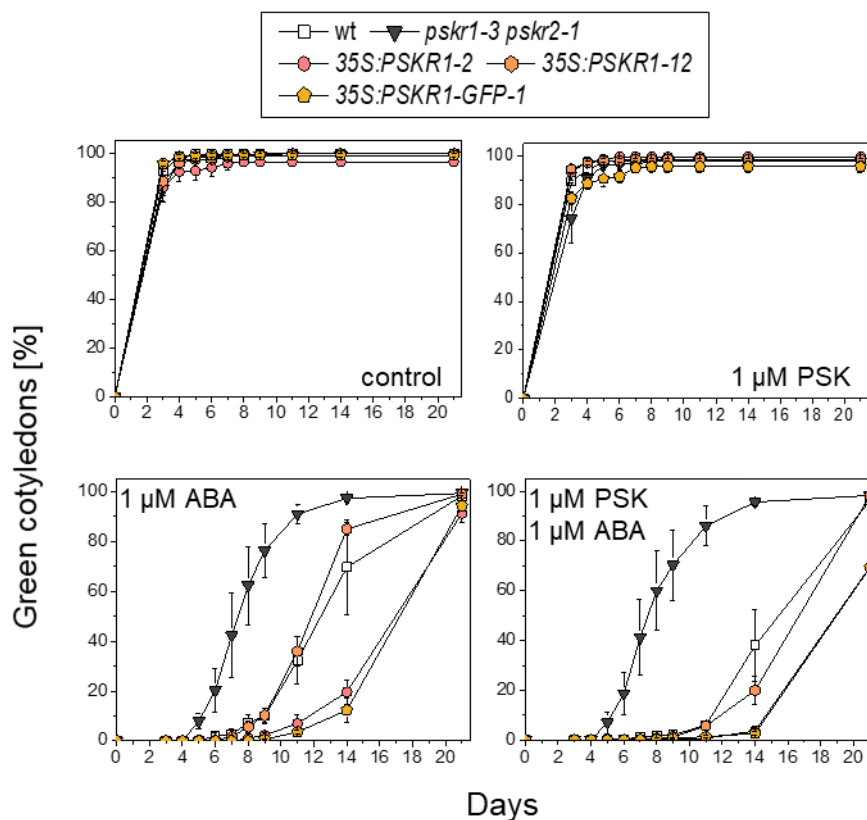
Supplemental Figure S4. Inhibition of seed germination by ABA is not dependent on PSK receptor signaling.

Germination rates were determined in response to 1 μ M PSK and 1 μ M ABA. Values are means (\pm SE) from three independent biological experiments each with 100 seeds analyzed. Seeds with a visible radicle were scored as germinated.



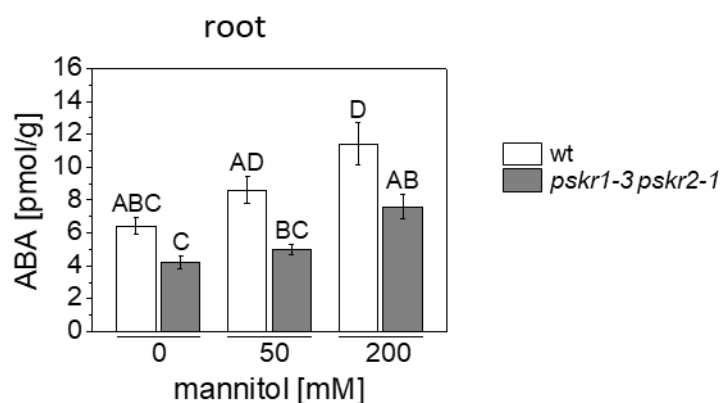
Supplemental Figure S5. Repression of early seedling development by ABA or mannitol is mediated by PSK receptor signaling.

(A) Cotyledon greening of wild type, *pskr1-3 pskr2-1*, and *PSKR1* overexpressing seedlings exposed to 1 μM ABA or 350 mM mannitol or no treatment for the times indicated. The scheme on the lower left side indicates the genotypes grown on each plate. (B) Cotyledon greening of 8-day-old wild type seedlings, *PSKR* knockout and of three independent *PSKR1* overexpressing lines treated with 1 μM PSK, 1 μM ABA, or both. Data are means ±SE of 3 independent experiments each evaluating 100 seeds per genotype. Different letters indicate significantly different values (one-way ANOVA, Tukey's test, $p < 0.05$). (C) Cotyledon greening of 8-day-old wild type seedlings, *PSKR* knockout and of three independent *PSKR1* overexpressing lines treated with 1 μM PSK, 350 mM mannitol, or both. Data are means ±SE of 3 independent experiments each evaluating 100 seeds per genotype. Different letters indicate significantly different values (one-way ANOVA, Tukey's test, $p < 0.05$).



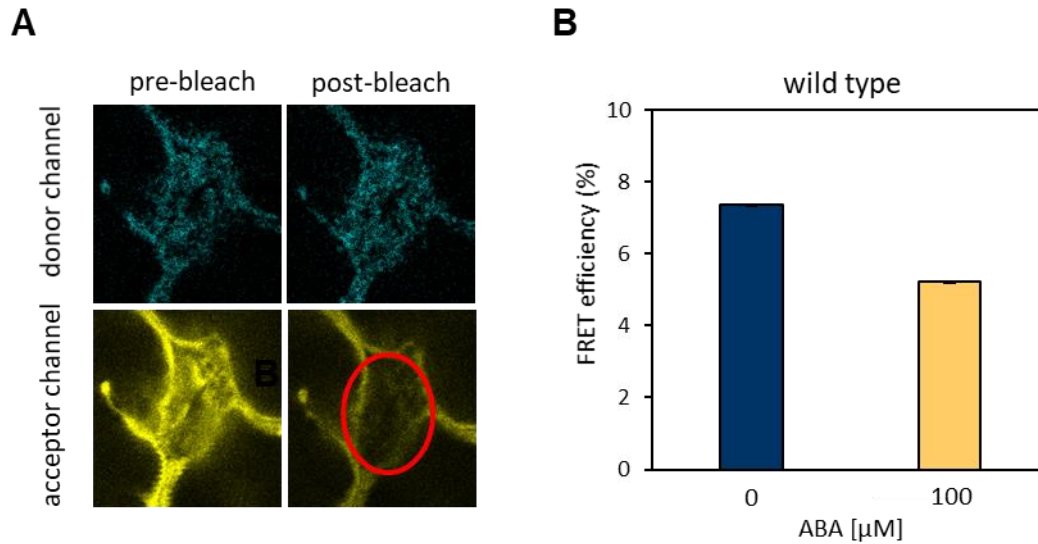
Supplemental Figure S6: Inhibition of cotyledon greening by ABA is partially dependent on PSKR signaling.

Time course analysis of cotyledon greening in response to ABA and PSK. Values are means \pm SE of three independent biological experiments, each evaluating 100 seedlings. Seedlings with green expanded cotyledons were scored.



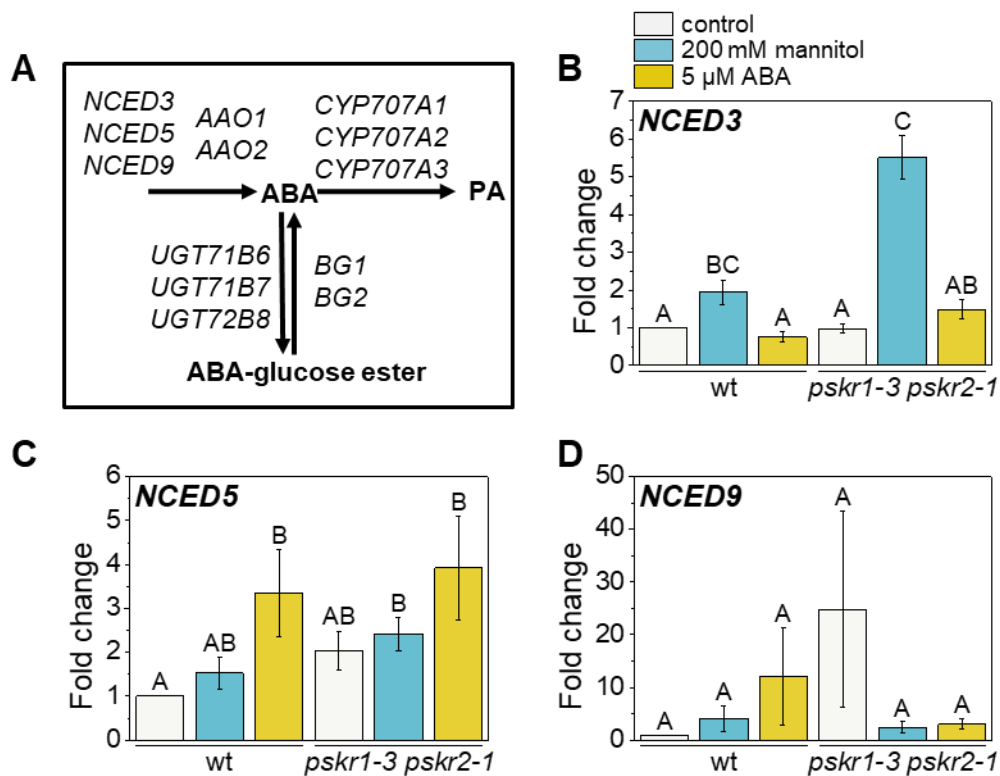
Supplemental Figure S7. ABA accumulation under mannitol stress in roots.

Four-day-old wild type and *pskr1-3 pskr2-1* seedlings were transferred to 0 mM, 50 mM or 200 mM mannitol and ABA levels in the root were determined after 7 days. Different letters indicate statistically significant differences (Kruskal-Wallis, Tukey's test, $p < 0.05$, 5 biological replicates).



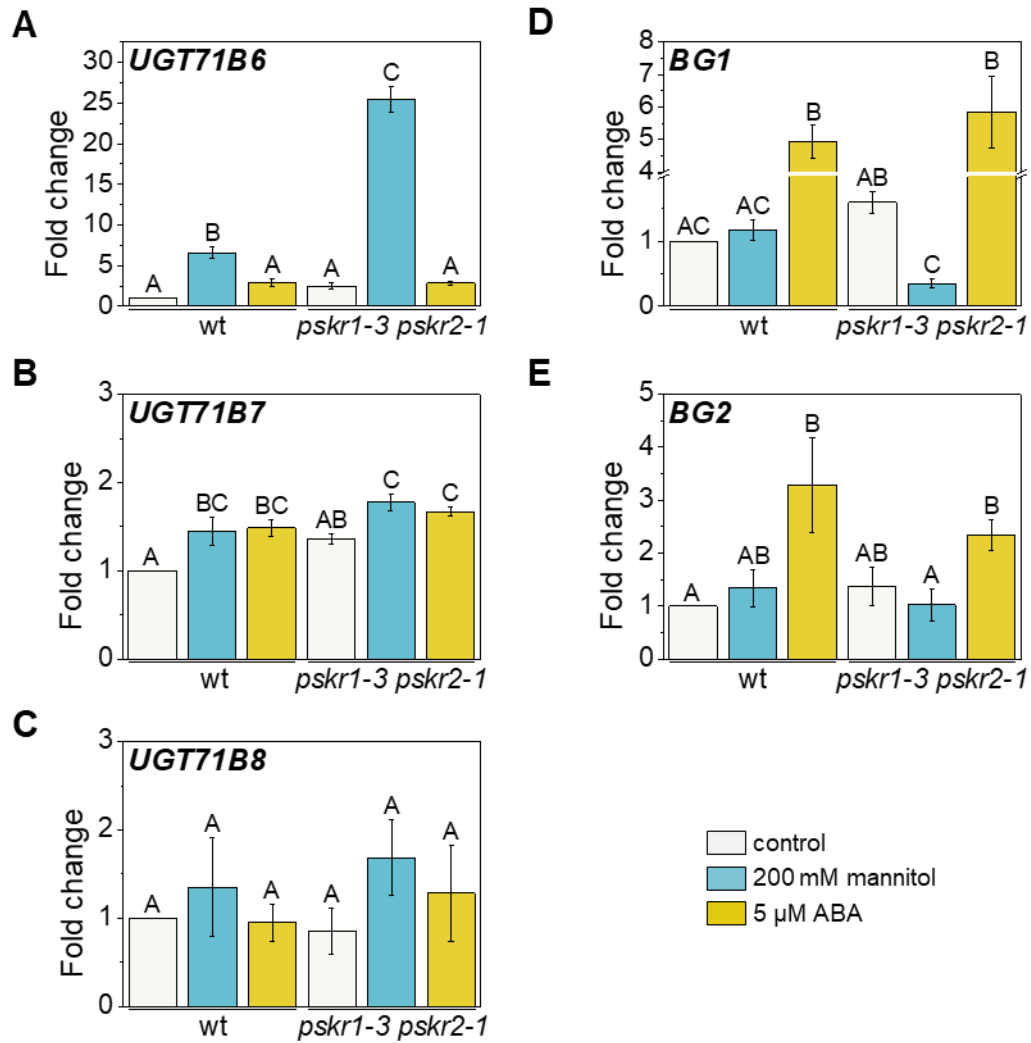
Supplemental Figure S8. Differences in ABA concentration were measured using the FRET-based ABA sensor ABAlleon.

(A) Acceptor photobleaching FRET in wild type Arabidopsis leaves co-expressing the mTurquoise (donor) and cpVenus173 (acceptor) construct. The images were excited sequentially at 458 and 514 nm and emission recorded with adequate filter sets. The region of the cell indicated by a red circle was photobleached at 514 nm for 10 sec. Post-bleach images were captured at 458 nm excitation. FRET is visualized as an increase in mTurquoise fluorescence following cpVenus173 photobleaching, which shows a distinct increase in donor post-bleaching; scale bar = 20 μ m. **(B)** Seven-day-old wild type seedlings were transferred to media with or without 100 μ M ABA and were analyzed after 1 day. FRET efficiency of the ABA sensor ABAlleon was measured using acceptor photobleaching.



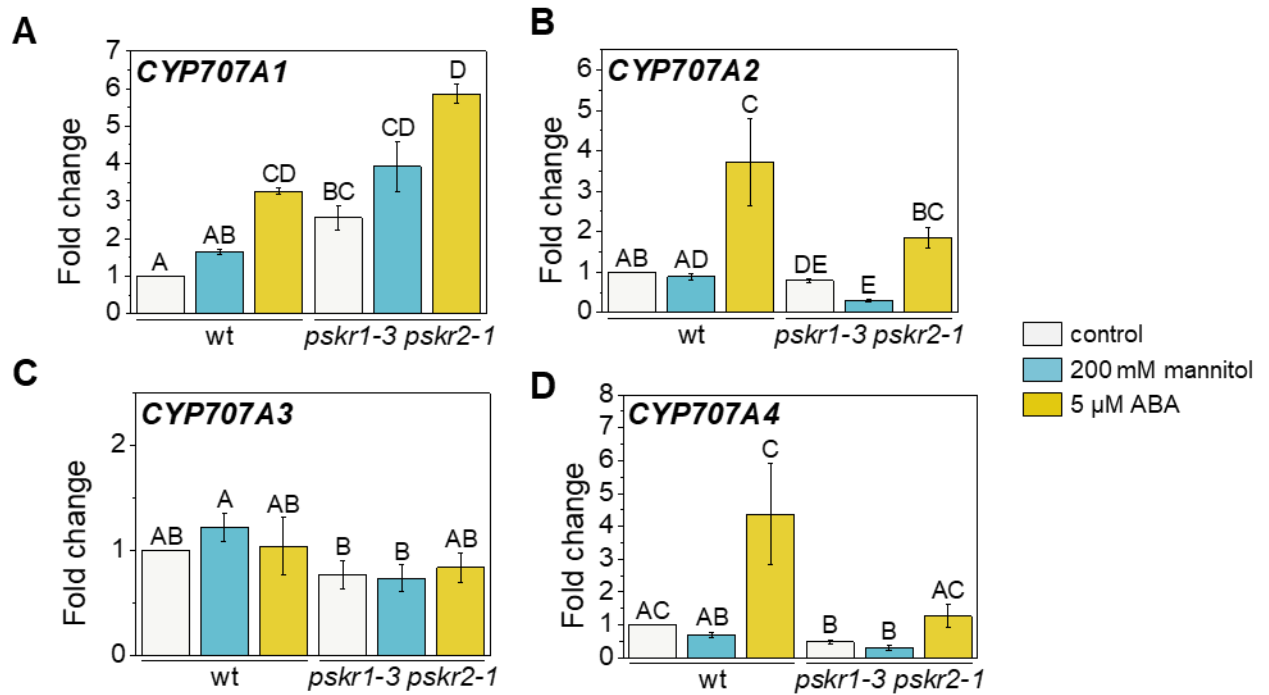
Supplemental Figure S9. Regulation of *NCED* expression by mannitol and ABA.

Seven-day-old wild type and *pskr1-3 pskr2-1* seedlings were exposed to 200 mM mannitol or 5 μ M ABA for 24 h to analyze relative *NCED3*, 5 and 9 transcript levels in true leaves. **(A)** Overview of genes encoding for enzymes of ABA synthesis (*NCEDs*, *AAOs*), degradation (*CYP707As*), inactivation (*UGT71Bs*) and mobilization (*BGs*). PA=phaseic acid. **(B-D)** Changes in *NCED3*, *NCED5* and *NCED9* transcript levels in response to mannitol, ABA and genotype. Values are means (\pm SE) with different letters indicating significant differences (Kruskal-Wallis, $p < 0.05$; $n=6$, 3 biological replicates).



Supplemental Figure S10. Regulation of *UGT71B* and *BG* transcripts by mannitol, ABA and PSKR signaling.

Seven-day-old wild type and *pskr1-3 pskr2-1* seedlings were exposed to 200 mM mannitol or 5 μ M ABA for 24 h for RT-qPCR analysis in true leaves. Values are means (\pm SE) of 3 biological replicates with different letters indicating significant differences. (A-C) Relative mRNA levels of *UGT71B6-8* in response to genotype and treatment (Kruskal-Wallis, Tukey's test, $p < 0.05$). (D, E) Relative mRNA levels of *BG1* and *2* in response to genotype and treatment (one-way ANOVA, Tukey's test, $p < 0.05$).



Supplemental Figure S11. Regulation of *CYP707A* ABA-8'-hydroxylase transcripts by mannitol, ABA and PSKR signaling.

Seven-day-old wild type and *pskr1-3 pskr2-1* seedlings were exposed to 200 mM mannitol or 5 μ M ABA for 1 day and analyze by RT-qPCR for gene expression in true leaves. (A-D) Relative *CYP707A1-4* transcript levels in response to genotype and treatment (Kruskal-Wallis, Tukey's test, $p < 0.05$, $n=6$, 3 biological replicates). Values are means (\pm SE) with different letters indicating significant differences (Kruskal-Wallis, Tukey's test, $p < 0.05$, $n=6$; 3 biological replicates).

Supplemental Table 1. Primer sequences used for qRT-PCR. for: forward, rev comp: reverse complement.

Gene name	Accession number	Orientation	Sequence 5' - 3'
<i>ACT2</i>	At3g18780	for	ACATTCCAGCAGATGTGGATCTC
		rev comp	GATCCCATTCATAAAACCCAGC
<i>GAPC1</i>	At3g04120	for	GATTCTACAATGGCTGACAAGAAGA
		rev comp	ATGAAGGGGTCGTTGACAGC
<i>PSKR1</i>	At2g02220	for	AGCGAGGTTTTCGATCCGTT
		rev comp	CTGTTGAGTCGTTGGCCTCT
<i>PSKR2</i>	At5g53890	for	GTTCTGCTCAAGAGGAGATCA
		rev comp	CCGGTGCCCGTGTTGTAT
<i>PSK1</i>	At1g13590	for	CCATCTCCACACACATGA
		rev comp	TCGGTGTGAGCAGCTACTGT
<i>PSK2</i>	At2g22860	for	ACTGCTGCCGATCCATGTAA
		rev comp	GCGACCAAAGTCCTCCTCAT
<i>PSK3</i>	At3g44735	for	CTTGTGCCTGGCAGTTCTCT
		rev comp	ACTGAGTCCTTCCACTGATG
<i>PSK4</i>	At3g49780	for	GACAACCACCGCTTTGTCCA
		rev comp	GGTGTGAAGAACAAGGCTTCG
<i>PSK5</i>	At5g65870	for	CTCTGCTCCACGCTAACACA
		rev comp	TCTTCTCCAACACCTTCACAGA
<i>CYP707A1</i>	At4g19230	for	GAACCACTCGTGTCTGG
		rev comp	GTTTTGGGAAGCGCAATG
<i>CYP707A2</i>	At2g29090	for	GGATCAAAAACGCAACGGCT
		rev comp	GCTCCCTGGAGACTTCTTGG
<i>CYP707A3</i>	At5g45340	for	CCGTAGCTCCTCCACGAAAC
		rev comp	GGGCTCGAGATCATCACACAT
<i>CYP707A4</i>	At3g19270	for	CGAAGCCGAATACATTATGCC
		rev comp	TCCCTTCACTTCCATCGGAAA
<i>AAO1</i>	At5g20960	for	GCAAACAGGAGGACCTGTGA
		rev comp	TTACTTCAACCTCGCTCGC
<i>AAO2</i>	At3g43600	for	CTGCGGTGAAGGAGGATGT
		rev comp	ACGCTGCAGAGGAGTGTAAAG
<i>ABI1</i>	At4g26080	for	CATGTCGAGATCCATTGGCGA
		rev comp	TCACACGCTTCTTCATCCGT
<i>ABI2</i>	At5g57050	for	AGATCCATTGGCGATAGATACCTT
		rev comp	CCAAATCGGCACACTTCTTCGT
<i>BG1</i>	At1g52400	for	TGCCGAGAATGGATACGGAG
		rev comp	TTGTCCTTGCAAATGGCGTC
<i>BG2</i>	At2g32860	for	ACTGTAAAAAGGTCGAGGGTGG
		rev comp	TGGTACTCGAGGGATCGTCT

4

Functional analysis of receptor domains of phytosulfokine receptors PSKR1 and PSKR2

Komathy Rajamanickam, Margret Sauter

Plant Developmental Biology and Plant Physiology, University of Kiel,
Kiel, Germany

4.1 ABSTRACT

PSK is a plant peptide growth hormone which is perceived by the leucine-rich repeat receptor-like kinases (LRR-RLK) PSKR1 and PSKR2 in *Arabidopsis thaliana*. Our recent data revealed that PSK/PSKR signaling is important for shoot growth maintenance and is predominantly mediated by PSKR1, but not PSKR2. It is, however, unknown why PSKR2 is ineffective. Likewise, another report on pathogen stress showed that PSK signaling mediated by PSKR1 attenuates pattern-triggered immunity (PTI) and stimulates plant growth but no functionality of PSKR2 has been demonstrated in this context. Both receptors are structurally similar sharing 48.6% amino acid identity, facilitating the exploration of PSKR2 protein functionality using a chimeric receptor approach. We generated chimeras of PSKRs in which we switched the promoters, the LRR and the kinase domain of *PSKR1* and *PSKR2* and expressed the hybrid receptor genes in the receptor-deficient *pskr1-3 pskr2-1* background. Our results based on functional analysis of the chimeras reveal that all the PSKR chimeras expressed under the control of the *PSKR1* promoter remain to be functional under osmotic and pathogen stress conditions indicating that the PSKR2 domains functionality is dependent on the promoter activity. Furthermore, an *in-silico* promoter analysis revealed that the *PSKR2* promoter may lack important regulatory regions or elements required for stress responses. We furthermore show that the LRR and kinase domains of PSKR1 slightly improved PSKR activity in comparison to PSKR2 domains depending on the nature and extent of the stress applied.

4.2 INTRODUCTION

Plant peptides are now recognized as signaling molecules that mediate long-range or short distance cell-to-cell signaling (Oh et al., 2018; Stührwohldt and Schaller, 2019) thereby participating in various plant processes including growth and development (Ghorbani et al., 2015; Tavormina et al., 2015), abiotic (Takahashi and Shinozaki, 2019) and biotic stress responses (Hu et al., 2018; Liu et al., 2018). One among such peptides is phytosulfokine (PSK).

PSK is the first secreted and post-translationally modified peptide hormone identified in plants (Matsubayashi and Sakagami, 1996; Kaufmann and Sauter, 2019). It is a disulfated pentapeptide (YIYTQ) that is biologically active at nanomolar concentrations (Stührwohldt et al., 2011; Sauter 2015) and was initially discovered as a growth factor that promotes cell proliferation in *Asparagus officinalis* cell cultures (Matsubayashi and Sakagami, 1996). PSK interaction with a receptor protein was first identified in *Daucus carota* (DcPSKR) (Matsubayashi et al., 2002) and is conserved among different plant species (Hanai et al., 2000; Kaufmann and Sauter, 2019). In *Arabidopsis thaliana*, two orthologues of DcPSKR were identified: PSKR1 and PSKR2 (Matsubayashi et al., 2006; Amano et al., 2007). PSK/PSKRs ligand-receptor pair identification helped to determine numerous physiological functions of PSK signaling in plants (Wheeler and Irving, 2010; Matsubayashi, 2014; Sauter, 2015).

In *Arabidopsis*, PSK signaling promotes root growth and hypocotyl elongation through cell expansion (Kutschmar et al., 2009; Stührwohldt et al., 2011). In *Medicago truncatula*, PSK promotes root growth by repressing the expression of pectin methylesterase inhibitor (PMEI) genes (Yu et al., 2020). PSK has also been shown to promote primary root growth and adventitious root formation in *Cunninghamia lanceolata* (Wu et al., 2019). Overexpression of *GhPSK* enhances fiber elongation in cotton (Han et al., 2014a). Besides promoting growth, PSK also participates in plant reproduction by promoting pollen germination in tobacco (Chen et al., 2000) and providing funicular pollen tube guidance in *Arabidopsis* (Stührwohldt et al., 2015). Furthermore, PSK attenuates immune responses activated by hemibiotrophs or biotrophs and provides resistance against fungal necrotrophic pathogens in *Arabidopsis* (Loivamäki et al., 2010; Igarashi et al., 2012; Mosher et al., 2013; Rodiuc et al., 2016). In tomato, PSK triggers auxin-dependent immune responses against the

necrotroph *Botrytis cinerea* (Zhang et al., 2018). In addition to participating in plant immunity, PSK was recently identified to play a role in osmotic and drought stress tolerance responses (Rajamanickam et al., bioRxiv; Stührwohldt et al., 2021).

PSKR1 and PSKR2 belong to the >200 membered leucine-rich repeat receptor-like kinases (LRR-RLKs) gene family. Both receptors share 48.6 % amino acid identity (Amano et al., 2007) and are structurally similar containing an extracellular LRR domain, a transmembrane domain, and an intracellular kinase domain. PSK interacts with PSKRs at the island domain present within the extracellular LRRs (Matsubayashi et al., 2006; Amano et al., 2007). PSKRs are anchored into the plasma membrane by a single transmembrane helix. Binding of PSK to PSKR1 facilitates heterodimerization and interaction with the promiscuous somatic embryogenesis receptor like kinases (SERKs) SERK1, SERK2 and BRI1-associated receptor kinase 1 (BAK1)/SERK3. Furthermore, PSKR1 directly interacts with the H⁺-ATPases AHA1 and AHA2. The PSKR1-AHAs complex in turn associates with the cyclic nucleotide-gated cation channel 17 (CNGC17). However, there is no experimental evidence that PSKR1 directly binds to CNGC17, and that this functional complex regulates cell expansion leading to root growth and hypocotyl elongation (Matsubayashi et al., 2006; Kutschmar et al., 2009; Stührwohldt et al., 2011; Ladwig et al., 2015). PSKR2 is also known to promote root growth (Kutschmar et al., 2009) probably through the same mechanism observed for PSKR1.

In our recent study, we showed that PSKR1 signaling is required to maintain shoot growth under osmotic stress, while PSKR2 signaling had no effect (Rajamanickam et al., bioRxiv). In terms of pathogen attack, a similar observation has been reported where PSKR1 attenuated pattern-triggered immunity (PTI) and stimulated seedling growth, while PSKR2 did not significantly contribute to PTI (Igarashi et al., 2012). Because both PSKRs share structural features and PSKR2 is known to have a redundant role in PSK signaling during plant growth, it was interesting to understand why PSKR2 was ineffective in maintaining shoot growth under stress conditions. To investigate functional differences between PSKRs, we employed the construction of chimeric receptors, a technique that is widely used to study functionally redundant receptors or orphan receptors (Tauszig et al., 2000; Tsujita et al., 2004). Using this technique, we can determine if the promoter or domains are responsible for differential activities of the PSKRs. Chimeric receptors were generated by fusing the promoter

regions of *PSKRs* to coding regions of LRRs with the coding regions of the kinase domain of *PSKRs* and expressed the hybrid receptor genes in the receptor-deficient *pskr1-3 pskr2-1* background. Our main goal was to analyze growth efficiency of plants expressing hybrid receptor genes upon osmotic stress using the osmoticum mannitol and on pathogen stress by employing flg22 (bacterial flagellin) and elf18 (Elongation factor thermal unstable) elicitors. Our results revealed that the promoter of *PSKR1* is the key player in driving PSKR receptor activity with contributions from the PSKR1 domains to gain improved PSKR activity.

4.3 MATERIALS AND METHODS

4.3.1 Plant material and growth conditions

The *Arabidopsis thaliana* (L.) Heynh. ecotype Columbia (Col-0), *pskr1-3* (Kutschmar et al., 2009; Stührwohltdt et al., 2011), *pskr2-1* (Amano et al., 2007; Stührwohltdt et al., 2011), *pskr1-3 pskr2-1* (Stührwohltdt et al., 2011; Hartmann et al., 2013), *PSKR1ox2* and *PSKR1ox12* (Hartmann et al., 2013) mutants in the Col-0 background were used in this work. Seeds were directly planted to soil composing 2:3 sand:humus mixture or surface-sterilized for 25 min in 2% (v/v) sodium hypochlorite solution, washed with autoclaved water for four times and plated on half-strength MS medium (Murashige & Skoog, 1962; basal salt mixture, Duchefa Biochemie) and 1% (w/v) sucrose, solidified with 0.4% Gelrite (Duchefa Biochemie). After stratification at 4°C for 2 d in the dark, seedlings were grown in a controlled environment at 60% relative humidity and 22°C with 16h/8h light/dark conditions (70 μM photons $\text{m}^{-2} \text{s}^{-1}$).

4.3.2 Cloning strategy for developing domain swapping constructs

For designing chimeric receptor proteins, the extracellular domain and intracellular domains were predicted using TMHMM version 2.0 (<https://services.healthtech.dtu.dk/service.php?TMHMM-2.0>; Krogh et al., 2001). In this study, the signal peptide, leucine rich repeats and transmembrane helix were defined as extracellular domain (LRR). The juxtamembrane and kinase domains were defined as intracellular domain (KD). The promoter sequences used for PSKR1 is 1602 bp and for PSKR2 is 1545 bp upstream of the respective receptors were amplified from genomic DNA and cloned into the destination vector pB7FWG2. The positive clones were verified by sequencing. The promoter of the 35S RNA was removed from pB7FWG2 and the corresponding PSKR promoter was ligated into pB7FWG2 vector. The defined LRR and KD regions were then amplified from cDNA of Col-0 *A. thaliana* and fused together using overlapping PCR. This fused full-length receptor was later cloned into the pENTR1A vector. For further cloning in destination vectors, the GatewayTM-technology was used. This way, eight different combinations of receptor protein genes were generated, and all constructs were introduced into *Agrobacterium*

tumefaciens strain *EHA105* and transformed into *Arabidopsis pskr1-3 pskr2-1* mutant plants using the floral dip method (Clough and Bent, 1998). Transformed plants were selected with BASTA®. At least three to four independent lines from the T3 generation were used for analysis and the transgene expression of these lines was confirmed by isolating RNA from seven-day-old seedlings.

4.3.3 Shoot growth and root elongation assay

Seedlings were pregrown for 4 days before transferring onto new plates supplemented with 50 mM mannitol, 0.6 nM flg22 or 0.7 nM elf18. Shoot growth was analyzed after fourteen days of transfer by excising shoots from the seedling and its fresh weight was recorded using a fine scale. To determine root elongation, the transferred seedlings were grown for an additional seven days, and the plates were photographed. Using ImageJ (National Institutes of Health, <http://rsb.info.nih.gov/ij>) root lengths were measured from the photographs. Relative growth was determined and for simple interpretation, the shoot fresh weight/root length of seedlings up to four independent lines from each transgenic line were averaged together.

4.3.4 Total RNA isolation and expression analysis

Total RNA was isolated from true leaves of wild type seedlings (four-day-old prior to transfer) that were untreated or treated with 50 mM mannitol, 0.6 nM flg22 or 0.7 nM elf18 and sampled after 1-, 7- or 14-days using TRI reagent (Merck) following manufacturer's instructions. Isolated RNA was treated with DNase I (Thermo Fischer Scientific) to remove genomic DNA. 1 µg of RNA was used based on OD measurements at 260 nm with a NanoDrop 2000 (Thermo Fischer Scientific) to synthesize cDNA by reverse transcription with oligo(dT) primers and RevertAid Reverse Transcriptase (Thermo Fischer Scientific). cDNA was amplified by PCR with the forward primer 5'-CAAAGACCAGCTCTTCCATCG-3' and the reverse primer 5'-CTGTGAACGATTCCTGGACCT-3' for *Actin2* to test for equal amounts of RNA and no traces of genomic DNA.

To analyze the expression of *PSKR1* and *PSKR2*, quantitative RT-PCR was performed with Rotor Gene SYBR Green PCR kit (Qiagen) in a Rotor gene Q cycler (Qiagen) as

instructed by the manufacturer. The primers used for qPCR are listed in Table 1. 10 ng cDNA each in 15 μ l sample volume were employed. *ACTIN2* and GLYCERALDEHYDE-3-PHOSPHATE DEHYDROGENASE 1 (*GAPC1*) were used as reference genes for data normalization. $\Delta\Delta$ CP method (Pfaffl, 2001) was applied to calculate the relative transcript abundance in relation to each reference gene. Results obtained were values averaged from three independent biological repeats with two technical repeats each. The expression level at control conditions was set to 1 and all other values are presented as multiples of that.

4.3.5 Cloning, protein expression and purification

For expression in *Drosophila melanogaster* Schneider 2 (S2) cells (Thermo Fischer Scientific), the extracellular regions excluding the transmembrane helix of PSKR1/PSKR2 (LRRs) were amplified and used for cloning into pECIA2 (Addgene) vector to express recombinant proteins with a C-terminal His6-tag. A colony-PCR was initially performed to screen for positive clones and the error-free clone was confirmed by sequencing. The LRRs cloned into pECIA2 vector were expressed by transient transfection of S2 cells cultured in Schneider's *Drosophila* medium (Genaxxon Bioscience) supplemented with 10% heat-inactivated fetal bovine serum (FBS, Thermo Fischer Scientific) according to the manual described by the manufacturer. The viability of S2 cells was verified by trypan blue staining before transfection.

For expression in *Escherichia coli* cells (*E. coli*), the LRR regions were amplified with a His6-tag by PCR and the product was ligated into pMAL[™]-c5x (New England Biolabs, NEB) which resulted in a C-terminally His-tagged PSKR1/2-LRR domain. The verified clone was transformed into *E. coli* BL21 (DE3) cells. The transformed cells were precultured overnight at 37°C in lysogeny broth (LB) Luria/Miller liquid medium with 0.2% (w/v) glucose and 100 μ g ml⁻¹ ampicillin. 1 ml from the preculture was used to inoculate 50 ml of fresh LB medium and the cells were grown at 37°C until OD₆₀₀ reached ~0.5-0.6. After a brief cooling of the cells on ice for 15 minutes, the recombinant protein expression was induced with 0.3 mM isopropyl- β -D-thiogalactopyranoside (IPTG) and incubated at 22°C for 4 hours. The cells were then harvested at 4000 g, 4°C for 10 minutes and resuspended in 4 ml chilled extraction buffer (50 mM NaPi pH 7.4, 500 mM NaCl, 1% Triton X-100, 20 mM imidazole, 10%

glycerol), disrupted in a French Press (SIM-AMINCO, Spectronic Instruments) at 1000 PSIG, sonicated three times for 15 s with a SONIFIER® B-12 Cell Disruptor (Branson Sonic Power Company) and the cell debris was removed by centrifugation at 20 000 g, 4°C for 30 minutes. The supernatant was incubated with TALON Metal Affinity Resin (Takara Bio) for 1 h in a rotator at room temperature (RT). Purification was done in a Pierce® Spin Column (Thermo Fischer Scientific). The resin was washed with 40 bed volumes of the washing buffer (50 mM NaPi pH 7.4, 500 mM NaCl, 20 mM imidazole, 10% glycerol) with increasing concentrations (30 mM and 40 mM) of imidazole. The remaining target proteins bound to the column were eluted with elution buffer (50 mM NaPi pH 7.4, 500 mM NaCl, 250 mM imidazole, 10% glycerol). The concentration of the protein was determined based on OD measurements at 280 nm with a NanoDrop 2000 (Thermo Fischer Scientific).

4.3.6 Biolayer interferometry

The interaction between PSK and its receptors PSKR1-LRR or PSKR2-LRR was done by biolayer interferometry (Octet RED96e, FortéBio). The receptors carrying a His₆-tag on the C-terminus and MBP-His₆ serving as a control were bound to Anti-Penta-HIS (HIS1K) biosensors (FortéBio) in reaction buffer (50 mM NaPi pH 7.4, 500 mM NaCl, 10% glycerol) for 60 min. Unreacted His₆-sites were blocked by adding 10 µg ml⁻¹ biocytin for 10 min. For tracking association, different concentrations of PSK (10 µM, 50 µM, 100 µM) in reaction buffer were added to the inhibitor-coated sensors followed by biolayer interference for 60 min at room temperature and shaking at 1000 rpm. For tracking dissociation, the sensors were placed in reaction buffer of the same composition without any protein and shaking at 500 rpm. We also tried a reverse interaction technique where PSK was treated with biotin-*N*-hydroxysuccinimide (Thermo Fischer Scientific) by following manufacturer's instructions to obtain biotinylated PSK that can be bound to streptavidin-coated sensors (SA sensor, FortéBio) and followed the same steps for biolayer interference as described above.

4.3.7 Databases and prediction tools

DNA and protein sequences of PSKR1 and PSKR2 were retrieved from TAIR (<https://www.arabidopsis.org/>). The LRR, transmembrane, juxtamembrane and kinase domains were predicted by TMHMM (<http://www.cbs.dtu.dk/services/TMHMM/>) (Krogh et al., 2001). For promoter analysis, PLACE (<https://www.dna.affrc.go.jp/PLACE/?action=newplace>) and CARE (<http://bioinformatics.psb.ugent.be/webtools/plantcare/html/>) databases were used to identify *cis*-regulatory motifs in the promoter regions of PSKR1 and PSKR2. The LRR repeats were identified using PhytoLRR (<https://phytolrr.com/findlrr>) (Chen, 2021).

4.3.8 Statistical analysis

Minitab® 16.1 was used for statistical analysis. Data were checked for normal distribution and if normally distributed then checked for equal variances. All data represented in this study are not distributed normally and therefore were evaluated using a Kruskal-Wallis or Mann-Whitney test for pairwise comparison.

4.3.9 Accession numbers

ACT2 - At3g18780, *GAPC1* - At3g04120, *PSKR1* - At2g02220, *PSKR2* - At5g53890

4.4 Results

4.4.1 PSKR1 but not PSKR2 is important for shoot growth under mild osmotic stress

PSK is perceived by two LRR-RLK receptors, PSKR1 and PSKR2, in Arabidopsis and is known to promote plant growth (Matsubayashi et al., 2006; Amano et al., 2007; Sauter 2015). From our recent study on PSK receptor signaling under mild osmotic stress (Rajamanickam et al., bioRxiv), we found that PSKR1 is required to maintain shoot growth whereas knockout of its close homolog PSKR2 had no effect (Fig. 1).

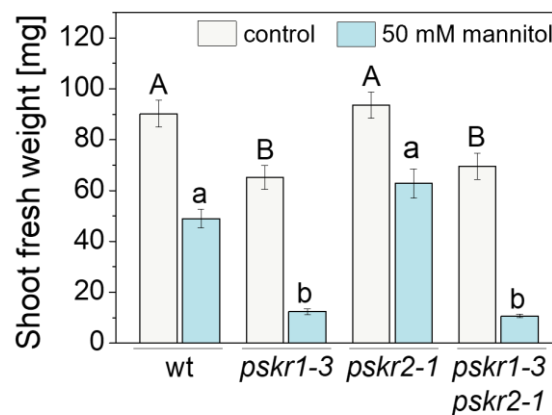


Figure 1. PSKR1 is crucial for growth promotion under mannitol stress.

Four-day-old wild type (wt), *pskr1-3*, *pskr2-1*, and *pskr1-3 pskr2-1* seedlings were transferred to media with or without 50 mM mannitol and average shoot fresh weights (\pm SE) of seedlings were determined after 3 weeks. Different capital and minor letters indicate significant differences between genotypes and treatments, respectively (Kruskal-Wallis, Tukey's test, $P < 0.05$, $n = 36$, 3 independent experiments).

We next tested the effect of exogenous PSK on shoot growth under osmotic stress as PSK was previously shown to promote growth when applied externally (Matsubayashi et al., 1999). Four-day-old wild type seedlings were transferred to plates containing 0.1 μ M or 1 μ M PSK in addition to (\pm) 50 mM mannitol and shoot fresh weights were measured after 2 weeks (Fig. 2A). No significant changes were induced by PSK in either control or mannitol conditions, suggesting that endogenous PSK levels were sufficient for PSK/PSKR signaling under osmotic stress. Next, we used the *PSKR1* overexpression lines, *PSKR1ox2* and *PSKR1ox12* (Hartmann et al., 2013) to test if

receptor abundance was limiting shoot growth under osmotic stress. Four-day-old wild type, *PSKR1ox2* and *PSKR1ox12* seedlings were transferred to plates containing 50 mM mannitol and shoot fresh weights were measured after 2 weeks. Shoot fresh weights of *PSKR1ox2* and *PSKR1ox12* of mannitol-treated seedlings were higher in comparison to the wild type (Fig. 2B) indicating that PSKR1 rather than its ligand PSK is a limiting factor in PSK/PSKR signaling of shoot growth under osmotic stress.

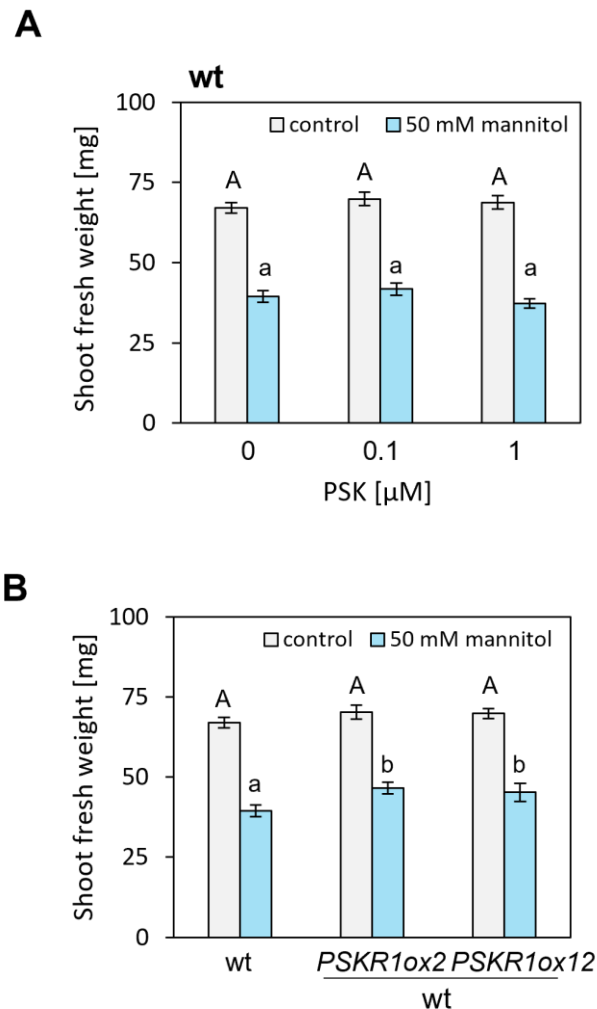


Figure 2. *PSKR1* expression limits PSK/PSKR signaling of shoot growth under mannitol stress.

(A) For testing the effect of PSK application on shoot fresh weight under mannitol stress, four-day-old wt seedlings were transferred to medium supplemented with (\pm) 50 mM mannitol and (\pm) 0.1 μ M or 1 μ M PSK. Shoot fresh weights were determined after 14 days. Significantly different values for control and mannitol treatments are denoted by capital and small letters (one-way ANOVA, Tukey's test, $P < 0.05$, $n = 36$, 3 independent experiments). (B) To test the effect of *PSKR1* overexpression, four-day-old *PSKR1ox2* and *PSKR1ox12* seedlings expressed in the wt background were transferred to medium supplemented with (\pm) 50 mM mannitol. Shoot fresh weights were determined after 14 days. Significantly

different values for control and mannitol treatments are denoted by capital and small letters (one-way ANOVA, Tukey's test, $P < 0.05$, $n = 36$, 3 independent experiments).

These results indicate a critical role of *PSKR1* in plant shoot growth which prompted us to investigate the functional differences with its paralog *PSKR2*, that was shown to also function as a PSK receptor (Amano et al., 2007). Both receptors have an extracellular leucine-rich repeat domain (LRR), a single transmembrane domain (TM) and an intracellular kinase domain (KD). It is, however, not known why *PSKR2* is ineffective in maintaining shoot growth under osmotic stress conditions despite being similar in structure to *PSKR1*.

4.4.2 Functional analysis of PSK receptor chimeras reveal that the promoter, LRR and kinase domain of *PSKR1* are collectively important for an effective PSK signaling under osmotic and pathogen stress conditions

To find out whether the promoter or specific receptor domains of *PSKR1* and *PSKR2* are responsible for differences in shoot growth between *pskr1-3* and *pskr2-1* under osmotic stress, we engineered eight chimeric *PSKR* genes by fusing either promoter region of *PSKR1* and *PSKR2* to the coding regions of the N-terminal extracellular and transmembrane domains (LRR+TM; from here on referred to collectively as LRR) with the coding regions of the juxtamembrane region and the kinase domain (JM+KD; from here on referred to collectively as KD) and expressed the hybrid receptor genes in the receptor-deficient *pskr1-3 pskr2-1* background (Fig. 3).

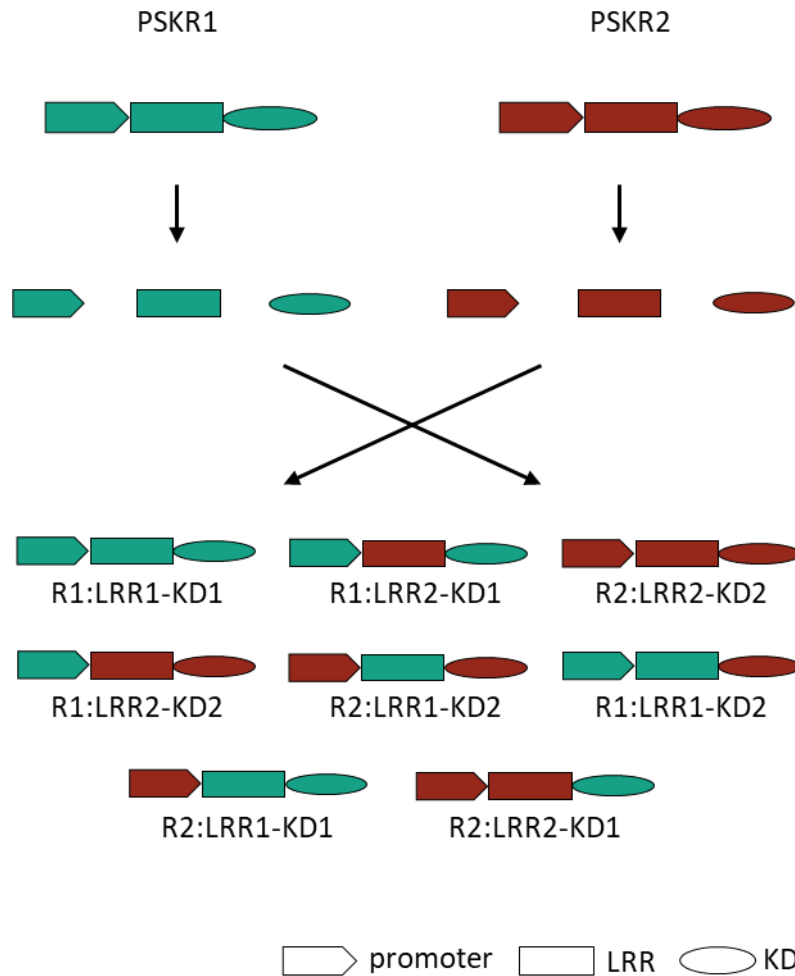
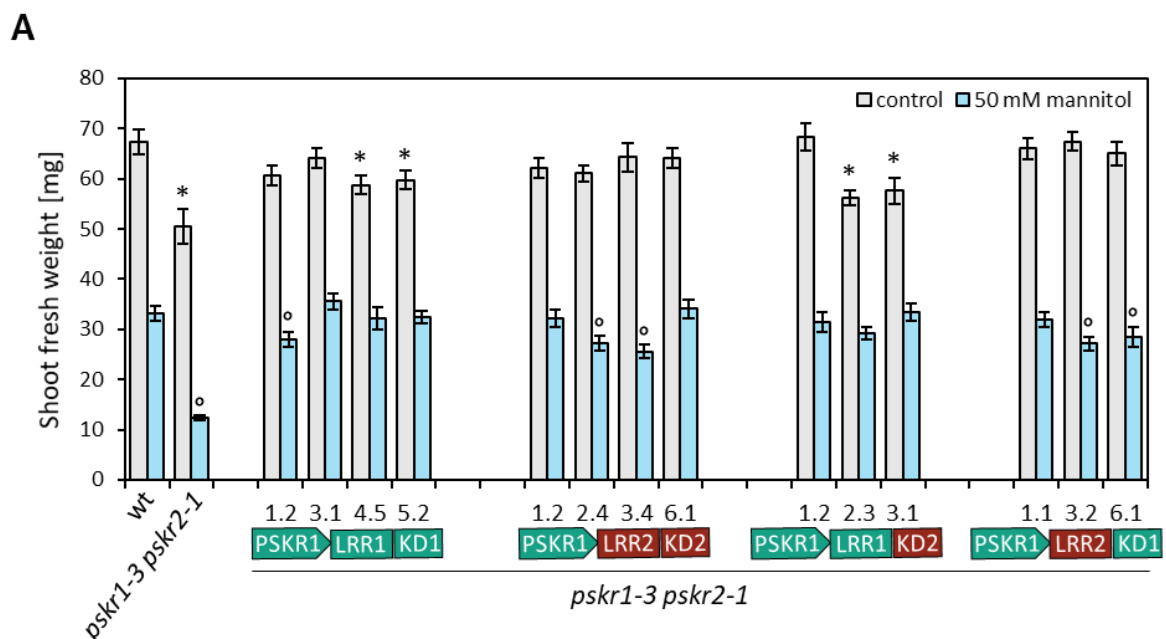


Figure 3. Schematic representation depicting the promoter region and domains that were swapped between the PSK receptors.

Eight hybrid receptor genes were generated and transformed into the *pskr1-3 pskr2-1* background. Green and red colours represent the domains from *PSKR1* and *PSKR2*, respectively.

The eight different hybrid receptor genes were transformed and three to four independent homozygous lines for each gene were used for functional analysis. We first analyzed shoot growth of plants expressing hybrid receptor genes on mild osmotic stress with 50 mM mannitol. Root elongation was not analyzed because we observed earlier that 50 mM mannitol did not alter root growth in *pskr1-3 pskr2-1* compared to the wild type (Rajamanickam et al., bioRxiv). Four-day-old seedlings were transferred to mannitol and shoot fresh weights were measured after two weeks (Fig. 4). Among the eight hybrid receptors, *PSKR1:LRR1-KD1* and *PSKR2:LRR2-KD2* are reconstituted native *PSKR*s that were included as gain-of-function controls. Shoot growth under mild mannitol stress of plants expressing hybrid receptors under the

control of the *PSKR1* promoter was increased compared to *pskr1-3 pskr2-1* and was nearly comparable to wild type except for *PSKR1:LRR1-KD1* line 1.2, *PSKR1:LRR2-KD2* lines 2.4 and 3.4, *PSKR1:LRR2-KD1* lines 3.2 and 6.1. Two out of four lines of *PSKR1:LRR2-KD2* and two out of three lines of *PSKR1:LRR2-KD1* showed slight reduction in shoot fresh weight in comparison to the wild type indicating that LRR2 may reduce PSKR growth signaling compared to LRR1. On the other hand, all hybrid receptors whose expression was driven by the *PSKR2* promoter exhibited reduced shoot growth compared to the wild type, except for *PSKR2:LRR1-KD1* line 2.5 (Fig. 4B), suggesting a major impact of the promoter on receptor activity under osmotic stress. Nonetheless, expression of *PSKR2:LRR1-KD1*, *PSKR2:LRR1-KD2* and *PSKR2:LRR2-KD1* improved shoot growth under mannitol treatment compared to *pskr1-3 pskr2-1* (Supplemental Fig. S1B), revealing specific contributions of the LRR and KD to overall receptor activity. To allow for an overall comparison of the hybrid receptor lines, we averaged the shoot fresh weights from independent lines of each hybrid receptor to represent one hybrid complementation group. This was done separately for control and mannitol treatments and relative shoot fresh weight in mannitol compared to control conditions was calculated to evaluate the contributions of the promoter, LRR and KD (Fig. 5).



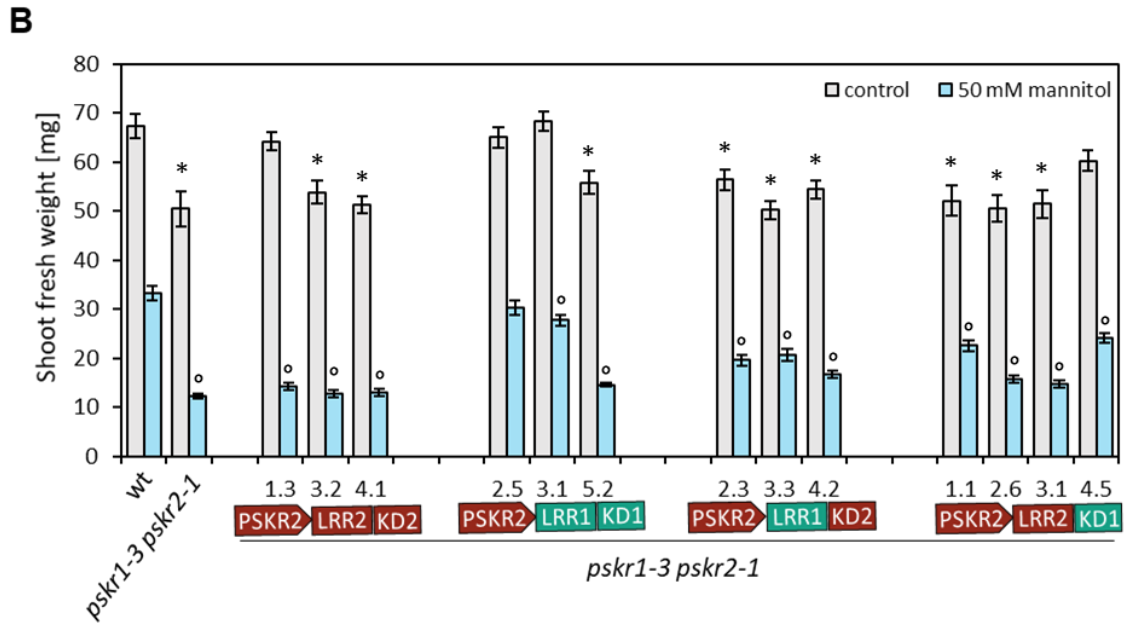


Figure 4. Effect of osmotic stress on shoot growth of lines each expressing a hybrid receptor gene.

Seedlings were pregrown for four days and then transferred to medium supplemented with or without 50 mM mannitol. Average shoot fresh weights (\pm SE) were determined after two weeks. At least 12 seedlings per independent line and per condition were analyzed. The numbers on the x-axis represent independent lines each expressing a receptor hybrid. Results are averages obtained from three independent experiments. Green represents the promoter region and domains of *PSKR1*, and red represents *PSKR2*. Shoot fresh weights of hybrid receptor lines expressed under control of the (A) *PSKR1* promoter and (B) *PSKR2* promoter. * and ° indicate significant differences in comparison to the wild type in control and mannitol treatments, respectively (Kruskal-Wallis test, $P < 0.05$, $n = 36$).

As seen before (Fig. 4), the major difference in PSKR activities was dependent on the promoter region. In addition, hybrid receptor lines under control of the *PSKR1* promoter but with LRR2 rather than LRR1, *PSKR1:LRR2-KD2* and *PSKR1:LRR2-KD1*, exhibited reduced growth compared to *PSKR1:LRR1-KD1* and *PSKR1:LRR1-KD2* indicating that LRR1 additionally contributes to full receptor activity. When expressed under control of the *PSKR2* promoter, hybrid receptor lines with either LRR1 or KD1 or both, *PSKR2:LRR1-KD1*, *PSKR2:LRR1-KD2*, *PSKR2:LRR2-KD1*, increased shoot growth compared to *pskr1-3 pskr2-1* and *PSKR2:LRR2-KD2* under osmotic stress indicating that the promoter region, LRR and KD of *PSKR1* and *PSKR2* are functionally different.

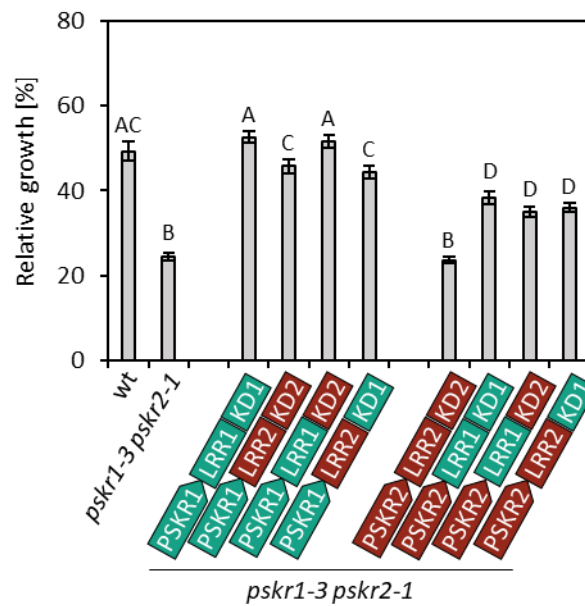


Figure 5. The promoter region, LRR and KD of *PSKR1* collectively contribute to mannitol stress resistance.

Four-day-old seedlings were transferred to control media or 50 mM mannitol and shoot fresh weight was measured after two weeks. Shoot fresh weights of 3-4 independent lines each expressing a hybrid receptor type were averaged (\pm SE) and shoot growth under mannitol relative to the control was determined (Kruskal-Wallis test, $P < 0.05$, $n = 36$ from each independent line, 3 biological replicates).

Next, we investigated if activities of the receptor hybrids also differed in response to molecular patterns that activate pathogen response based on the previous finding that PSKR signaling modulates biotic stress responses (Igarashi et al., 2012; Mosher et al., 2013; Sauter, 2015). In 2012, Igarashi and co-workers demonstrated that *PSKR1* but not *PSKR2* attenuates pattern-triggered immunity (PTI) and stimulates seedling growth when treated with the microbe-associated molecular patterns (MAMPs) flg22 or elf18, peptides that evoke PTI and originate from bacterial flagellin and EF-Tu (Elongation factor thermal unstable) (Felix et al., 1999; Kunze et al., 2004). Therefore, we examined shoot growth of the hybrid receptor lines in the presence of flg22 or elf18 using the same set-up as described for mannitol treatment.

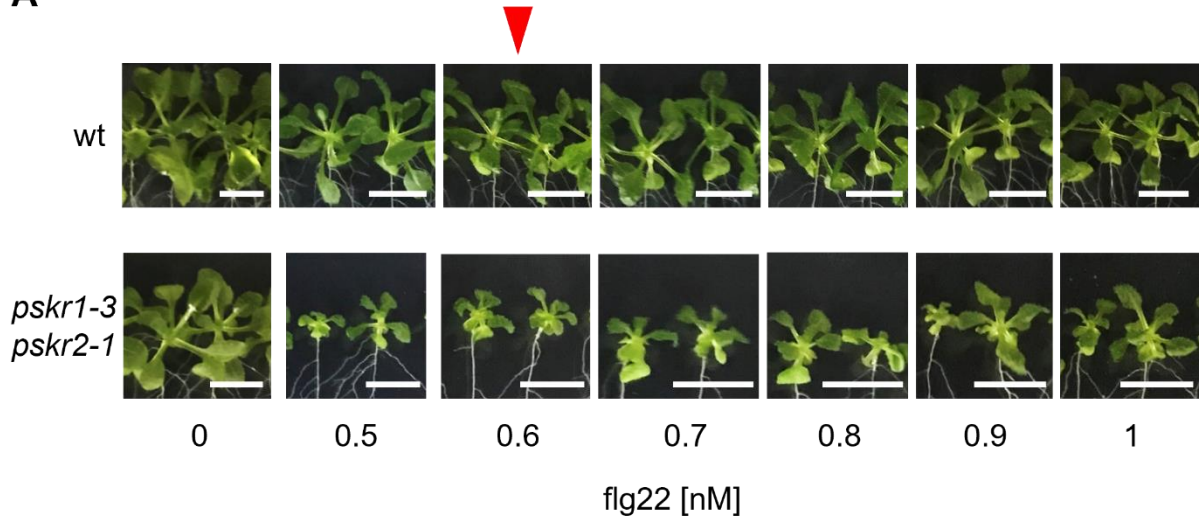
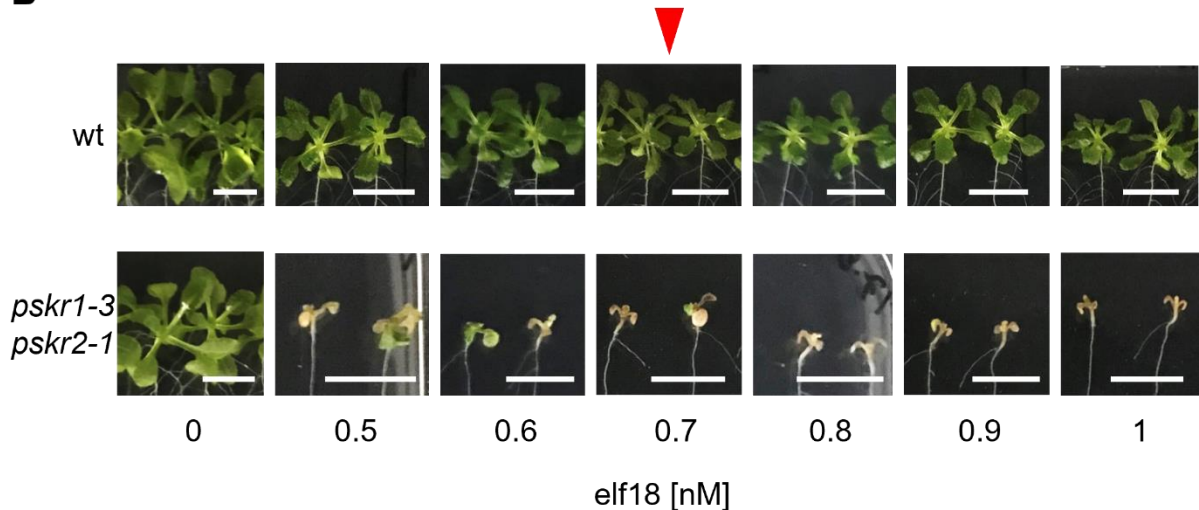
A**B**

Figure 6. Shoot phenotypes of wt and *pskr1-3 pskr2-1* on increasing concentrations of flg22 and elf18.

Four-day-old wt and *pskr1-3 pskr2-1* seedlings were transferred to media containing flg22 or elf18 as indicated. Shoot phenotypes of wt and *pskr1-3 pskr2-1* plants after two weeks of growth on (A) flg22 and (B) elf18 were analyzed. Scale bars = 10 mm. Red arrows indicate the concentration chosen for further analysis.

To choose a concentration of elicitors to use in further analysis, we performed a dose-response experiment (Fig. 6). Shoot growth was consistently reduced in *pskr1-3 pskr2-1* at 0.6 nM flg22 (Fig. 6A). For elf18, concentrations higher than 0.7 nM were lethal for *pskr1-3 pskr2-1* (Fig. 6B) therefore 0.6 nM for flg22 and 0.7 nM for elf18 were chosen for further analysis.

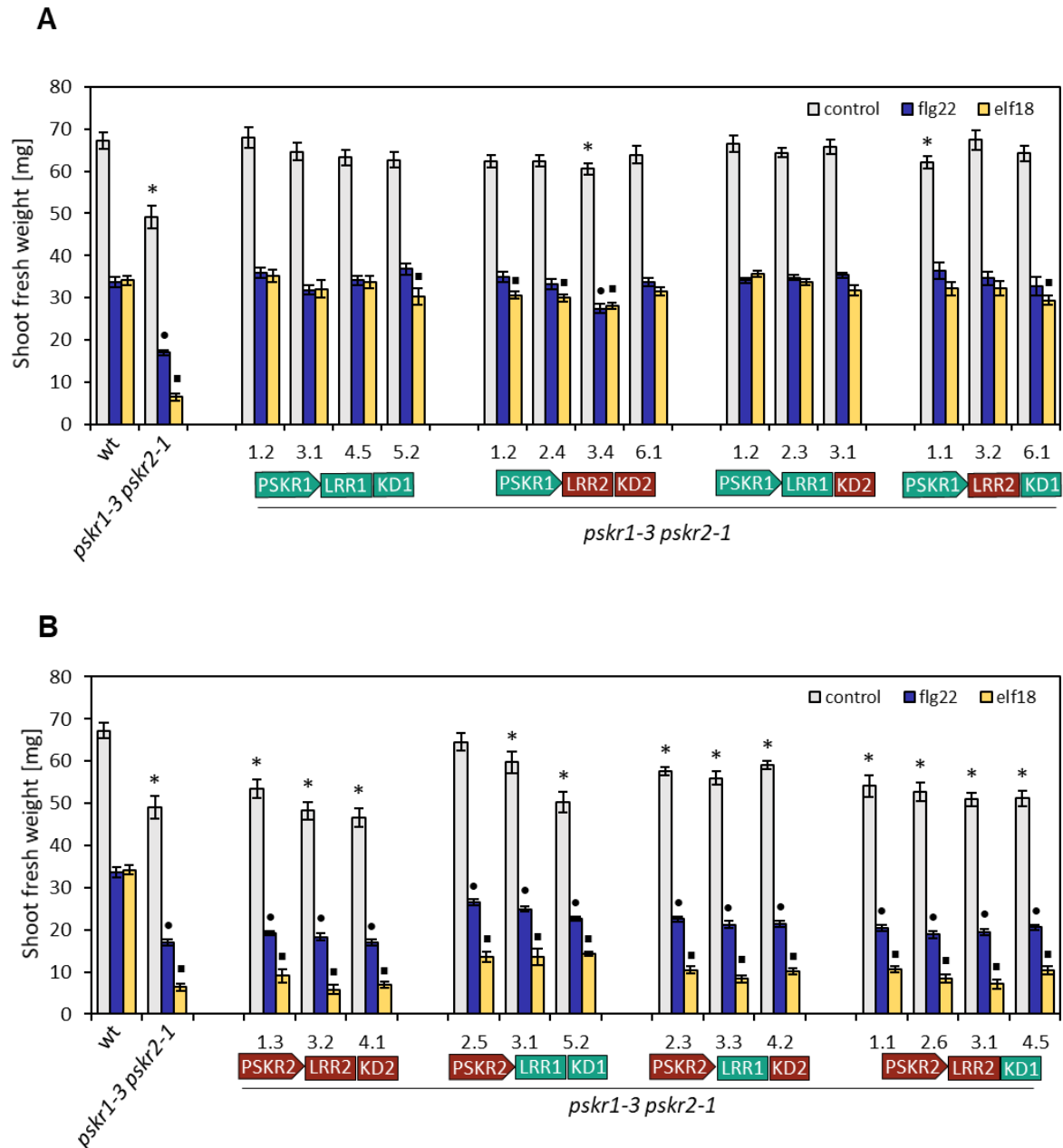


Figure 7. Effect of MAMPs on shoot growth of lines each expressing a hybrid receptor gene.

Seedlings were pregrown for four days and then transferred to medium supplemented with or without 0.6 nM flg22 or 0.7 nM elf18. Average shoot fresh weights (\pm SE) were determined after two weeks. At least 12 seedlings per independent line and per condition were analyzed. The numbers on the x-axis represent independent lines each expressing a receptor hybrid. Results are averages obtained from three independent experiments. Green represents the promoter region and domains of *PSKR1*, and red represents *PSKR2*. Shoot fresh weights of hybrid receptor lines expressed under control of the (A) *PSKR1* promoter and (B) *PSKR2* promoter. *, • and ▪ indicate significant differences in comparison to the wild type under control, flg22 and elf18 treatments, respectively (Kruskal-Wallis test, $P < 0.05$, $n = 36$).

Four-day-old seedlings were transferred to control or flg22 or elf18 containing media and shoot fresh weights were measured after 14 days (Fig. 7). Plants expressing hybrid receptors under control of the *PSKR1* promoter reached close to wild type shoot growth upon flg22, except line *PSKR1:LRR2-KD2* 3.4 (Fig. 7A). Most lines from *PSKR1:LRR1-KD1*, *PSKR1:LRR1-KD2* and *PSKR1:LRR2-KD1*, but not *PSKR1:LRR2-KD2*, showed similar shoot growth as wild type in response to elf18. Three out of four *PSKR1:LRR2-KD2* lines displayed slightly reduced shoot fresh weight compared to the wild type on elf18 indicating that the LRR and KD of the two receptors are not fully redundant (Fig. 7A). In contrast, shoot growth of all plants expressing hybrid receptors under control of the *PSKR2* promoter was significantly reduced when compared to wild type in response to both elicitors (Fig. 7B) demonstrating a critical role of the *PSKR1* promoter as this also mirrored results from osmotic stress. Another similar response observed in both osmotic and pathogen stress was that *PSKR2:LRR1-KD1* had increased shoot growth in comparison to *pskr1-3 pskr2-1* (Supplemental Fig. S2B) suggesting LRR1 and KD1 together improved receptor activity.

To compare all receptor hybrids together we averaged data from independent lines of each receptor hybrid together and determined relative shoot growth on flg22 and elf18 separately as described earlier for osmotic stress (Fig. 8). Shoot growth of plants expressing hybrid receptors driven by the *PSKR1* promoter in response to both elicitors were comparable to wild type implying that LRR and KD from both PSKRs regulated receptor activity in an equal manner when expressed under control of the *PSKR1* promoter. Although *PSKR1:LRR2-KD2* and *PSKR1:LRR2-KD2* on elf18 had similar shoot growth as wild type, a minor reduction in shoot growth in comparison to *PSKR1:LRR1-KD2* was observed revealing LRR2 may have reduced activity. All receptor hybrid lines driven by the *PSKR2* promoter displayed reduction in shoot growth when compared to wild type but *PSKR2:LRR1-KD1* improved shoot growth in relation to *pskr1-3 pskr2-1* once again highlighting the importance of LRR1 and KD1 (Fig. 8A). Same observation was detected in case of elf18 elicitation (Fig. 8B).

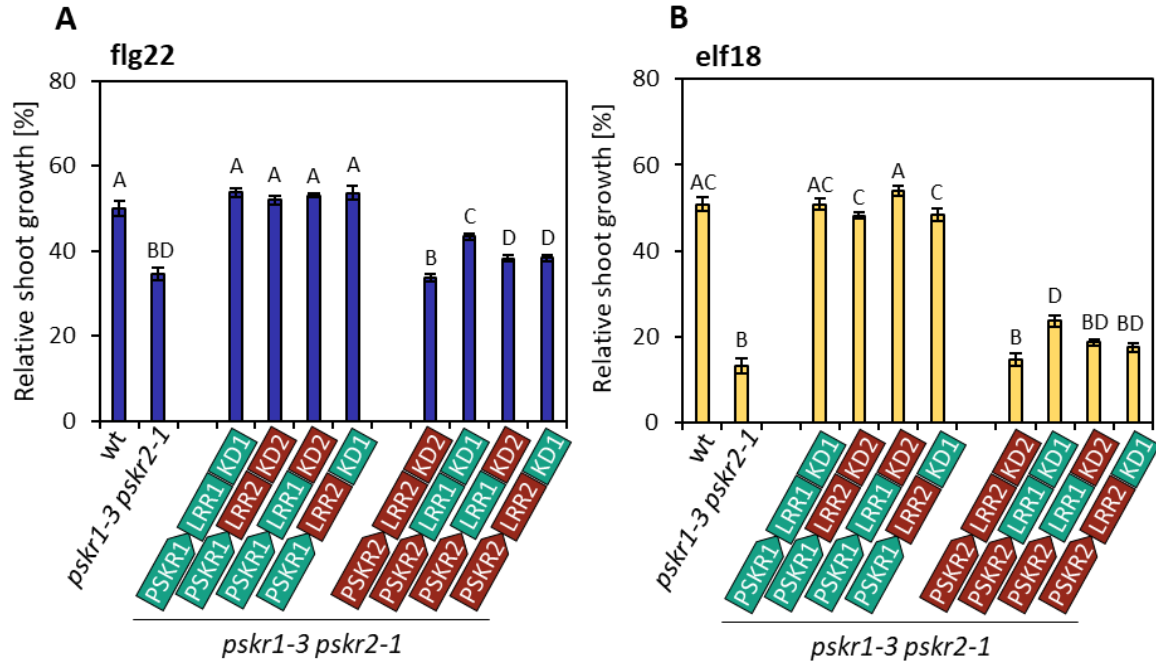


Figure 8. The promoter region and domains of *PSKR1* collectively improve shoot growth on MAMP treatment.

Seedlings were pregrown for four days and then transferred to medium supplemented with or without 0.6 nM flg22 or 0.7 nM elf18 and shoot fresh weight was measured after two weeks. Shoot fresh weight of three or four independent lines each expressing a specific hybrid receptor were averaged (\pm SE) and shoot growth relative to wild type on (A) flg22 and (B) elf18 treatments was determined (Statistics: Kruskal-Wallis test, $P < 0.05$, $n = 36$, from each independent line).

We next analyzed the root growth on MAMP treatment as we observed a difference in root elongation between wild type and *pskr1-3 pskr2-1* at our working concentration. To do so, four-day-old seedlings were transferred to flg22, elf18 or control plates and root lengths were measured after seven days.

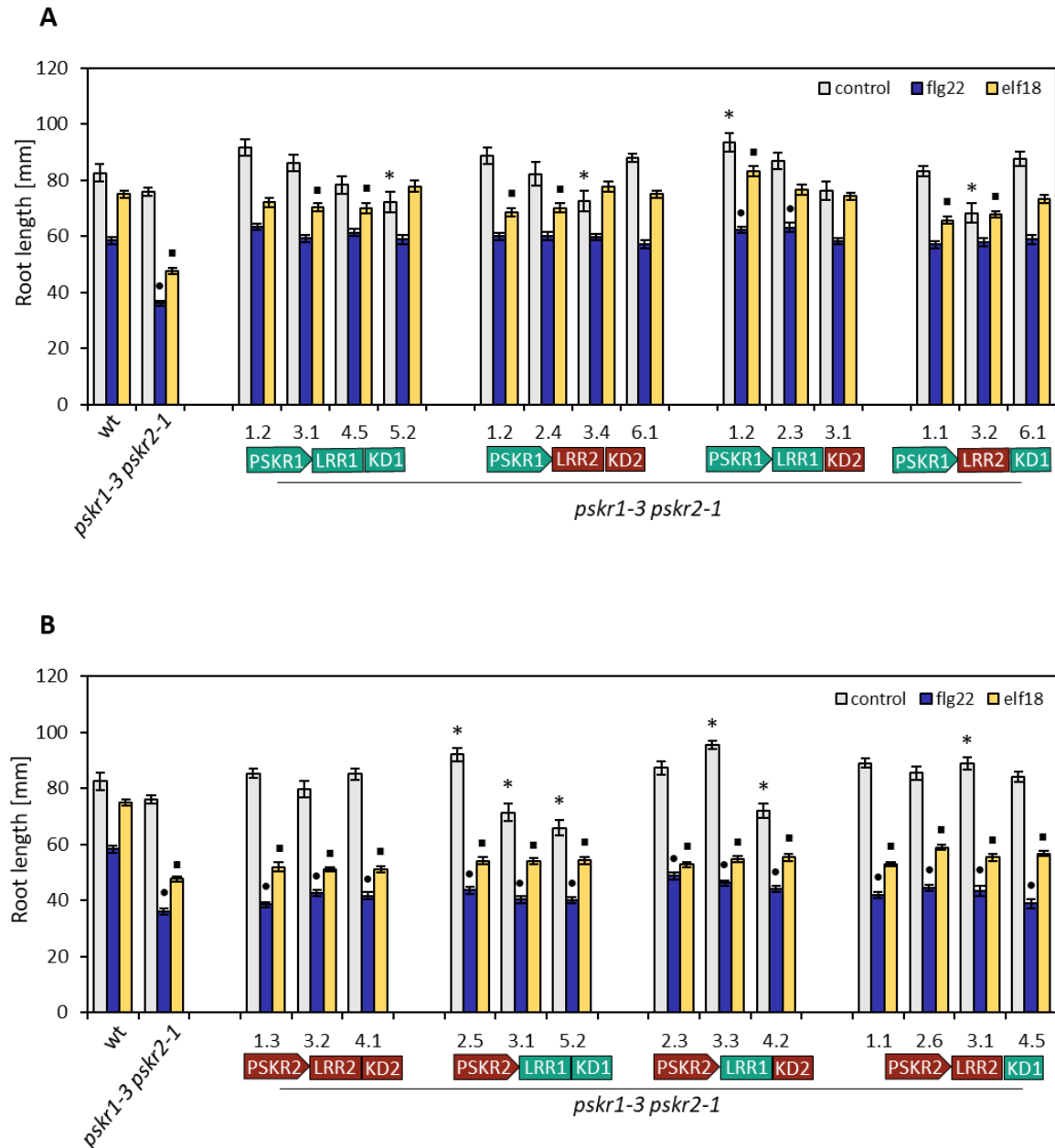


Figure 9. Effect of MAMPs on root growth of lines each expressing a hybrid receptor gene.

Seedlings were pregrown for four days and then transferred to medium supplemented with or without 0.6 nM flg22 or 0.7 nM elf18. Average root lengths (\pm SE) were determined after seven days. At least 12 seedlings per independent line and per condition were analyzed. Results are averages obtained from three independent experiments. Green represents the promoter and domains of *PSKR1*, and red represents *PSKR2*. Root lengths of hybrid receptors expressed under the control of (A) *PSKR1* promoter and (B) *PSKR2* promoter. *, • and ▪ indicate significant differences in comparison to wild type upon control, flg22 and elf18 treatments, respectively (Kruskal-Wallis test, $P < 0.05$, $n = 36$).

Plants expressing hybrid receptors under control of the *PSKR1* promoter showed similar root lengths as the wild type on flg22 except for *PSKR1:LRR1-KD2* lines 1.2 and 2.3. In contrast, the root lengths of *PSKR1:LRR1-KD1* lines 3.1 and 4.5; *PSKR1:LRR2-KD2* lines 1.2 and 2.4; *PSKR1:LRR2-KD1* lines 1.1 and 3.2 were significantly different to the wild type after elf18 treatment (Fig. 9A). On the other hand, root elongation of all receptor hybrids driven by the *PSKR2* promoter showed reduced root growth in comparison to wild type upon both elicitors (Fig. 9B). Once again, we averaged the root lengths of single lines together from respective receptor hybrids as described for osmotic stress and determined relative root growth of each hybrid receptor line on flg22 and elf18 separately (Fig. 10). Significant differences in root growth compared to the wild type was observed only in plants expressing hybrid receptors driven by the *PSKR2* promoter. It should be noted here, however, that *PSKR2:LRR1-KD1* on both elicitors and *PSKR2:LRR1-KD2* on flg22 showed improved root growth in comparison to *pskr1-3 pskr2-1*.

Taken together, these results show that among the three components of *PSKR*s tested in different combinations using the chimeric receptor approach, the *PSKR1* promoter is primarily important for a functional *PSKR* under osmotic and pathogen stress. On the other hand, assuming the *PSKR2* promoter is weaker or inactive under these stress conditions, still *PSKR2:LRR1-KD1* improved growth compared to other hybrid lines driven by the *PSKR2* promoter revealing that both receptors differ not only in their promoter regions but also have functionally different LRRs and KDs. It was also interesting to notice that *PSKR1:LRR2-KD2* gained almost full receptor activity upon all conditions implying that LRR2 and KD2 activity depends on the promoter region. *PSKR1:LRR1-KD1* and *PSKR1:LRR1-KD2* showed marginal increase on mannitol and elf18 when analyzed for shoot growth in comparison to *PSKR1:LRR2-KD1* and *PSKR1:LRR2-KD2* indicating that LRR1 is important for full receptor activity even when the expression of these receptor hybrids was driven by the primarily important component, the *PSKR1* promoter. *PSKR2:LRR1-KD2* improved shoot growth on mannitol and root growth on flg22 whereas *PSKR2:LRR2-KD1* promoted shoot growth on mannitol indicating that the LRR and KD have altered activity depending on the stress and tissues analyzed. Altogether it is clear that the promoter of *PSKR1* modulates *PSKR* activity majorly compared to the *PSKR2* promoter. Among the LRRs and KDs, LRR1 and LRR2 showed increased or reduced activity depending on the

stress condition. The promoter region, LRR and KD of *PSKR1* all in different degrees improve PSK/PSKR signaling when compared to *PSKR2* receptor components.

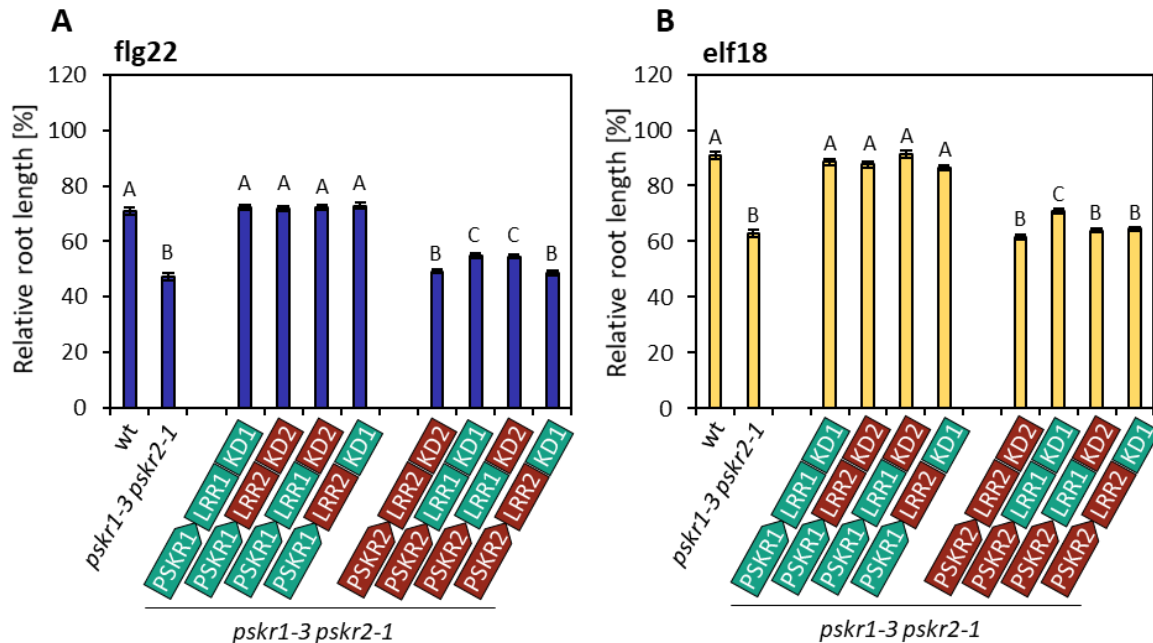


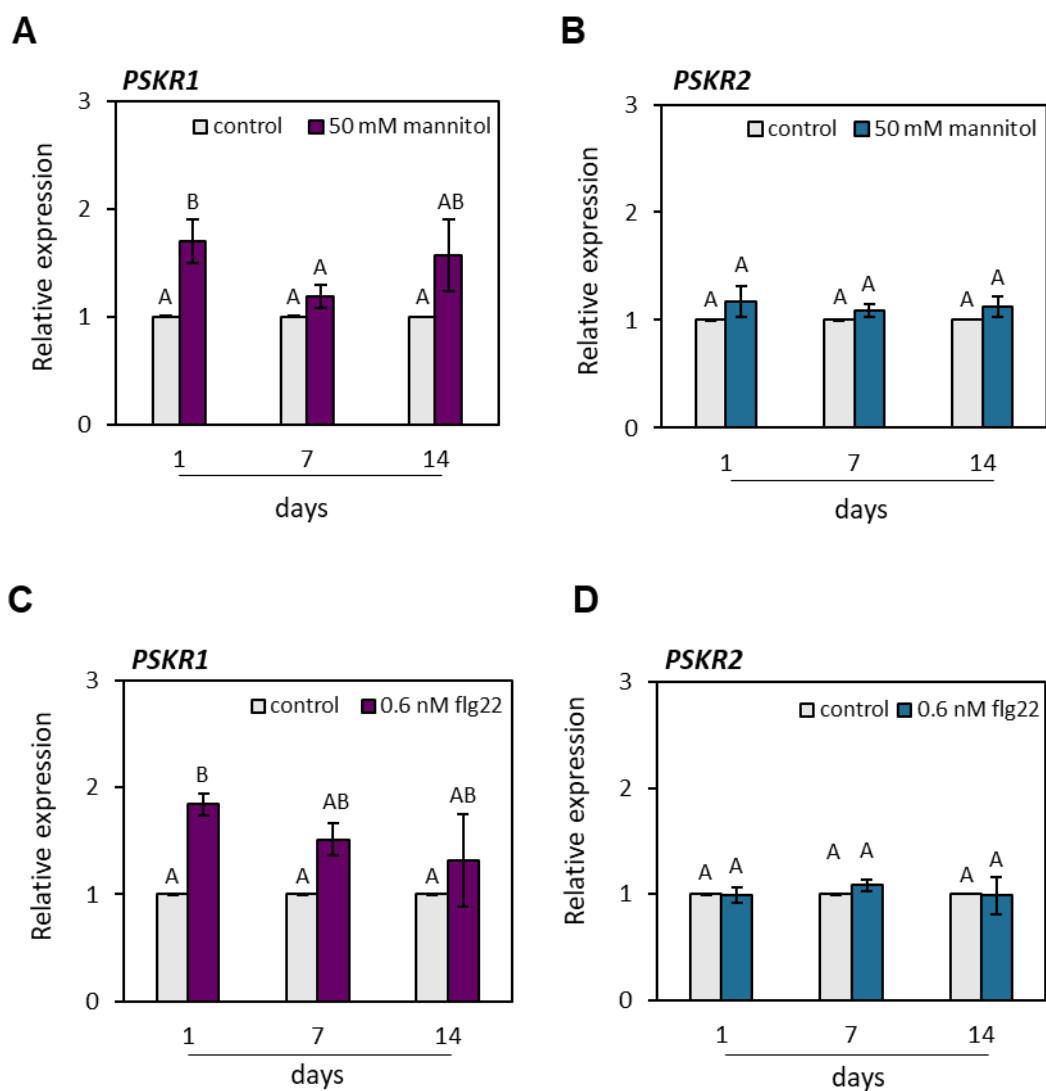
Figure 10. The promoter region and domains of *PSKR1* are important to improve root growth on MAMP treatment.

Seedlings were pregrown for four days and then transferred to medium supplemented with or without 0.6 nM flg22 or 0.7 nM elf18. Root length of three or four independent lines each expressing a specific hybrid receptor were averaged (\pm SE) from which relative root length on (A) flg22 and (B) elf18 treatments were determined (Statistics: Kruskal-Wallis test, $P < 0.05$, $n = 36$, from each independent line).

4.4.3 *PSKR1* is transcriptionally regulated upon osmotic and MAMP stress while *PSKR2* remains unaltered

The difference between an active and inactive PSKR was largely dependent on the promoter regions and since promoters play an important role in gene expression, we examined the expression of both *PSKR1* and *PSKR2* in response to mannitol, flg22 and elf18. Four-day-old wild type seedlings were transferred to control and stress treatments and true leaves were sampled after one, seven and 14 days to detect early-to-end expression changes. RT-qPCR data revealed that *PSKR1* was induced after one day of exposure to all three treatments (Fig. 11A, C and E). After seven and 14

days, the expression of *PSKR1* on mannitol and flg22 were comparable to the control. However, *PSKR1* expression remained to be elevated on elf18 even after seven days. On the contrary, *PSKR2* expression was unaltered under all tested conditions and time points (Fig. 11B, D and F).



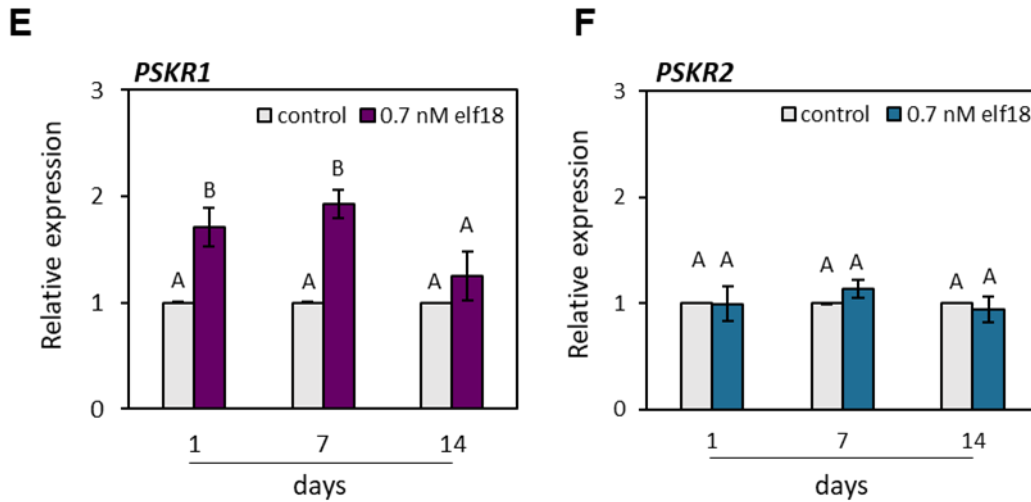


Figure 11. *PSKR1* expression is induced up on mannitol and MAMPs while *PSKR2* shows no regulation.

Four-day-old wt seedlings exposed to different treatments or left untreated as control were sampled after one, seven and 14 days for expression analysis by RT-qPCR in true leaves. Relative transcript levels of (A, C, E) *PSKR1* and (B, D, F) *PSKR2* in response to mannitol, flg22 or elf18. Results (\pm SE) are averages from three biological replicates with two technical repeats each. Different letters indicate significant differences (A, C, E: Kruskal-Wallis test, $P < 0.05$; B, D, F: one-way ANOVA, Tukey's test, $P < 0.05$; $n = 3$).

In addition, transcript levels of *PSKR1* and *PSKR2* on each condition were determined. Transcript abundance of *PSKR1* was invariably higher compared to *PSKR2* regardless of the treatment and time points tested (Fig. 12), except on control and mannitol conditions after one and seven days, respectively (Fig. 12A). Interestingly, *PSKR1* expression was increased after seven and 14 days even under control conditions indicating a development-dependent expression pattern of *PSKR1*, but not *PSKR2*. So, loss or basal transcriptional activation of *PSKR2* could be a major reason why *PSKR2* is ineffective to compensate for the tested stress conditions that largely relies on the *PSKR2* promoter.

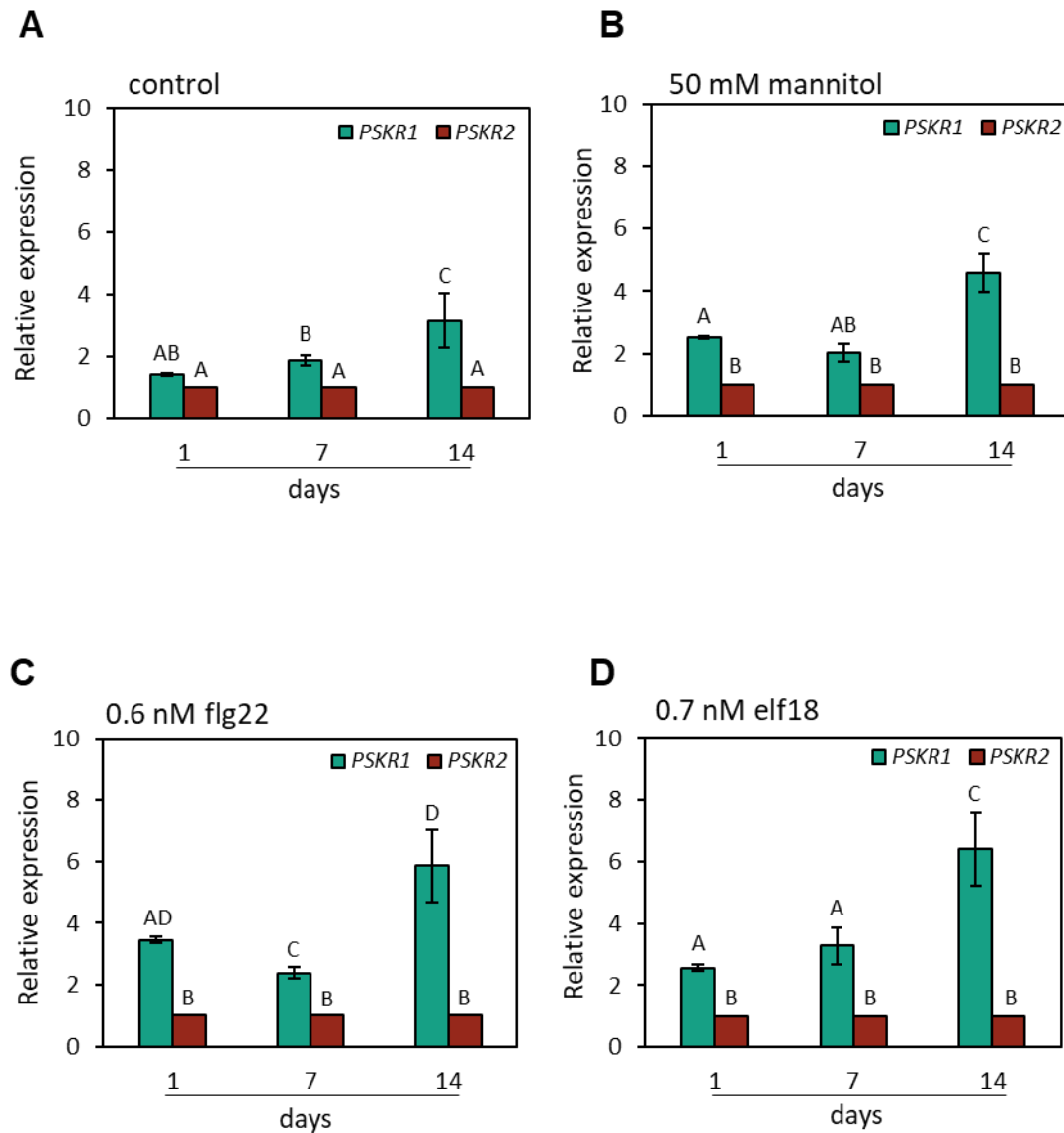


Figure 12. *PSKR2* expression is relatively low compared to *PSKR1* on different conditions.

Four-day-old wt seedlings exposed to various treatments or left untreated as control were sampled after one, seven and 14 days for expression analysis by RT-qPCR. Changes in *PSKR1* transcript compared to *PSKR2* transcript abundance on (A) control (B) 50 mM mannitol (C) 0.6 nM flg22 and (D) 0.7 nM elf18. Results (\pm SE) are averages from three biological replicates with two technical repeats each. Different letters indicate significant differences (Kruskal-Wallis test, $P < 0.05$, $n = 3$).

4.4.4 The *PSKR1* promoter contains regulatory regions that influence both dehydration and elicitor responses

Any differential expression of target genes is likely attributable to the regulatory elements in their promoter regions (Wu et al. 2012). To comprehend the differences in transcriptional regulation between *PSKR1* and *PSKR2*, *in silico* promoter analysis was carried out using PLACE (<https://www.dna.affrc.go.jp/PLACE/?action=newplace>) (Higo et al., 1999) and PlantCARE (<http://bioinformatics.psb.ugent.be/webtools/plantcare/html/>) (Lescot et al., 2002) databases to identify important *cis*-acting regulatory elements (CAREs) that likely regulate *PSKR* gene expression by binding potential transcription factors under osmotic and pathogen stress conditions used in this study. Putative promoter regions that were used for generating hybrid receptor lines were subjected to *in silico* analysis. The results showed many common putative CAREs in promoter regions of both *PSKR1* and *PSKR2* including CAAT-box and TATA-box, the core regulatory elements (Bilas et al., 2016). But we intended to determine motifs that were exclusive to the *PSKR1* promoter in order to understand lack of which specific CAREs in the *PSKR2* promoter contributed to differential expression between the *PSKR*s. We also determined motifs that are unique to the *PSKR2* promoter to check for the possibility of repressor binding that intervened gene expression (Fig. 13).

In total, 24 motifs could be identified that were unique to the *PSKR1* promoter region, while 9 motifs were found to be unique to the *PSKR2* promoter. The predicted CAREs in the *PSKR1* promoter region were categorized into seven different groups based on its putative function (Table 1). Among the five motifs in the hormone responsive category, PYRIMIDINEBOXHVEPB1 and TCA-element CAREs regulate gene expression in response to ABA/gibberellins and salicylic acid, respectively (Cercós et al., 1999). There were five motifs grouped into the stress responsive category including DRECRTCOREAT, a dehydration-responsive element that regulates gene expression in response to drought stress in *Arabidopsis* (Yamaguchi-Shinozaki and Shinozaki, 1994), TC-rich repeats that regulate defense and stress responses (Sun et al., 2010), WBOXNTCHN48, an elicitor responsive element (Yamamoto et al., 2004), BOXLCOREDPCAL that binds MYB transcription factors in response to elicitor treatments (Maeda et al., 2005) and MYBST1 that binds ANAC074, a transcription

factor that regulates promoters of ethylene and stress responsive genes (He et al., 2018).

A	PSKR1	B	PSKR2
	<div><div>➤</div>TATAPVTRNALEU</div> <div><div>➤</div>CAREOSREP1</div> <div><div>➤</div>GARE2OSREP1</div> <div><div>➤</div>BOXLCOREDCPAL</div> <div><div>➤</div>10PEHVPSBD</div> <div><div>➤</div>PYRIMIDINEBOXHVEPB1</div> <div><div>➤</div>SURE1STPAT21</div> <div><div>➤</div>CTRMCAMV35S</div> <div><div>➤</div>AE-box</div> <div><div>➤</div>TCA-element</div> <div><div>➤</div>TGA-element</div> <div><div>➤</div>PYRIMIDINE-rich stretch</div> <div><div>➤</div>TATABOX2</div> <div><div>➤</div>TATABOX4</div> <div><div>➤</div>MYBST1</div> <div><div>➤</div>AMYBOX1</div> <div><div>➤</div>SEF1MOTIF</div> <div><div>➤</div>PROLAMINBOXOSGLUB1</div> <div><div>➤</div>WBOXNTCHN48</div> <div><div>➤</div>HDZIP2ATATHB2</div> <div><div>➤</div>MYBGAHV</div> <div><div>➤</div>DRECRTCOREAT</div> <div><div>➤</div>SEF3MOTIFGM</div> <div><div>➤</div>TC-rich repeats</div>	<div><div>➤</div>ABRE</div> <div><div>➤</div>TGACG-motif</div> <div><div>➤</div>DPBFCOREDCDC3</div> <div><div>➤</div>ARFAT</div> <div><div>➤</div>CGTCA-motif</div> <div><div>➤</div>ARE</div> <div><div>➤</div>SURECOREATSULTR11</div> <div><div>➤</div>L1BOXATPDF1</div> <div><div>➤</div>ANAERO1CONSENSUS</div>	

Figure 13. *Cis*-acting regulatory elements identified in *PSKR* promoter regions.

Putative *cis*-elements found exclusively in promoter regions of *PSKR1* or *PSKR2* are shown above. Motifs in bold denote responsiveness to ABA or different stresses. **A)** Motifs identified only in the *PSKR1* promoter. **B)** Motifs identified only in the *PSKR2* promoter.

Table 1. Predicted *cis*-elements specific to the *PSKR1* promoter.

Category	Identified CAREs	Consensus sequence	Position	Function
Hormone responsive	CAREOSREP1	CAACTC	-256, -1338	Gibberellin regulated proteinase expression
	GARE2OSREP1	TAACGTA	-1162	Gibberellin responsive
	TCA-element	TCAGAA	-107, -268	Salicylic acid responsive
	TGA-element	AACGAC	-549, -1052	Auxin responsive
	PYRIMIDINEBOXHV EPB1	TTTTTCC	-1063	ABA and Gibberellin responsive
Stress responsive	TC-rich repeats	ATTTCTTC	-562	Defense and stress responsive
	WBOXNTCHN48	CTGACY	-854	Elicitor responsive element that binds WRKY1, WRKY2 and WRKY4 transcription factors
	BOXLCOREDCPAL	ACCWWCC	-1113	Elicitor responsive
	MYBST1	GGATA	-1568	Stress responsive and binding site for ANAC074
	DRERTCOREAT	RCCGAC	-1417	CBFs/DREBs interact and control the expression of drought and many stress-inducible genes
Enhancers	PYRIMIDINE-rich stretch	TTCTTCTCT	-47	Conferring high transcription levels
	CTRMCAV35S	TCTCTCTCT	-156, -235	Gene expression enhancer
Light responsive	HDZIP2ATATHB2	TAATMATTA	-812	Light responsive
	AE-box	AGAAACAT	-647	Part of a module for light response

Table 1. (Continued) Predicted *cis*-elements specific to the *PSKR1* promoter.

Category	Identified CAREs	Consensus sequence	Position	Function
Conserved promoter motifs	TATAPVTRNALEU	TTTATATA	-1373, -1394	TATA-like motif
	TATABOX2	TATAAAT	-691	Members of TATA-box
	TATABOX4	TATATAA	-1370, -1393	Members of TATA-box
Embryo related	PROLAMINBOXOSGLUB1	TGCAAAG	-921	Endosperm specific
	SEF3MOTIFGM	AACCCA	-799	Embryo specific
	SEF1MOTIF	ATATTTAWW	-338	Modulates embryo development
Miscellaneous	10PEHVPSBD	TATTCT	-25	Chloroplast related
	SURE1STPAT21	AATAGAAAA	-960	Sucrose responsive element
	AMYBOX1	TAACARA	-391	Amylase element

Table 2. Predicted *cis*-elements specific to the *PSKR2* promoter.

Category	Identified CAREs	Consensus sequence	Position	Function
Hormone responsive	ABRE	ACGTG	-158	ABA responsive
	TGACG-motif	TGACG	-371	MeJA responsive
	DPBFCOREDCDC3	ACACNNG	-759	ABA responsive
	ARFAT	TGTCTC	-16, -547	Auxin responsive
	CGTCA-motif	CGTCA	-489	MeJA responsive
Miscellaneous	ARE	TGGTTT	-233	Anaerobic induced
	SURECOREATSULTR11	GAGAC	-513, -748	Core of sulfur-responsive element
	L1BOXATPDF1	TAAATGYA	-1314	Embryo specific
	ANAERO1CONSENSUS	AAACAAA	-777	Oxygen-responsive element

Another important category of *cis*-elements that could be found in the *PSKR1* promoter region was the enhancers. A PYRIMIDINE-rich stretch identified at 47 bp, CTRMCAMV35S at 156 bp and 235 bp upstream, but in close proximity to the ATG codon might facilitate increased transcription rates of *PSKR1*. Additionally, three conserved TATA-box like motifs were identified of which two were TATAPVTRNALEU motifs, one TATABOX2 and two TATABOX4. Other categories included CAREs that respond to environmental stimuli such as light or that are responsible for organ-specific expression patterns (Table 1).

Conversely, there was only one important category observed in the *PSKR2* promoter that contained two ABA responsive elements, ABRE that binds AREB transcription factors directly and initiates expression in response to ABA-mediated signaling pathways while DPBFCOREDCDC3 binds bZIP transcription factors that are indirectly regulated by ABA-dependent signaling pathways (Tiwari et al., 2016) and two methyl jasmonate (MeJA) motifs, TGACG and CGTCA.

Altogether, we predicted almost three times more CAREs in the *PSKR1* promoter region compared to the *PSKR2* promoter. Presence of dehydration and elicitor responsive elements predicted only in the *PSKR1* promoter region reveals the possibility that *PSKR1* transcription could depend on these CAREs for activation upon osmotic and pathogen stress treatments. In addition, the presence of enhancers and TATA-box members might be responsible for high transcript levels of *PSKR1* compared to *PSKR2* under control conditions as these elements tightly regulate initiation and enhance transcription. Alternatively, the ABA-responsive elements identified in the *PSKR2* promoter region were probably not crucial elements required for *PSKR2* activation on tested stress treatments. Thus, from prediction studies it is apparent that absence of essential CAREs in the *PSKR2* promoter led to weak or no transcription and could ultimately account for non-functional *PSKR2*.

4.4.5 Potential differences in LRR2 contrastive to LRR1 determined through computational analysis

Followed by our finding that LRR1 is required for full activation of the PSK receptor, we were intrigued to explore how LRR2 differed in action compared to LRR1. It is well-established that in *Arabidopsis*, PSKR1 contains 21 LRR repeats with an island domain that provides an interface for PSK interaction and is located between LRR17 and LRR18 (Matsubayashi et al., 2002; Wang et al., 2015; Sauter 2015; Chakraborty 2019). The crystal structure of PSK-LRR1 and LRR1-SERK1 is also available (Wang et al., 2015) and PSK interacts with PSKR1 at a dissociation constant of 7.7 nM (Matsubayashi et al., 2006). But so far, no appropriate information on the number of LRR repeats in PSKR2, the crystal structure or the binding affinity of PSK-LRR2 is known which hampers our efforts to fully elucidate the differences between both LRRs. Therefore, in an attempt to understand this, we started out to first investigate if both the receptors varied in the number of LRR repeats. This was important because the LRR tandem repeats facilitate formation of a slender conformation thereby maximizing the surface area making it ideal for protein-protein interactions (Padmanabhan et al., 2008) stipulating that a change in numbers can contribute to alterations in PSK or co-receptor interactions with LRRs.

A LRR consensus

LRR consensus	LxxLxLxxNxLGxIPxxLxxLxx	23
---------------	-------------------------	----

B PSKR1

PSKR1-LRR1	77	VIRLELGNNKLSGKLSLSESLGKLDE	24
PSKR1-LRR2	101	IRVLNLSRNFIKDSIPLSIFNLKN	24
PSKR1-LRR3	125	LQTLDLSSNDLSGGIPTSLNLP	23
PSKR1-LRR4	148	LQSFDLSSNKFNGSLPSHICHNSTQ	25
PSKR1-LRR5	173	IRVVKLAVNYLAGNFTSGFGKCVL	24
PSKR1-LRR6	197	LEHLCLGMNDLTGNIPEDLFLHKL	24
PSKR1-LRR7	221	LNLLGIQENRLSGSLREIRNLSS	24
PSKR1-LRR8	245	LVRDLVSWNLFSGEIPDVFDLPQ	24
PSKR1-LRR9	269	LKFFLGQTNGFIGGIPKSLANSPS	24
PSKR1-LRR10	293	NLLNLRNNSLSGRLMLNCTAMIA	23
PSKR1-LRR11	317	NSLDLGTNRFNGLPENLPDCKR	23
PSKR1-LRR12	341	KNVNLRNTFHGQVPESFKNFES	23
PSKR1-LRR13	365	LSYFSLSNSSLANISSALGILQHCKN	26
PSKR1-LRR14	391	LTTLVLTLNFHGEALPDDSSLHFKEK	25
PSKR1-LRR15	416	LKVLVAVNCRLTGSMRWLSSSNE	24
PSKR1-LRR16	440	LQLDLNRLTGAIPSWIGDFKA	24
PSKR1-LRR17	464	LFYDLNNSFTGEIPKSLTKLESLSRNISVNEPSPDFPFMKNESARALQYNQIFGF	60
PSKR1-LRR18	524	PPTIELGHNNLSGPIWEEFGNLKK	24
PSKR1-LRR19	548	LHVFDLKNALSGSIPSSLSGMTS	24
PSKR1-LRR20	572	LEALDLNRLSGSIPVSLQQLSF	24
PSKR1-LRR21	596	LSKFSVAYNNLSGVIIPSGGQFQTFPNSSSFESNHLCEHRFPCSEGTESALIKRSRRSRGGDI	62

C PSKR2

PSKR2-LRR1	65	VTKLVLPEKGLEGVISKSLGELTE	24
PSKR2-LRR2	89	LRVLDLSRNQLKGEVPAEISKLEQ	24
PSKR2-LRR3	113	LQVLDLSHNLSSGSLGVVSGKL	24
PSKR2-LRR4	137	IQSLNLSNLSGKLSGVGVFP	23
PSKR2-LRR5	160	LVMLNVSNNLFEGEIHPELCSSSGG	25
PSKR2-LRR6	185	IQVLDLSMNLVGNLDGLYNCSKS	24
PSKR2-LRR7	209	IQQLHIDSNGLTGQLPDYLYSIRE	24
PSKR2-LRR8	233	LEQLSLSGNYLSGELSKNLNLSG	24
PSKR2-LRR9	257	LKSLISENRFSGVIPDVFGNLTQ	24
PSKR2-LRR10	281	LEHLDVSSNKFSGRFPSPSLQCSK	24
PSKR2-LRR11	305	LRVLDLRNNSLSGSINLNTGFTD	24
PSKR2-LRR12	329	LCVLDLASNHFSGLPDSLGHCPK	24
PSKR2-LRR13	353	MKILSLAKNEFRGKIPDTFKNLQS	24
PSKR2-LRR14	377	LLFLSLSNNSFVDFSETMNVLQHCRN	26
PSKR2-LRR15	403	LSTLILSKNFIEGEEIPNNVTGFDN	24
PSKR2-LRR16	427	LAILALGNCGLRGQIPSWLLNCKK	24
PSKR2-LRR17	451	LEVLDLSWNHFGYGTIPHWIGKMS	24
PSKR2-LRR18	475	LFYIDFSNNTLTGAIPVAITELKNLIRLNGTASQMTDSSGIPLYVKRNKSSNGLPYNQVSRF	62
PSKR2-LRR19	537	PPSIYLNNNRLNGTILPEIGRLKE	24
PSKR2-LRR20	561	LHMDLSRNFTGTIPDSISGLDN	24
PSKR2-LRR21	585	LEVLDLSYNHLYGSIPLSFQSLTF	24
PSKR2-LRR22	609	LSRFSVAYNRLTGAIPSGGQFYSPHSSFEGLGLCRAIDSPCDVLMNMLNPKGSSRRNNNGGKFGFR	68

Figure 14. Determination of LRR repeats in PSKR1 and PSKR2.

The amino acid sequences of LRRs from PSKR1 and PSKR2 without the signal sequence and transmembrane helix were used to identify the leucine rich repeats (LRRs). A web-based tool Phyto-LRR, (<https://phytolrr.com/findlrr>) was used for the determination of LRR repeats (Chen, 2021). (A) The LRR consensus sequence is highlighted. (B) 21 LRR repeats were identified in PSKR1 as previously described (Matsubayashi et al., 2002) and (C) 22 LRR repeats were identified in PSKR2. The island domain is underlined red.

Amino acid residues from PSKR-LRRs were fed into PhytoLRR (<https://www.phytolrr.com/findlrr>), an online database tool used for predicting LRR repeats (Chen, 2021). The tool accurately predicted 21 LRRs in PSKR1 as previously reported (Matsubayashi et al., 2002; Wang et al., 2015; Sauter 2015; Chakraborty 2019) and 22 LRRs in PSKR2 (Fig. 14). The LRR2 featured highly regular LRR repeats mostly about 24 aa length and the island domain was located between LRR18 and LRR19. Hence, an additional LRR repeat was identified in LRR2 compared to LRR1 and how much this affects signaling requires further studies.

Since the crystal structure of PSK-LRR1 and LRR1-SERK1 is solved, the amino acid residues in LRR1 that interact with PSK and SERK1 are known. Therefore, we performed a sequence alignment with amino acid residues of LRR1 and LRR2 to check if PSK-LRR and SERK1-LRR interaction between the LRRs were conserved (Fig. 15). Most PSK-interacting residues of LRR1 were highly conserved or similar in LRR2. Out of 16 residues identified in LRR1 that interact with PSK, three residues, Leu-399, Ala-423 and Ala-515 were replaced by Lys, Gly and Gly in LRR2.

PSKR1-LRR	PEDLFHLKRL	NLLGIQENRL	SGSLSRREIRN	LSSLVRLDVS	252
PSKR2-LRR	PDYLYSIREL	EQLSLSGNYL	SGELSKNLSN	LSGLKSL LIS	264
PSKR1-LRR	WNLFSGEIPD	VFDELPQLKF	FLGQTNGFIG	GIPKSLANS P	292
PSKR2-LRR	ENRFSGVIPD	VFGNLTQLEH	LDVSSNKESG	RFPPSLSQCS	304
PSKR1-LRR	S L N L L N L R N N	S L S G R I M L N C	T A M I A L N S L D	L G T N R F N G R L	332
PSKR2-LRR	K L R V L D L R N N	S L S G S I N L N F	T G F T D L C V L D	L A S N H F S G P L	344
PSKR1-LRR	P E N L P D C K R L	K N V N L A R N T F	H G Q V P E S F K N	F E S L S Y F S L S	372
PSKR2-LRR	P D S L G H C P K M	K I L S L A K N E F	R G K I P D T F K N	L Q S L L F L S L S	384
PSKR1-LRR	N S S L A N I S S A	L G I L Q H C K N L	T T L V L T L N F H	G E A L P D D S S L	412
PSKR2-LRR	N N S F V D F S E T	M N V L Q H C R N L	S T L I L S K N F I	G E E I P N N V T -	423
PSKR1-LRR	H F E K L K V L V V	A N C R L T G S M P	R W L S S S N E L Q	L L D L S W N R L T	452
PSKR2-LRR	G F D N L A I L A L	G N C G L R G Q I P	S W L L N C K K L E	V L D L S W N H F Y	463
PSKR1-LRR	G A I P S W I G D F	K A L F Y L D L S N	N S F T G E I P K S	L T K L E S L T S R	492
PSKR2-LRR	G T I P H W I G K M	E S L F Y I D F S N	N T L T G A I P V A	I T E L K N L I R L	503
PSKR1-LRR	N I S V N E - - P S	P D F P F F M K R N	E S A R A L Q Y N Q	I F G F P P T I E L	530
PSKR2-LRR	N G T A S Q M T D S	S G I P L Y V K R N	K S S N G L P Y N Q	V S R F P P S I Y L	543
PSKR1-LRR	G H N N L S G P I W	E E F G N L K K L H	V F D L K W N A L S	G S I P S S L S G M	570
PSKR2-LRR	N N N R L N G T I L	P E I G R L K E L H	M L D L S R N N F T	G T I P D S I S G L	583
PSKR1-LRR	T S L E A L D L S N	N R L S G S I P V S	L Q Q L S F L S K F	S V A Y N N L S G V	610
PSKR2-LRR	D N L E V L D L S Y	N H L Y G S I P L S	F Q S L T F L S R F	S V A Y N R L T G A	623
PSKR1-LRR	I P S G G Q F Q T F	P N S S F E S N - H	L C G E H R F P C S	E G T E S A L - I K	648
PSKR2-LRR	I P S G G Q F Y S F	P H S S F E G N L G	L C R A I D S P C D	V L M S N M L N P K	663
PSKR1-LRR	R - S R R - S R G G	D I - -	658		
PSKR2-LRR	G S S R R N N N G G	K F G R	677		

Figure 15. PSK perception and SERK1 interaction with PSKRs are mostly conserved.

A ClustalW sequence alignment was performed using the amino acid sequences of LRRs from PSKR1 and PSKR2. Conserved and similar sequences are highlighted in black and grey, respectively. The red rectangular boxes denote the residues that are involved in interaction with PSK, and the blue circles denote the residues interacting with SERK1.

The SERK-interacting residues were also mostly conserved in LRR2 where out of 11 amino acid residues identified only 2 residues, Gly-523 and Gln-618 in LRR1 were replaced by Arg and Tyr in LRR2.

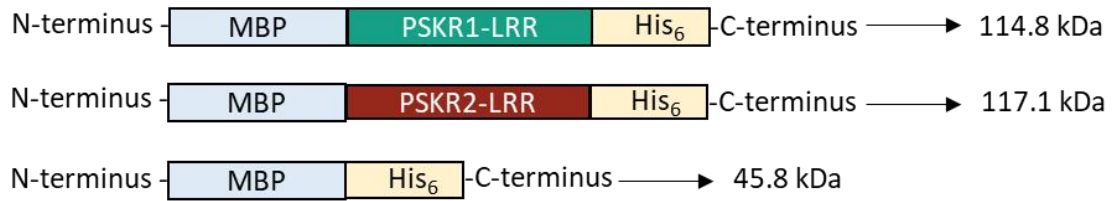
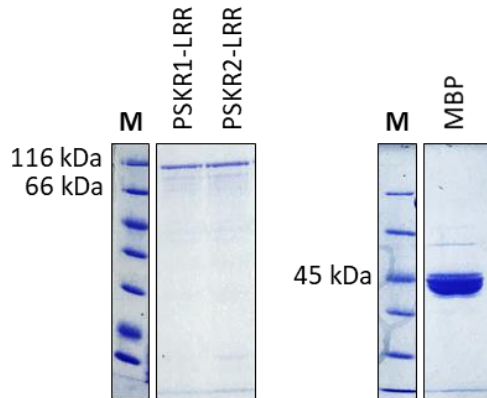
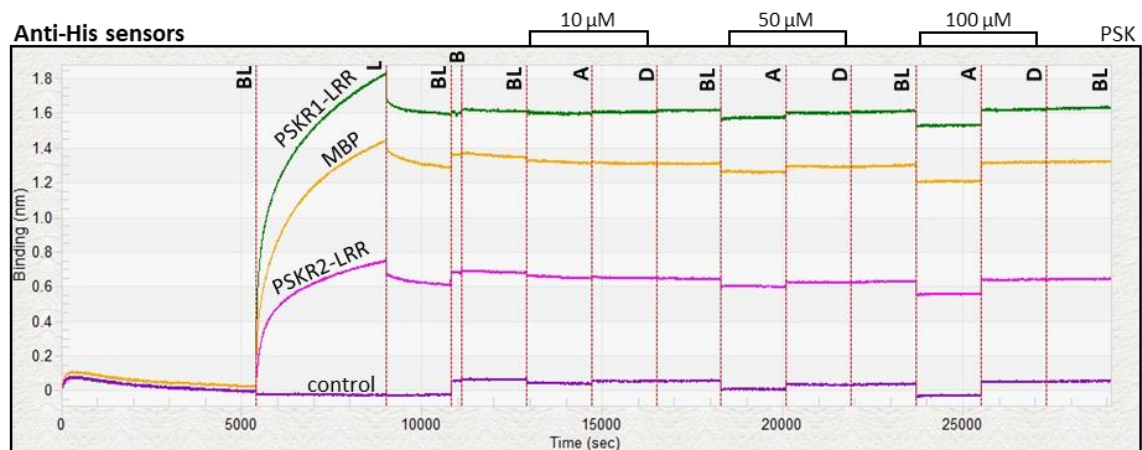
A**B****C**

Figure 16. Assessing binding of PSK to immobilized PSKRs by biolayer interferometry (BLI).

The LRR regions of PSKRs without the transmembrane helix were used for expression of PSKR-LRR proteins containing an MBP-tag and a His-tag. Anti-His sensors were used for affinity binding analysis with the BLI system. (A) Schematic representation of the protein constructs used and their respective molecular weights. (B) SDS-PAGE of the proteins. (C) PSKR-LRRs and MBP protein bound onto anti-His sensors with no possible interaction at different concentrations of PSK (BL – baseline; B – blocking with biocytin; L – loading; A – association; D – dissociation).

To obtain further insights into PSK interaction with PSKRs, we employed bio-layer interferometry (BLI) to analyze the binding affinities of PSK to LRRs. BLI is a label-free system that measures biomolecular interactions by analyzing the interference patterns of white light reflected from the surface of a biosensor tip. The protein of interest is coupled to the biosensor and subsequently dipped into a ligand containing solution to monitor binding events. For this, we expressed and purified recombinant PSKR-LRR proteins in *E. coli*, carrying an MBP-tag at the N-terminus and a His₆-tag at the C-terminus (Fig. 16A). The His₆-tag was important to bind Anti-His sensors (His1K), while the MBP-tag facilitates solubilization of recombinant proteins.

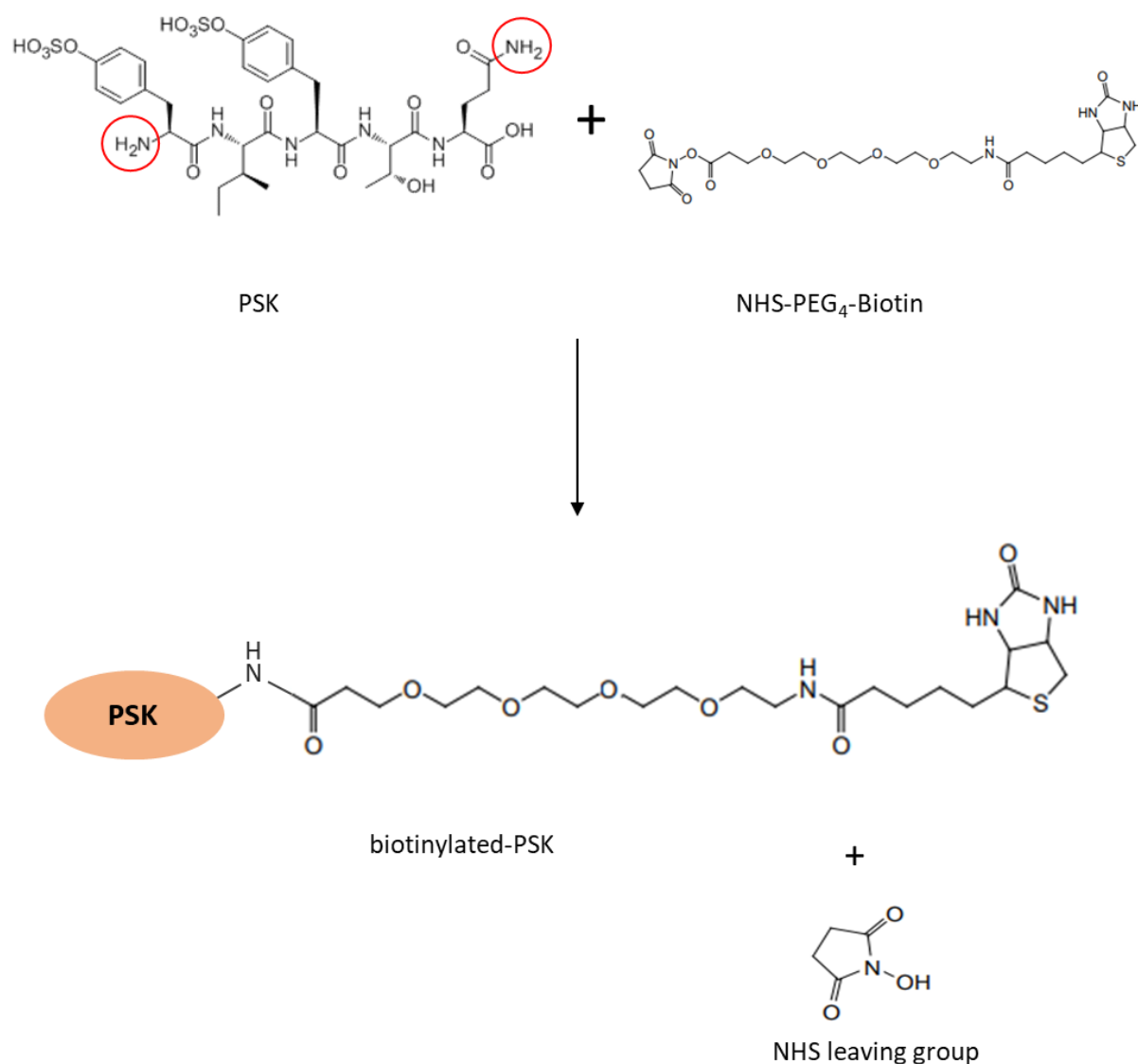


Figure 17. Reaction of NHS-PEG₄-Biotin with primary amines of PSK.

The peptide, PSK, was incubated with biotin for two hours on ice to facilitate binding to streptavidin sensors. The red circles show the amine groups in PSK that can potentially be labelled with some proportions of the biotin molecules during the reaction. *N*-hydroxysuccinimide (NHS) is the leaving group in the reaction.

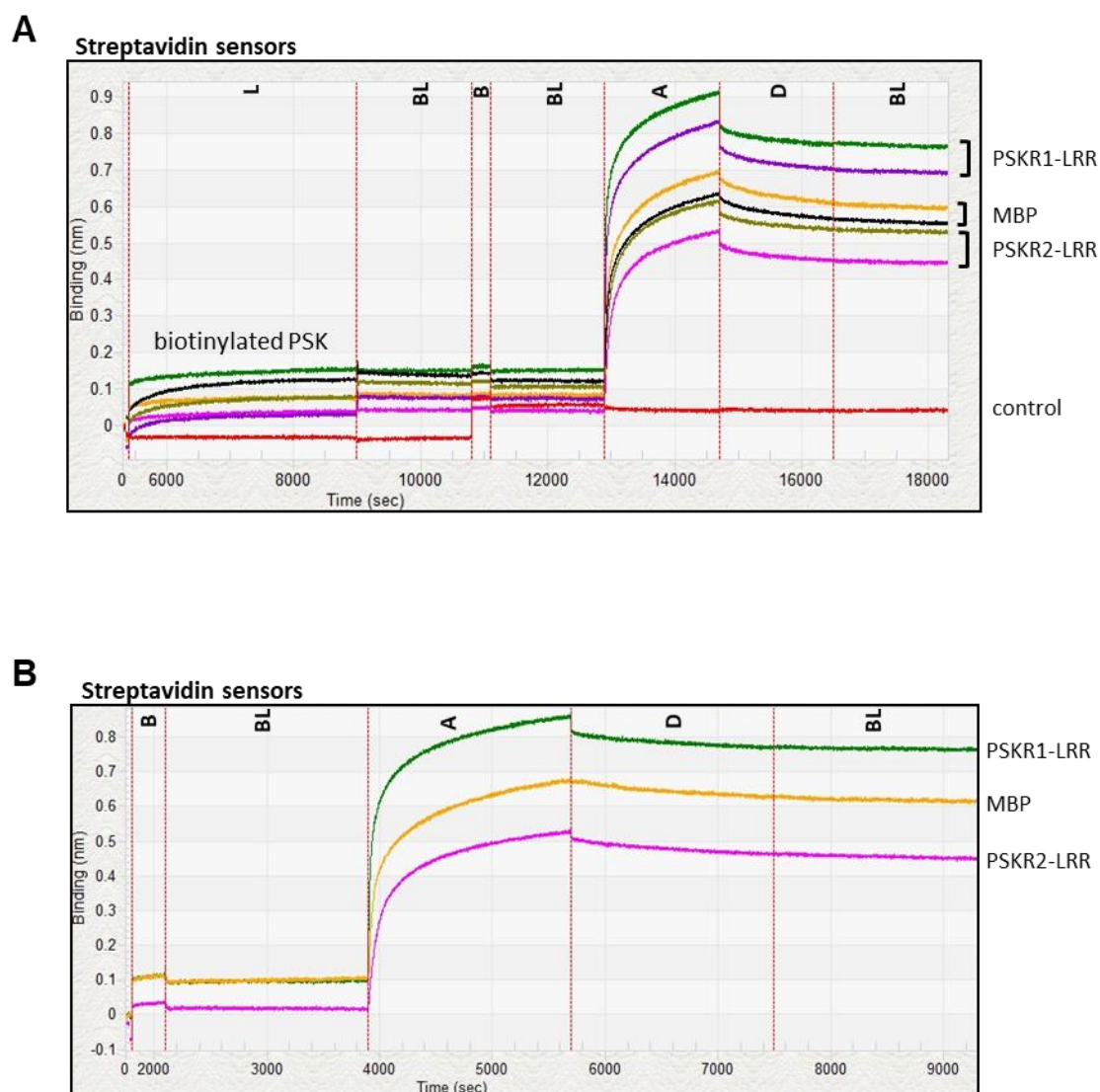


Figure 18. Biotinylated-PSK immobilized to bind PSKR-LRRs.

(A) Two different concentrations of PSK (100 μ M and 200 μ M) were biotinylated to bind streptavidin sensors and their interaction with PSKR-LRRs and MBP is shown. (B) PSKR-LRRs and MBP let to bind streptavidin sensors to check non-specific binding (BL – baseline; B – blocking with biocytin; L – loading; A – association; D – dissociation).

Since MBP was fused to the N-terminus, we wanted to include an MBP-His₆-tag protein as a control to detect the possibilities of any non-specific interaction of PSK to the LRRs. After successful expression (Fig. 16B), we started out by coupling PSKR-LRRs and MBP recombinant proteins to His1K sensors followed by blocking of untreated His1K sensors using biocytin. Despite good loading efficiency (Fig. 16C), subsequent exposure to different concentrations of PSK showed no signals above the background noise indicating that this approach might not be feasible owing to the detergent used in the purification of recombinant proteins. The size of the solubilizing detergent (Triton

X-100) micelles could have limited the density of immobilized protein at the sensor surface. Hence, we reversed the setup of the assay by binding the small molecule, PSK to the sensor. For this, we biotinylated PSK by incubating PSK with NHS-PEG₄-Biotin (Fig. 17). The biotinylated PSK carries a biotin moiety which enabled coupling of PSK to streptavidin-coated sensors (SA). 100 μ M and 200 μ M concentrations of PSK were used for monitoring interaction. This time we observed quite good signals denoting interaction with PSKR-LRRs at both concentrations of PSK (Fig. 18A) and to reassure this result, we used free-SA sensors and subsequently exposed to PSKR-LRRs/MBP proteins to check for non-specific binding (Fig. 18B). Since biotin is absent in PSKR-LRRs/MBP recombinant proteins there should be no signal but to our dismay, we observed good peaks signifying non-specific interaction. Therefore, this approach needs further optimization in the future. This was unfortunate and therefore we were only able to show computational differences between LRRs.

4.5 DISCUSSION

Based on the finding that only PSKR1 but not PSKR2 drives growth-promoting effects of PSK and positively regulates shoot growth under osmotic and pathogen stress conditions (Rajamanickam et al., bioRxiv; Igarashi et al., 2012) prompted us to investigate whether differential gene expression or specific receptor characteristics are responsible for the differences in receptor activity between the PSKRs. Using a chimeric receptor approach followed by functional analysis of hybrid receptors, we were able to dissect which receptor component of PSKR2 contributed to its non-functionality in response to the above-mentioned stress conditions.

4.5.1 Transcriptional control of *PSKR1* by putative osmotic- and PTI-responsive CAREs is absent in the promoter region of *PSKR2*

We show that the promoter of *PSKR1* is crucial for PSKR activity and *PSKR2* expressed under the control of the *PSKR1* promoter regained receptor activity suggesting that PSKR2 domains are functional. This led us to the conclusion that the promoter of *PSKR2* accounted for the complete loss of PSKR2 activity. To proof this, we tested the expression of *PSKR1* and *PSKR2* upon both osmotic and pathogen stress and observed that only *PSKR1* was induced, indicating that *PSKR2* was not responsive to these stress conditions, or the developmental stage tested in this study to exert a response. This pattern, that control of *PSKR1* expression by its native promoter is important for PSKR1 function was also reported in positive regulation of growth against pathogen infection (Igarashi et al., 2012). On the other hand, *PSKR2* was constitutively expressed at relatively low levels even in untreated shoots after seven and 14 days of transfer which we hypothesized to be the reason for physiological differences in shoot growth observed between knock-out mutants *pskr1-3* and *pskr2-1* under control conditions (Fig. 1).

The activation and inactivation of genes participating in signaling pathways is regulated by several mechanisms, including the binding of transcription factors (TFs) to *cis*-elements in the promoter regions of target genes, which thereby become activated or suppressed (Lindl f et al., 2009). To the best of our knowledge, no study to date has

examined the *cis*- and *trans*-factors that regulate *PSKR*s expression. Therefore, we characterized CAREs of *PSKR*s and identified their potential function through *in-silico* analysis.

Interestingly, only the promoter of *PSKR1* contained a DRE/CRT (dehydration-responsive element/C-repeat) *cis*-element which is commonly found in promoters of numerous stress-inducible genes and is responsible for ABA-independent induction of several genes in response to osmotic stress in many plants including *Arabidopsis* (Yamaguchi-Shinozaki and Shinozaki, 1994, 2005; Singh and Laxmi, 2015). On the other hand, one copy of the ABRE (ABA-responsive element) *cis*-element was identified exclusively in the promoter region of *PSKR2*. Most ABA-responsive genes are regulated by ABRE in their promoter region and is therefore responsible for ABA-dependent regulation of gene expression under drought stress (Nakashima et al., 2009; Yoshida et al., 2015). It is known that both ABA-dependent and ABA-independent pathways regulate the transcriptional response of TFs upon drought stress (Nakashima et al., 2009). However, a single copy of an ABRE is not sufficient to induce a response and requires other copies of ABRE in proximity or coupling element to function as an active CARE and induce ABA-responsive gene expression (Choi et al., 2000; Uno et al., 2000; Fujita et al., 2011). In contrast, a single copy of DRE/CRT is sufficient to induce genes under osmotic stress (Yamaguchi-Shinozaki and Shinozaki, 1994). Therefore, we hypothesize that the DRE/CRT in the promoter region of *PSKR1* contributes to its osmotic stress-responsiveness and a single copy of ABRE in the promoter region of *PSKR2* could not render this response.

Two elicitor-responsive CAREs were identified in the promoter region of *PSKR1*, WBOXNTCHN48 (Yamamoto et al., 2004) and BOXLCORED CPAL (Maeda et al., 2005) that maybe responsible for regulating transcription upon PTI. On the contrary, no potential elicitor-responsive CAREs could be identified in the promoter region of *PSKR2* which could be the reason why *PSKR1* but not *PSKR2* is induced upon PTI.

While we do not have experimental evidence yet to conclude that the CAREs, DRE/CRT, WBOXNTCHN48 and BOXLCORED CPAL are essential for regulation of *PSKR1* upon osmotic and pathogen stress conditions, their identification as candidate regulators is a step forward for more detailed future analysis of the molecular factors required for transcriptional regulation and biological function of *PSKR*s. Taken together

these results point to differential molecular regulation of *PSKR1* and *PSKR2* expression.

4.5.2 Computational analysis identified a residue that differed between the LRRs which is crucial for a functional ligand binding domain

We next observed that *PSKR1* expressed under the control of the *PSKR2* promoter slightly improved PSKR activity compared to *PSKR2* expressed under the control of the *PSKR2* promoter upon tested stress conditions, even though we report that the promoter of *PSKR2* exerts weak activity, suggesting that the LRRs and KDs of both PSKRs also differed in their activity.

Binding of PSK to the LRR of PSKR induces signaling mediated by Ca^{2+} /CaM binding and the kinase activity of PSKR (Hartmann et al., 2014), suggesting that ligand binding activates the KD of PSKR, a pattern observed in well-studied receptor-like kinases (RLKs) such as flagellin insensitive 2 (FLS2) and brassinosteroid insensitive 1 (BR11) (Belkhadir et al., 2014). Also, PSKRs utilize a member of the somatic embryogenesis receptor-like kinases (SERKs) that generally act as co-receptors and are required for their activation (Belkhadir et al., 2014; Han et al., 2014b).

Since the KD of *PSKR1* (Hartmann et al., 2015; Kaufmann and Sauter, 2017) and *PSKR2* (Kaufmann, 2018) are functional as reported earlier, we examined only the LRRs of both receptors to detect potential differences between them that caused the LRR of *PSKR1* to contribute for full activation of PSK/PSKR signaling.

Our efforts to determine the binding affinities of PSK to PSKRs could not be achieved in this study as further optimization of the ligand binding assays were required. This was unfortunate and therefore we were only able to show computational differences between LRRs. Nevertheless, computational prediction is the first critical step in analyzing protein-protein interactions (Zahiri et al., 2013). The crystal structure of PSK-LRR1 and LRR1-SERK1 was solved (Wang et al., 2015). Using these data, we performed a sequence alignment and determined the PSK- and SERK1-interacting amino acid residues in LRR2. Only three residues differed between the LRRs that interacted with PSK. Among them, Leu-399 that is a critical residue interacting with the sulfate moiety in PSK. Substitution of this residue has been shown to compromise

PSK-LRR1 association (Wang et al., 2015). Ala substitution by Gly should possibly not make a huge difference as Gly is conserved in carrot DcPSKR, an orthologue of PSKR (Wang et al., 2015). Only two residues differed between the LRRs that interacted with SERK1. Until today, there is no information regarding substitutions at these residues that could intervene the interaction between SERK1 and LRRs. So, further studies are required to elucidate this.

At this stage we can only describe that the differences in LRR activities could be originating from the diversification of amino acid residue Leu-399 in LRR1 substituted by Lys predicted in LRR2 that is crucial for PSK interaction. This correlates with findings by Wang et al. (2015) where they showed root length analysis performed with mutation at this residue compromised root lengths. Thus, weak association of PSK to LRR2 might contribute to the minor reduction observed in shoot and root growth analysis of plants expressing hybrid receptors under osmotic and pathogen stress.

4.6 CONCLUSION

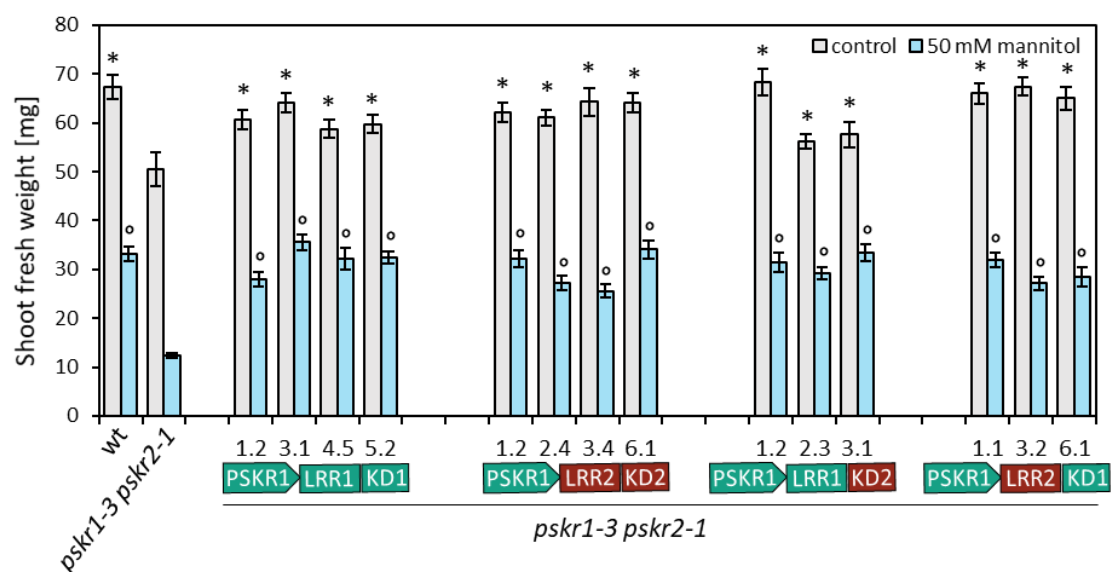
In this study, we started out with the knowledge that PSKR2 is functionally redundant to PSKR1 but was non-functional upon osmotic and pathogen stress while PSKR1 showed tolerance. To decipher differences in their receptor activity we utilized a chimeric receptor approach. Overall, our results show that the promoter of *PSKR2* is not responsive to these stress conditions as it lacked the important CAREs required for transcription. The PSKR2 domains regained receptor activity under the control of the *PSKR1* promoter. LRR2 exhibited minor differences compared to LRR1 in receptor activity which arises from lack of an essential amino acid at the PSK-LRR2 interaction site. In conclusion, PSKR2 might not be contributing to PSK/PSKR activity under osmotic and pathogen stress conditions. However, other stress conditions and developmental stages need to be examined properly to conclude its function.

4.7 AUTHOR CONTRIBUTIONS

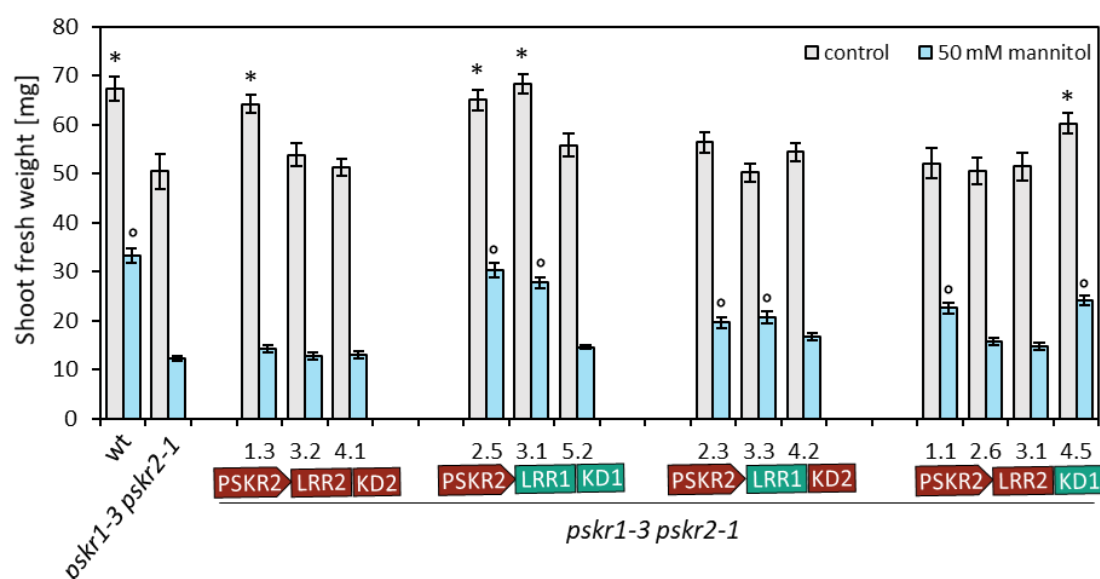
Margret Sauter conceived the project. Margret Sauter and I designed the experiments. Timo Staffel generated the hybrid receptor lines. I did the research. The data were analyzed by me and Margret Sauter. I wrote the chapter.

4.8 SUPPLEMENTARY MATERIAL

A



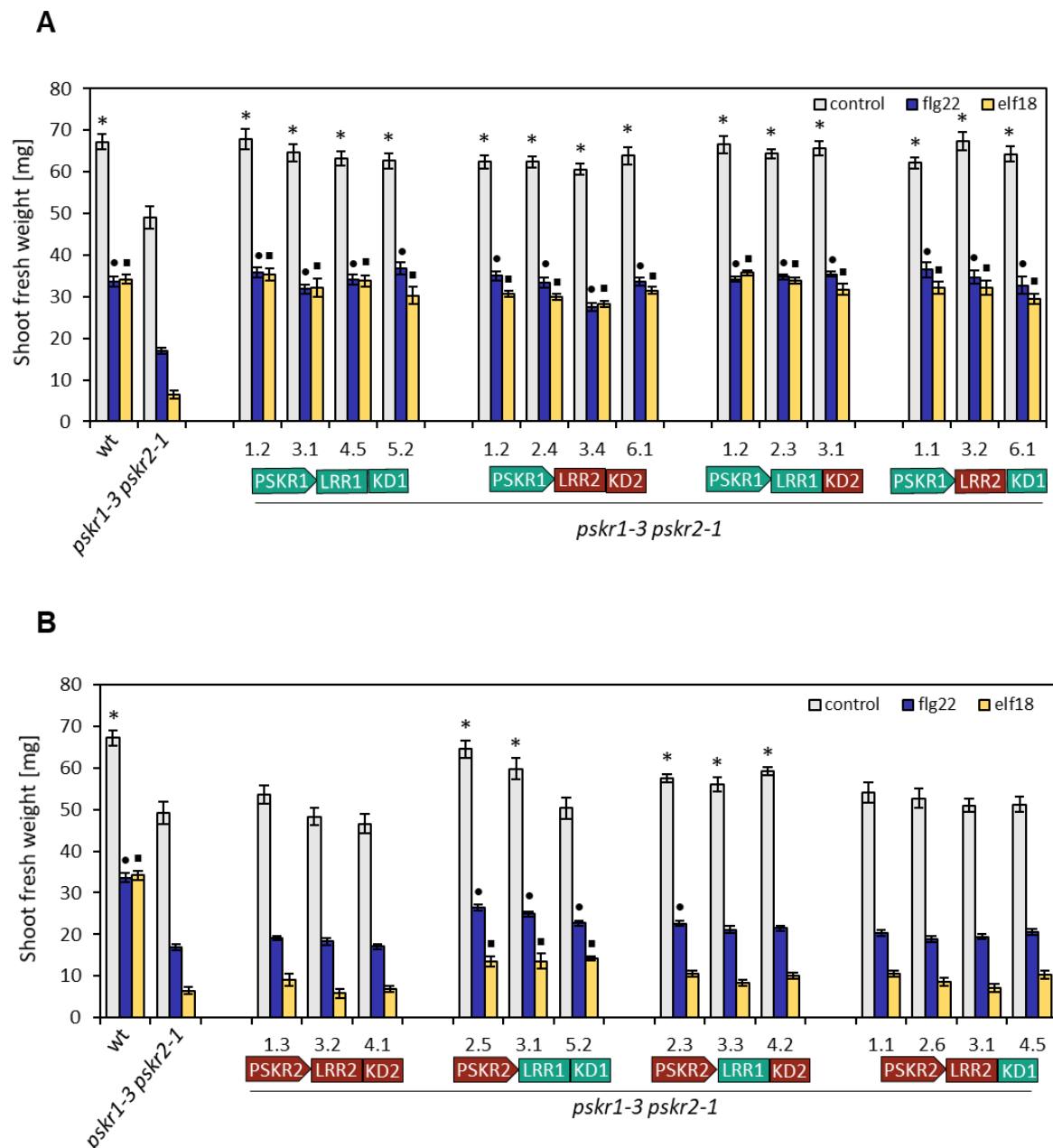
B



Supplementary Figure S1. Effect of osmotic stress on shoot growth of lines each expressing a hybrid receptor gene.

Seedlings were pregrown for four days and then transferred to medium supplemented with or without 50 mM mannitol. Average shoot fresh weights (\pm SE) were determined after 2 weeks. At least 12 seedlings per independent line and per condition were analyzed. The numbers on the x-axis represent independent lines each expressing a receptor hybrid. Results are averages obtained from three independent experiments. Green represents the promoter and domains of *PSKR1*, and red represents *PSKR2*. Shoot fresh weights of hybrid receptor lines expressed under control of the (A) *PSKR1* promoter

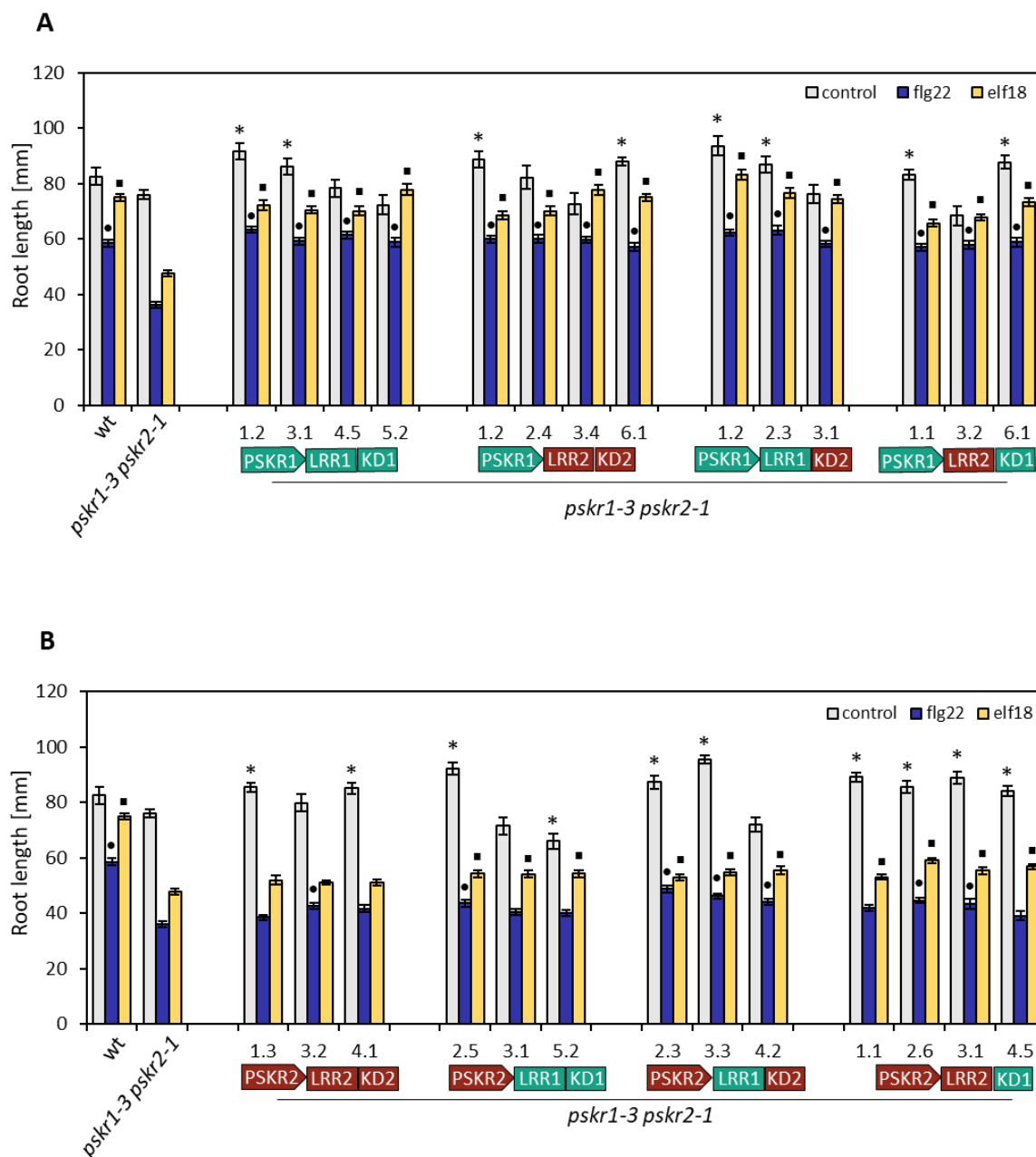
and (B) *PSKR2* promoter. * and ° indicate significant differences in comparison to *pskr1-3 pskr2-1* in control and mannitol treatments, respectively (Kruskal-Wallis test, $P < 0.05$, $n = 36$).



Supplementary Figure S2. Effect of MAMPs on shoot growth of lines each expressing a hybrid receptor gene.

Seedlings were pregrown for four days and then transferred to medium supplemented with or without 0.6 nM flg22 or 0.7 nM elf18. Average shoot fresh weights (\pm SE) were determined after 2 weeks. At least 12 seedlings per independent line and per condition were analyzed. The numbers on the x-axis represent independent lines each expressing a receptor hybrid. Results are averages obtained from three independent experiments. Green represents the promoter and domains of *PSKR1*, and red represents *PSKR2*. Shoot fresh weights of hybrid receptor lines expressed under control of the (A)

PSKR1 promoter and **(B)** *PSKR2* promoter. *, • and ▪ indicate significant differences in comparison to *pskr1-3 pskr2-1* under control, flg22 and elf18 treatments, respectively (Kruskal-Wallis test, $P < 0.05$, $n = 36$).



Supplementary Figure S3. Effect of MAMPs on root growth of lines each expressing a hybrid receptor gene.

Seedlings were pregrown for four days and then transferred to medium supplemented with or without 0.6 nM flg22 or 0.7 nM elf18. Average root lengths (\pm SE) were determined after 7 days. At least 12 seedlings per independent line and per condition were analyzed. The numbers on the x-axis represent

independent lines each expressing a receptor hybrid. Results are averages obtained from three independent experiments. Green represents the promoter and domains of *PSKR1*, and red represents *PSKR2*. Root lengths of hybrid receptors expressed under control of the (A) *PSKR1* promoter and (B) *PSKR2* promoter. *, • and ▪ indicate significant differences in comparison to *pskr1-3 pskr2-1* up on control, flg22 and elf18 treatments, respectively (Kruskal-Wallis test, $P < 0.05$, $n = 36$).

Supplementary Table S1. Primer sequences used for RT-PCR.
for: forward, rev comp: reverse complement.

Gene name	Accession number	Orientation	Sequence 5' - 3'
<i>PSKR1</i>	At2g02220	for	GAGCGTTGCAATACAATCAG
		rev comp	CTAGACATCATCAAGCCAAGAGA
<i>PSKR2</i>	At5g53890	for	CCGAAAGGTTCTTCGCGTAG
		rev comp	GGCCTAAGCAACCTCGCTAA

Supplementary Table S2. Primer sequences used for qRT-PCR.
for: forward, rev comp: reverse complement.

Gene name	Accession number	Orientation	Sequence 5' - 3'
<i>ACT2</i>	At3g18780	for	ACATTCCAGCAGATGTGGATCTC
		rev comp	GATCCCATTCATAAAACCCAGC
<i>GAPC1</i>	At3g04120	for	GATTCTACAATGGCTGACAAGAAGA
		rev comp	ATGAAGGGGTCGTTGACAGC
<i>PSKR1</i>	At2g02220	for	AGCGAGGTTTTGATCCGTT
		rev comp	CTGTTGAGTCGTTGGCCTCT
<i>PSKR2</i>	At5g53890	for	TGGCGGATTGGTCTTGTGT
		rev comp	TTCCGCTCGAGACAATGCTT

5 CONCLUSIVE DISCUSSION AND PERSPECTIVES

Increasing lines of evidence show the importance of plant peptides through their respective receptors mediating cell-to-cell communication to coordinate a variety of plant processes. Among them, PSK which was previously identified as a growth hormone (Sauter, 2015) and participated in biotic stress responses (Loivamäki et al., 2010) is recently found to respond towards abiotic stress as well, particularly in providing osmotic-stress tolerance (Stührwohldt et al., 2021). In relation to that, our work establishes PSK/PSKR1 signaling as a key regulator of shoot growth maintenance under water-deficit conditions in an ABA-dependent manner.

Drought induces osmotic stress that affects the plant water status. These unfavorable conditions result in the synthesis of ABA, an important stress hormone responsible for coordinating a complex gene regulatory network that enables plants to cope with stress (Raghavendra et al., 2010). Numerous studies in the past revealed crosstalk between PSKR-mediated signaling and different hormonal signaling (Mosher et al., 2013; Sauter, 2015; Zhang et al., 2018) inspiring us to investigate if PSK enhances drought tolerance via the ABA signaling pathway.

5.1 PSK/PSKR is associated with ABA signaling

ABA is known to inhibit seed germination and post germinative growth under stress conditions. We showed (**Chapter 3**) that ABA-inhibited seed germination was not dependent on PSKR signaling. Post germinative growth is characterized by cotyledon greening. Cotyledon greening assay performed in this study revealed that the PSKR null mutant *pskr1-3 pskr2-1* was insensitive to ABA and showed enhanced cotyledon greening whereas *PSKR1* overexpressors were hypersensitive to ABA providing initial evidence that ABA responsiveness specifically in seedling establishment was controlled by PSK/PSKR signaling. Determining the molecular mechanisms involving the integration of PSKR signaling in ABA-induced post germinative inhibition and which component facilitates this crosstalk is a separate topic of research and requires further investigation. An ideal candidate to explore would be abscisic acid insensitive5 (*ABI5*), a basic leucine zipper transcription factor which is an important factor in the regulation

of ABA mediated post germinative inhibition (Lopez-Molina et al., 2002; Guan et al., 2014).

ABA is also known to regulate vegetative growth under water-deficit conditions and our findings exhibit that the absence of *PSKRs* markedly decreased sensitivity to ABA in shoot growth experiments upon exogenous application of ABA. Thus, PSK/PSKR appears to positively regulate ABA signaling in two different developmental stages tested in this study.

5.2 PSK/PSKR signaling maintains shoot growth upon osmotic stress by regulating ABA levels

Growth and stress responses are two processes that require a large amount of energy and other resources (Ali et al., 2007). Since plants must balance growth programs against stress responses, it is crucial for plants to properly allocate limited resources to gain better fitness. Plants facilitate this through crosstalk between plant hormones. Our results on mannitol-induced growth experiments (**Chapter 3**) showed that PSK/PSKR signaling was required to specifically maintain shoot growth under such stress conditions possibly by regulating ABA accumulation. We also showed that PSKR signaling impacts expression of genes related to ABA metabolism and ABA signaling in response to mannitol which explains ABA elevation in wild type but not in *pskr1-3 pskr2-1* shoots. In the context of ABA signaling, central ABA signaling proteins predominantly localized in the cytosol are often dragged to the plasma membrane so that they can be in close proximity of their interaction partners. Type 2C PP2C phosphatases and PYR/PYL/RCAR ABA receptors which are negative and positive regulators of ABA signaling, respectively, are believed to be localized not only in the cytosol and nucleus but also at the plasma membrane to regulate the activity of membrane proteins (Gao et al., 2013; Bueso et al., 2014; Rodriguez et al., 2014; Diaz et al., 2016). Since PSKR is a RLK member and is localized at the plasma membrane it would be interesting to identify molecular interactions of PSKR with core ABA signaling components using a bimolecular fluorescence complementation (BiFC) assay and determine physical targets of PSKR in the ABA signaling pathway, in the future.

5.3 PSKR does not mediate long-distance drought signaling

In nature, plants recognize drought via roots and transmit drought signals from the roots to shoots which then leads to accumulation of ABA that provides adaptation. Lately, novel findings reveal that hormone-like peptides serve as mobile signals in the vasculature to integrate long-distance root-to-shoot signal communication and mediate drought responses (Takahashi et al., 2020). We performed grafting experiments and treated grafts with mannitol to understand if PSK/PSKR participated in long-distance drought signaling. The roots deficient in PSKRs grafted to wild type shoots conferred better shoot growth compared to shoots deficient in PSKRs grafted to wild type roots indicating that PSKR signaling did not participate in long-distance communication and the presence of PSKRs in the shoots was enough to maintain shoot growth under osmotic stress. However, we could not confirm if the peptide PSK functioned as a mobile signal due to difficulties in obtaining a pertinent PSK null mutant. We did try to optimize the desorption electrospray ionization mass spectrometry imaging (DESI-MSI) to detect endogenous PSK directly from tissue sections but turned out unsuccessful. One reason could be that PSK seems to function in planta at extremely low concentrations (Matsubayashi et al., 2018) and are difficult to detect due to technical limitations. Thus, a key goal in the future is to develop highly sensitive biosensors capable of detecting these low abundant peptides.

5.4 PSKR1 is the main transducer of PSK signaling

In Arabidopsis, PSK has two binding partners, PSKR1 and PSKR2. Though both receptors are ubiquitously expressed (Sauter, 2015; Wu et al., 2016), PSK functions mainly via PSKR1, particularly in water-deficit conditions. We showed in our study (**Chapter 4**) that this resulted due to differential expression of *PSKRs* using a chimeric receptor approach. Promoter analysis revealed an important drought-related *cis-element* that was specific to the promoter region of *PSKR1* and absent in the *PSKR2* promoter. These results were obtained from computational analysis and therefore requires robust experiments to verify these data. Firstly, target genes are induced at the transcriptional level through the specific recognition of *cis-elements* in their

promoters by *trans*-acting sequence-specific DNA-binding transcription factors (TFs) (Cai et al., 2008). So, determination of all possible TFs specific to the DRE/CRT element identified in the *PSKR1* promoter can be predicted from available database such as PlantPAN 2.0 (Chang et al., 2008; Chow et al., 2015). The regulation of *PSKR1* activity by screened TFs can be verified using transient transactivation assays in Arabidopsis protoplasts to investigate TF interaction with the promoter (Yi et al., 2010). Also, promoter deletion analysis of the *PSKR1* specifically at the DRE/CRT region can provide more information if the predicted motif is actually responsible for activation of *PSKR1* upon water-deficiency.

5.5 PSK interaction at the LRR of PSKRs

PSK binds to a pocket that is formed by the LRR domain of the PSKR and a small island domain. This binding stabilizes the island domain and enables PSKR to interact with a SERK coreceptor, which is shared between many LRR-RLK signaling pathways (Wang et al., 2015; Hohmann et al., 2017). Our results (**Chapter 4**) showed that the LRR of PSKRs differed in receptor function. We started out with the speculation that the binding affinities of PSK to both the receptors could vary. To decipher this, we tried to analyze the binding affinities of PSK with LRRs using the BLI system. For this, we initially attempted to express the PSKR-LRRs in *Drosophila melanogaster* Schneider 2 (S2) cells. But we had to change the expression system as culturing of S2 cells was impossible often resulting in cell death which was extremely difficult to solve. The bacterial expression of PSKR-LRRs was successful but the BLI assay did not work. Further optimization of this system and use of fresh sensors could be the solution for the future. Therefore, we couldn't determine the binding affinities of PSK to PSKR-LRRs at this stage. Also, alternative methods such as the surface plasmon resonance (SPR) which does not require labeling of the ligand could also be used for determining the binding affinities. Computational analysis of both LRRs revealed that Leu-399 is required for PSK perception in LRR1 and at this position there is Lys in LRR2 which could be associated with weak binding, thereby differing in receptor function.

Collectively, our results reveal an important role for PSK/PSKR1 in plant responses to osmotic stress conditions in an ABA-dependent manner.

6 REFERENCES

- Ali, R., Ma, W., Lemtiri-Chlieh, F., Tsaltas, D., Leng, Q., von Bodman, S., & Berkowitz, G. A. 2007. Death don't have no mercy and neither does calcium: Arabidopsis CYCLIC NUCLEOTIDE GATED CHANNEL2 and innate immunity. *The Plant cell*, 19(3), 1081–1095.
- Angelica Lindlöf, Marcus Bräutigam, Aakash Chawade, Olof Olsson, Björn Olsson. 2009. *In silico* analysis of promoter regions from cold-induced genes in rice (*Oryza sativa* L.) and *Arabidopsis thaliana* reveals the importance of combinatorial control, *Bioinformatics*. 25:1345–1348.
- Augé, RM., Toler, HD., and Saxton, AM. 2015. Arbuscular mycorrhizal symbiosis alters stomatal conductance of host plants more under drought than under amply watered conditions: a meta-analysis. *Mycorrhiza*. 25:13–24.
- Belkhadir, Y., Yang, L., Hetzel, J., Dangl, J. L. & Chory, J. 2014. The growth-defense pivot: crisis management in plants mediated by LRR-RK surface receptors. *Trends Biochem. Sci.* 39: 447–456.
- Bilas, R., Szafran, K., Hnatuszko-Konka, K. et al. 2016. *Cis*-regulatory elements used to control gene expression in plants. *Plant Cell Tiss. Organ. Cult.* 127: 269–287.
- Bueso, E., Rodriguez, L., Lorenzo-Orts, L., Gonzalez-Guzman, M., Sayas, E., Muñoz-Bertomeu, J., Ibanñez, C., Serrano, R., and Rodriguez, P.L. 2014. The single-subunit RING-type E3 ubiquitin ligase RSL1 targets PYL4 and PYR1 ABA receptors in plasma membrane to modulate abscisic acid signaling. *Plant J.* 80:1057–1071.
- Cai, M., Qiu, D., Yuan, T., Ding, X., Li, H., Duan, L., et al. 2008. Identification of novel pathogen-responsive cis-elements and their binding proteins in the promoter of OsWRKY13, a gene regulating rice disease resistance. *Plant Cell Environ.* 31, 86–96.
- Cercós, M., Gómez-Cadenas, A. and Ho, THD. 1999. Hormonal regulation of a cysteine proteinase gene, *EPB-1*, in barley aleurone layers: *cis*- and *trans*-acting elements involved in the co-ordinated gene expression regulated by gibberellins and abscisic acid. *Plant J.* 19:107–118.
- Chakraborty, S., Nguyen, B., Wasti, SD., and Xu, G. (2019). Plant Leucine-Rich Repeat Receptor Kinase (LRR-RK): Structure, Ligand Perception, and Activation Mechanism. *Molecules*. 24: 3081.
- Chandrasekaran, M., Sonia, B., Hu, S., Oh, S. H., and Sa, T. 2014. A meta-analysis of arbuscular mycorrhizal effects on plants grown under salt stress. *Mycorrhiza*. 24: 611–625.
- Chang, W.C., Lee, T.Y., Huang, H.D., Huang, H.Y. and Pan, R.L. 2008. PlantPAN: Plant promoter analysis navigator, for identifying combinatorial cis-regulatory elements with distance constraint in plant gene groups. *BMC genomics*, 9, 561.

- Chen, D., Cao, Y., Li, H., Kim, D., Ahsan, N., Thelen, J., and Stacey, G.** 2017. Extracellular ATP elicits DORN1-mediated RBOHD phosphorylation to regulate stomatal aperture. *Nat. Commun.* 8: 1–13.
- Chen, T.** 2021. Identification and characterization of the LRR repeats in plant LRR-RLKs. *BMC Mol. and Cell. Biol.* 22: 9.
- Chen, Y., Matsubayashi, Y., and Sakagami, Y.** 2000. Peptide growth factor phytosulfokine-a contributes to the pollen population effect. *Plant Mol. Biol.* 211: 752–755.
- Chi-Nga Chow, Han-Qin Zheng, Nai-Yun Wu, Chia-Hung Chien, Hsien-Da Huang, Tzong-Yi Lee, Yi-Fan Chiang-Hsieh, Ping-Fu Hou, Tien-Yi Yang, and Wen-Chi Chang.** 2015. "PlantPAN 2.0: an update of plant promoter analysis navigator for reconstructing transcriptional regulatory networks in plants" *Nucleic Acids Res.*
- Choi, H., Hong, J., Ha, J., Kang, J., & Kim, S. Y.** 2000. ABFs, a family of ABA-responsive element binding factors. *J. Biol. Chem.*, 275: 1723–1730.
- Christine Kaufmann, Michael Motzkus, Margret Sauter.** 2017. Phosphorylation of the phytosulfokine peptide receptor PSKR1 controls receptor activity. *J. Exp. Bot.* 68: 1411–1423.
- Christmann, A., Hoffmann, T., Teplova, I., Grill, E., and Müller, A.** 2005. Generation of active pools of abscisic acid revealed by in vivo imaging of water-stressed *Arabidopsis*. *Plant Physiol.* 137: 209–219.
- Clough, S.J. and Bent, A.F.** 1998. Floral dip: A simplified method for *Agrobacterium* mediated transformation of *Arabidopsis thaliana*. *Plant J.* 16: 735–74.
- Comas, L.H., Becker, S.R., Cruz, V.M., Byrne, P.F., and Dierig, D.A.** 2013. Root traits contributing to plant productivity under drought. *Front. Plant Sci.* 4: 442.
- Cutler, S.R., Rodriguez, P.L., Finkelstein, R.R., and Abrams, S.R.** 2010. Absciscic acid: emergence of a core signaling network. *Annu. Rev. Plant Biol.* 61:651–669.
- Darko, E., Végh, B., Khalil, R., Marček, T., Szalai, G., Pál, M., & Janda, T.** 2019. Metabolic responses of wheat seedlings to osmotic stress induced by various osmolytes under iso-osmotic conditions. *PloS one.* 14: e0226151.
- Diaz, M., Sanchez-Barrena, M.J., Gonzalez-Rubio, J.M., Rodriguez, L., Fernandez, D., Antoni, R., Yunta, C., BeldaPalazon, B., Gonzalez-Guzman, M., and Peirats-Llobet, M.** 2016. Calcium-dependent oligomerization of CAR proteins at cell membrane modulates ABA signaling. *Proc. Natl. Acad. Sci. USA* 113:E396–E405.
- Felix, G., Duran, J.D., Volko, S. and Boller, T.** 1999 Plants have a sensitive perception system for the most conserved domain of bacterial flagellin. *Plant J.* 18: 265–276.
- Fletcher J.C.** 2020. Recent Advances in *Arabidopsis* CLE Peptide Signaling. *Trends in plant science.* 25:1005–1016.

Fujii, H., Chinnusamy, V., Rodrigues, A., Rubio, S., Antoni, R., Park, S. Y., Cutler, SR., Sheen, J., Rodriguez, PL., & Zhu, JK. 2009. In vitro reconstitution of an abscisic acid signalling pathway. *Nature*. 462: 660–664.

Fujita, Y., Fujita, M., Shinozaki, K., and Yamaguchi-Shinozaki, K. 2011. ABA-mediated transcriptional regulation in response to osmotic stress in plants. *J. Plant Res.* 124: 509–525.

Gao, H.-B., Chu, Y.-J., and Xue, H.-W. 2013. Phosphatidic acid (PA) binds PP2AA1 to regulate PP2A activity and PIN1 polar localization. *Mol. Plant* 6:1692–1702.

Ghorbani, S., Lin, Y. C., Parizot, B., Fernandez, A., Njo, M. F., Van de Peer, Y., Beeckman, T., & Hilson, P. 2015. Expanding the repertoire of secretory peptides controlling root development with comparative genome analysis and functional assays. *J. Exp. Bot.* 66: 5257–5269.

Gosti F, Beaudoin N, Serizet C, Webb AA, Vartanian N, Giraudat J. 1999. ABI1 protein phosphatase 2C is a negative regulator of abscisic acid signaling. *Plant Cell* 11: 1897–1910.

Gou, X., He, K., Yang, H., Yuan, T., Lin, H., Clouse, S. D., and Li, J. 2010. Genome-wide cloning and sequence analysis of leucine-rich repeat receptor-like protein kinase genes in *Arabidopsis thaliana*. *BMC genomics*. 11:19.

Han, J., Tan, J., Tu, L., and Zhang, X. 2014a. A peptide hormone gene, GhPSK promotes fibre elongation and contributes to longer and finer cotton fibre. *Plant Biotechnol. J.* 12: 861–871.

Han, Z., Sun, Y. & Chai, J. 2014b. Structural insight into the activation of plant receptorkinases. *Curr. Opin.* 20: 55–63.

Hanai H, Nakayama D, Yang H, Matsubayashi Y, Hirota Y, Sakagami Y. 2000. Existence of a plant tyrosylprotein sulfotransferase: Novel plant enzyme catalyzing tyrosine O-sulfation of preprophytosulfokine variants in vitro. *FEBS Letters* 470: 97–101.

Hartmann, J., Fischer, C., Dietrich, P., and Sauter, M. 2014. Kinase activity and calmodulin binding are essential for growth signaling by the phytosulfokine receptor PSKR1. *Plant J.* 78: 192–202.

Hartmann, J., Stührwoldt, N., Dahlke, R.I., and Sauter, M. 2013. Phytosulfokine control of growth occurs in the epidermis, is likely to be non-cell autonomous and is dependent on brassinosteroids. *Plant J.* 73: 579–590.

He, L., Xu, J., Wang, Y., and Yang, K. 2018. Transcription Factor ANAC074 Binds to NRS1, NRS2, or MybSt1 Element in Addition to the NACRS to Regulate Gene Expression. *Int. J. Mol. Sci.* 19: 3271.

Higo K, Ugawa Y, Iwamoto M, Korenaga T. 1999. Plant cis-acting regulatory DNA elements (PLACE) database: 1999. *Nucl. Acids Res.* 27: 297–300.

Hohmann, U., Lau, K. and Hothorn, M. 2017. The structural basis of ligand perception and signal activation by receptor kinases. *Annu. Rev. Plant Biol.* 68, 109-137. 10.1146/annurev-arplant-042916-040957.

Holzward, E., Huerta, A.I., Glöckner, N., Garnelo Gómez, B., Wanke, F., Augustin, S., Askani, J.C., Schürholz, A.-K., Harter, K., and Wolf, S. 2018. BRI1 controls vascular cell fate in the Arabidopsis root through RLP44 and phytosulfokine signaling. *Proc. Natl. Acad. Sci.* 115: 11838–11843.

Hu Z, Zhang H, and Shi K. 2018. Plant peptides in plant defense responses, *Plant Signal. Behav.* 13:8.

Igarashi, D., Tsuda, K., and Katagiri, F. 2012. The peptide growth factor, phytosulfokine, attenuates pattern-triggered immunity. *Plant J.* 71: 194–204.

Igasaki, T., Akashi, N., Ujino-Ihara, T., Matsubayashi, Y., Sakagami, Y., and Shinohara, K. 2003. Phytosulfokine Stimulates Somatic Embryogenesis in *Cryptomeria japonica*. *Plant Cell Physiol.* 44: 1412–1416

Jeon, B. W., Kim, M. J., Pandey, S. K., Oh, E., Seo, P. J., and Kim, J. 2021. Recent advances in peptide signaling during *Arabidopsis* root development. *J. Exp. Bot.* 72: 2889–2902.

Joshi-Saha, A., Valon, C., & Leung, J. 2011. Absciscic acid signal off the STARting block. *Molecular plant.* 4: 562–580.

Kalve, S., Sizani, B. L., Markakis, M. N., Helsmoortel, C., Vandeweyer, G., Laukens, K., Sommen, M., Naulaerts, S., Vissenberg, K., Prinsen, E., & Beemster, G. 2020. Osmotic stress inhibits leaf growth of *Arabidopsis thaliana* by enhancing ARF-mediated auxin responses. *The New phytologist.* 226:1766–1780.

Kaufmann, C. 2018. Regulation and activities of phytosulfokine receptor PSKR1 in *Arabidopsis thaliana*. Dissertation.

Kaufmann, C. and Sauter, M. 2019. Sulfated plant peptide hormones. *J. Exp. Bot.*: 1– 11.

Kim, J. S., Jeon, B. W., & Kim, J. 2021. Signaling Peptides Regulating Abiotic Stress Responses in Plants. *Front. Plant Sci.* 12: 704490.

Koevoets IT, Venema JH, Elzenga JTM and Testerink C. 2016. Roots withstanding their environment: Exploiting root system architecture responses to abiotic stress to improve crop tolerance. *Front. Plant Sci.* 7: 1335.

Komori, R., Amano, Y., Ogawa-Ohnishi, M., and Matsubayashi, Y. 2009. Identification of tyrosylprotein sulfotransferase in *Arabidopsis*. *Proc. Natl. Acad. Sci. U. S. A.* 106: 15067–15072.

Krogh, A., Larsson, B., von Heijne, G., and Sonnhammer, EL. (2001). Predicting transmembrane protein topology with a hidden Markov model: application to complete genomes. *J. Mol. Biol.* 305:567–580.

Kuhn JM, Boisson-Dernier A, Dizon MB, Maktabi MH, Schroeder JI. 2006. The protein phosphatase AtPP2CA negatively regulates ABA signal transduction in Arabidopsis. *Plant Physiol.* 140: 127–139.

Kunze, G., Zipfel, C., Robatzek, S., Niehaus, K., Boller, T. and Felix, G. 2004. The N terminus of bacterial elongation factor Tu elicits innate immunity in Arabidopsis plants. *Plant Cell.* 16: 3496–3507.

Kuromori, T., Seo, M., and Shinozaki, K. 2018. ABA Transport and Plant Water Stress Responses. *Trends Plant Sci.* 23: 513–522.

Kwezi, L., Ruzvidzo, O., Wheeler, JI., Govender, K., Iacuone, S., Thompson, PE., Gehring, C., and Irving, HR. 2011. The phytosulfokine (PSK) receptor is capable of guanylate cyclase activity and enabling cyclic GMP-dependent signaling in plants. *J. Biol. Chem.* 286: 22580–22588.

Lescot M, Dhais P, Thijs G, Marchal K, Moreau Y, Van de Peer Y, et al. 2002. PlantCARE a database of plant *cis*-acting regulatory elements and a portal to tools for *in silico* analysis of promoter sequences. *Nucleic Acids Res.* 30: 325–327.

Lindsey K, Casson S and Chilley P. 2002. Peptides: new signalling molecules in plants. *Trends Plant Sci.* 7: 78–83.

Liu Q, Luo L, Zheng L. Lignins. 1996. Biosynthesis and Biological Functions in Plants. *Int. J. Mol. Sci.* 19:335.

Loivamäki, M., Stührwohltd, N., Deeken, R., Steffens, B., Roitsch, T., Hedrich, R., and Sauter, M. 2010. A role for PSK signaling in wounding and microbial interactions in Arabidopsis. *Physiol. Plant.* 139: 348–357.

Lopez-Molina, L., Mongrand, S., McLachlin, DT., Chait, BT., and Chua NH. 2002. ABI5 acts downstream of ABI3 to execute an ABA-dependent growth arrest during germination. *Plant J* 32: 317–328.

Lorbiecke, R. and Sauter, M. 2000. Comparative analysis of PSK peptide growth factor precursor homologs. *Plant Sci.* 163: 321–332.

Lorbiecke, R., Steffens, M., Tomm, J. M., Scholten, S., von Wiegen, P., Kranz, E., Wienand, U., & Sauter, M. 2005. Phytosulphokine gene regulation during maize (*Zea mays* L.) reproduction. *J. Exp. Bot.* 56: 1805–1819.

Ma, Y., Cao, J., He, J., Chen, Q., Li, X., and Yang, Y. 2018. Molecular Mechanism for the Regulation of ABA Homeostasis During Plant Development and Stress Responses. *Int. J. Mol. Sci.* 19: 3643.

Maeda K, Kimura S, Demura T, Takeda J, Ozeki Y. 2005. DcMYB1 acts as a transcriptional activator of the carrot phenylalanine ammonia-lyase gene (DcPAL1) in response to elicitor treatment, UV-B irradiation and the dilution effect. *Plant Mol Biol* 59: 739–752.

Maggio A., Zhu JK., Hasegawa PM., and Bressan RA. 2006. Osmogenetics: Aristotle to *Arabidopsis*. Plant Cell 18: 1542–1557.

Matsubayashi Y. 2018. Exploring peptide hormones in plants: identification of four peptide hormone-receptor pairs and two post-translational modification enzymes. Proc. Jpn. Acad. B: Phys. Biol. Sci. 94: 59–74.

Matsubayashi, Y. 2014. Posttranslationally modified small-peptide signals in plants. Annu. Rev. Plant Biol. 65: 385–413.

Matsubayashi, Y., Hanai, H., Hara, O., and Sakagami, Y. 1996. Active Fragments and Analogs of the Plant Growth Factor, Phytosulfokine: Structure – Activity Relationships Proliferation of dispersed plant cells in culture is strictly dependent on cell density, and cells in a low-density culture can only grow in the. Biochem. Biophys. Res. Commun. 225: 209–214.

Matsubayashi, Y., Morita, A., Matsunaga, Furuya, A., Hanai, N., and Sakagami, Y. 1999. Physiological relationships between auxin, cytokinin, and a peptide growth factor, phytosulfokine- α in stimulation of asparagus cell proliferation. Planta. 207: 559–565.

Matsubayashi, Y., Ogawa, M., Morita, A., and Sakagami, Y. 2002. An LRR receptor kinase involved in perception of a peptide plant hormone, phytosulfokine. Science. 296: 1470–1472.

Merilo, E., Jalakas, P., Laanemets, K., Mohammadi, O., H  rak, H., Kollist, H., and Brosch  , M. 2015. Absciscic Acid Transport and Homeostasis in the Context of Stomatal Regulation. Molecular plant. 8: 1321–1333.

Morillo, SA., and Tax, FE. 2006. Functional analysis of receptor-like kinases in monocots and dicots. Curr. Opin. Plant Biol. 9: 460–469.

Mosher, S., Seybold, H., Rodriguez, P., Stahl, M., Davies, K.A., Dayaratne, S., Morillo, S.A., Wierzb  , M., Favery, B., Keller, H., Tax, F.E., and Kemmerling, B. 2013. The tyrosine-sulfated peptide receptors PSKR1 and PSY1R modify the immunity of Arabidopsis to biotrophic and necrotrophic pathogens in an antagonistic manner. Plant J. 73: 469–482.

Nakashima, K., Fujita, Y., Kanamori, N., Katagiri, T., Umezawa, T., Kidokoro, S., Maruyama, K., Yoshida, T., Ishiyama, K., Kobayashi, M., Shinozaki, K., & Yamaguchi-Shinozaki, K. 2009. Three Arabidopsis SnRK2 protein kinases, SRK2D/SnRK2.2, SRK2E/SnRK2.6/OST1 and SRK2I/SnRK2.3, involved in ABA signaling are essential for the control of seed development and dormancy. Plant & cell physiology. 50:1345–1363.

Nakashima, K., Yamaguchi-Shinozaki, K., and Shinozaki, K. 2014. The transcriptional regulatory network in the drought response and its crosstalk in abiotic stress responses including drought, cold, and heat. Front. Plant Sci. 5: 170.

Nishimura, N., Sarkeshik, A., Nito, K., Park, SY., Wang, A., Carvalho, PC., Lee, S., Caddell, DF., Cutler, SR., Chory, J., Yates, JR., & Schroeder, JI. 2010.

PYR/PYL/RCAR family members are major in-vivo ABI1 protein phosphatase 2C-interacting proteins in Arabidopsis. *The Plant journal*. 61: 290–299.

Oh, E., Seo, P. J., and Kim, J. 2018. Signaling peptides and receptors coordinating plant root development. *Trends Plant Sci.* 23: 337–351.

Olsson, V., Joos, L., Zhu, S., Gevaert, K., Butenko, M. A., and De Smet, I. 2019. Look Closely, the Beautiful May Be Small: Precursor-Derived Peptides in Plants. *Annu. Rev. Plant Biol.* 70. 153–186.

Osakabe, Y., Arinaga, N., Umezawa, T., Katsura, S., Nagamachi, K., Tanaka, H., Ohiraki, H., Yamada, K., Seo, S. U., Abo, M., Yoshimura, E., Shinozaki, K., & Yamaguchi-Shinozaki, K. 2013. Osmotic stress responses and plant growth controlled by potassium transporters in Arabidopsis. *The Plant cell*, 25. 609–624.

Padmanabhan, M., Cournoyer, P., and Dinesh Kumar, SP. 2009. The leucine-rich repeat domain in plant innate immunity: a wealth of possibilities. *Cellular microbiology*. 11: 191–198.

Patharkar, OR., and Walker, JC. 2016. Core mechanisms regulating developmentally timed and environmentally triggered abscission. *Plant Physiol.* 172: 510–520.

Pierik R and Testerink C. 2014. The art of being flexible: How to escape from shade, salt, and drought. *Plant Physiol.* 166: 5–22.

Raghavendra, A. S., Gonugunta, V. K., Christmann, A., and Grill, E. 2010. ABA perception and signalling. *Trends Plant Sci.* 15: 395–401.

Rajamanickam, K., Schönhof, M.D., Hause, B., and Sauter, M. 2021. PSK signaling controls ABA homeostasis and signaling genes and maintains shoot growth under osmotic stress. *bioRxiv* doi: <https://doi.org/10.1101/2020.10.20.347674>.

Rodiuc, N., Barlet, X., Hok, S., Perfus-Barbeoch, L., Allasia, V., Enger, G., et al. 2016. Evolutionary distant pathogens require the Arabidopsis phytosulfokine signalling pathway to establish disease. *Plant Cell Environ.* 39, 1396–1407.

Rodriguez PL. 1998. Protein phosphatase 2C (PP2C) function in higher plants. *Plant Mol. Biol.* 38: 919–927.

Rodriguez, L., Gonzalez-Guzman, M., Diaz, M., Rodrigues, A., Izquierdo-Garcia, A.C., Peirats-Llobet, M., Fernandez, M.A., Antoni, R., Fernandez, D., and Marquez, J.A. 2014. C2-domain abscisic acid-related proteins mediate the interaction of PYR/PYL/RCAR abscisic acid receptors with the plasma membrane and regulate abscisic acid sensitivity in Arabidopsis. *Plant Cell* 26:4802–4820.

Roychoudhury, A., Paul, S., & Basu, S. 2013. Cross-talk between abscisic acid-dependent and abscisic acid-independent pathways during abiotic stress. *Plant cell reports*. 32: 985–1006.

Saez, A., Robert, N., Maktabi, M. H., Schroeder, J. I., Serrano, R., and Rodriguez, PL. 2006. Enhancement of abscisic acid sensitivity and reduction of water consumption in Arabidopsis by combined inactivation of the protein phosphatases type 2C ABI1 and HAB1. *Plant Physiol.* 141: 1389–1399.

- Sauter M.** 2015. Phytosulfokine peptide signalling. *J. Exp. Bot.* 66: 5161–5169.
- Schwartz, S.H., Qin, X., and Jan AD. Zeevaart.** 2003. Elucidation of the Indirect Pathway of Absciscic Acid Biosynthesis by Mutants, Genes, and Enzymes. *Plant Physiol.* 131: 1591–1601.
- Segonzac, C., & Monaghan, J.** 2019. Modulation of plant innate immune signaling by small peptides. *Curr. Opin. Plant Biol.* 51. 22–28.
- Shinozaki K, Yamaguchi-Shinozaki K and Seki M.** 2003. Regulatory network of gene expression in the drought and cold stress responses. *Curr. Opin. Plant Biol.* 6: 410–417.
- Singh, D., & Laxmi, A.** 2015. Transcriptional regulation of drought response: a tortuous network of transcriptional factors. *Front. Plant Sci.* 6:895.
- Slama, I., Ghnaya, T., Hessini, K., Messedi, D., Savouré, A., & Abdelly, C.** 2007. Comparative study of the effects of mannitol and PEG osmotic stress on growth and solute accumulation in *Sesuvium portulacastrum*. *Environ. Exp. Bot.* 61:10-17.
- Smith, S., Zhu, S., Joos, L., Roberts, I., Nikonorova, N., Dai Vu, L., et al.** 2020. The CEP5 peptide promotes abiotic stress tolerance, as revealed by quantitative proteomics, and attenuates the AUX/IAA equilibrium in *Arabidopsis*. *Mol. Cell Proteomics* 19: 1248–1262.
- Srivastava, R., Liu, JX., and Howell, SH.** 2008. Proteolytic processing of a precursor protein for a growth-promoting peptide by a subtilisin serine protease in *Arabidopsis*. *Plant J.* 56: 219–227.
- Stührwohltdt, N., & Schaller, A.** 2019. Regulation of plant peptide hormones and growth factors by post-translational modification. *Plant biology (Stuttgart, Germany)*. 21: 49–63.
- Stührwohltdt, N., Dahlke, R.I., Kutschmar, A., Peng, X., Sun, M.X., and Sauter, M.** 2015. Phytosulfokine peptide signaling controls pollen tube growth and funicular pollen tube guidance in *Arabidopsis thaliana*. *Physiol. Plant.* 153: 643–653.
- Sun, Q., Gao, F., Zhao, L., Li, K., & Zhang, J.** 2010. Identification of a new 130 bp cis-acting element in the TsVP1 promoter involved in the salt stress response from *Thellungiella halophila*. *BMC plant biology.* 10: 90.
- Tauszig, S., Jouanguy, E., Hoffmann, JA., and Imler, JL.** 2000. Toll-related receptors and the control of antimicrobial peptide expression in *Drosophila*. *Proc. Natl. Acad. Sci. U.S.A.* 97: 10520–10525.
- Tavormina, P., De Coninck, B., Nikonorova, N., De Smet, I., and Cammuea, B.P.A.** 2015. The plant peptidome: An expanding repertoire of structural features and biological functions. *Plant Cell.* 27: 2095–2118.
- Tiwari, V., Patel, M. K., Chaturvedi, A. K., Mishra, A., and Jha, B.** 2016. Functional Characterization of the Tau Class Glutathione-S-Transferases Gene (SbGSTU) Promoter of *Salicornia brachiata* under Salinity and Osmotic Stress. *PloS one.* 11: e0148494.

Torii KU. 2004. Leucine-rich repeat receptor kinases in plants: structure, function, and signal transduction pathways. *Int. Rev. Cytol.* 234:1–46.

Tsujita T. et al. 2004. Sensing bacterial flagellin by membrane and soluble orthologs of Toll-like receptor 5 in rainbow trout (*Onchorhynchus mikiss*). *J. Biol. Chem.* 279: 48588–48597.

Umezawa, T., Nakashima, K., Miyakawa, T., Kuromori, T., Tanokura, M., Shinozaki, K., & Yamaguchi-Shinozaki, K. 2010. Molecular basis of the core regulatory network in ABA responses: sensing, signaling and transport. *Plant & cell physiology.* 51. 1821–1839.

Uno, Y., Furihata, T., Abe, H., Yoshida, R., Shinozaki, K., & Yamaguchi-Shinozaki, K. 2000. Arabidopsis basic leucine zipper transcription factors involved in an abscisic acid-dependent signal transduction pathway under drought and high-salinity conditions. *Proc. Natl. Acad. Sci. U.S.A.* 97: 11632–11637.

Vanstraelen M and Benková E. 2012. Hormonal interactions in the regulation of plant development. *Annu Rev. Cell Dev. Biol.* 28: 463-487.

Wang, J., Li, H., Han, Z., Zhang, H., Wang, T., Lin, G., Chang, J., Yang, W., and Chai, J. 2015. Allosteric receptor activation by the plant peptide hormone phytosulfokine. *Nature.* 525: 265–268.

Wang, YH., and Irving, HR. 2011. Developing a model of plant hormone interactions. *Plant Signal. Behav.* 6:494–500.

Wani, S. H., and Kumar, V. 2015. Plant stress tolerance: engineering ABA: a Potent phytohormone. *Transcriptomics: An Open Access.* 3:1000113.

Wheeler, J.I. and Irving, H.R. 2010. Evolutionary advantages of secreted peptide signalling molecules in plants. *Funct. Plant Biol.* 37: 382–394.

Wu, G., Shan, J., Pang, S., Wei, X., Zhang, H., & Yan, B. 2012. Genetic analysis of the promoter region of the GATA4 gene in patients with ventricular septal defects. *Transl Res: J Lab Clin Med.* 159: 376–382.

Wu, Y., Xun, Q., Guo, Y., Zhang, J., Cheng, K., Shi, T., He, K., Hou, S., Gou, X., and Li, J. 2016. Genome-Wide Expression Pattern Analyses of the Arabidopsis LeucineRich Repeat Receptor-Like Kinases. *Mol. Plant* 9: 289-300.

Wu, H., Zheng, R., Hao, Z., Meng, Y., Weng, Y., Zhou, X., et al. 2019. Cunninghamia lanceolata PSK peptide hormone genes promote primary root growth and adventitious root formation. *Plants.* 8:520.

Yamaguchi-Shinozaki, K., and Shinozaki, K. 1994. A novel cis-acting element in an *Arabidopsis* gene is involved in responsiveness to drought, low-temperature, or high-salt stress. *The Plant cell.* 6: 251–264.

Yamaguchi-Shinozaki, K., and Shinozaki, K. 2005. Organization of cis-acting regulatory elements in osmotic- and cold-stress-responsive promoters. *Trends in plant science*. 10: 88–94.

Yamakawa, S., Matsubayashi, Y., Sakagami, Y., Kamada, H., and Satoh, S. 1999. Promotive effects of the peptidyl plant growth factor, phytosulfokine- α , on the growth and chlorophyll content of *Arabidopsis* seedlings under high night-time temperature conditions. *Biosci. Biotechnol. Biochem.* 63: 2240–2243.

Yamakawa, S., Sakuta, C., Matsubayashi, Y. et al. 1998. The promotive effects of a peptidyl plant growth factor, phytosulfokine- α , on the formation of adventitious roots and expression of a gene for a root-specific cystatin in cucumber hypocotyls. *J. Plant Res.* 111: 453–458.

Yamamoto, S., Nakano, T., Suzuki, K., & Shinshi, H. 2004. Elicitor-induced activation of transcription via W box-related cis-acting elements from a basic chitinase gene by WRKY transcription factors in tobacco. *Biochimica et Biophysica Acta*. 1679: 279–287.

Yang, H., Matsubayashi, Y., Nakamura, K., and Sakagami, Y. 2001. Diversity of *Arabidopsis* genes encoding precursors for phytosulfokine, a peptide growth factor. *Plant Physiol.* 127: 842–851.

Yang, W., Zhang, B., Qi, G., Shang, L., Liu, H., Ding, X., and Chu, Z. 2019. Identification of the phytosulfokine receptor 1 (OsPSKR1) confers resistance to bacterial leaf streak in rice. *Planta*. 250:1603–1612.

Yi, J., Derynck, M. R., Li, X., Telmer, P., Marsolais, F., and Dhaubhadel, S. 2010. A single-repeat MYB transcription factor. GmMYB176, regulates CHS8 gene expression and affects isoflavonoid biosynthesis in soybean. *Plant J.* 62, 1019–1034.

Yoshida, T., Fujita, Y., Maruyama, K., Mogami, J., Todaka, D., Shinozaki, K., & Yamaguchi-Shinozaki, K. 2015. Four *Arabidopsis* AREB/ABF transcription factors function predominantly in gene expression downstream of SnRK2 kinases in abscisic acid signalling in response to osmotic stress. *Plant, cell and environment*, 38:35–49.

Yoshida, T., Nishimura, N., Kitahata, N., Kuromori, T., Ito, T., Asami, T., Shinozaki, K., & Hirayama, T. 2006. ABA-hypersensitive germination3 encodes a protein phosphatase 2C (AtPP2CA) that strongly regulates abscisic acid signaling during germination among *Arabidopsis* protein phosphatase 2Cs. *Plant Physiol.* 140: 115–126.

Yu, L., Zhou, W., Zhang, D., Yan, J., and Luo, L. 2020. Phytosulfokine- α promotes root growth by repressing expression of pectin methylesterase inhibitor (PMEI) genes in *Medicago truncatula*. *Phyton*. 89: 1–9.

Zahiri, J., Bozorgmehr, JH., and Masoudi-Nejad, A. 2013. Computational Prediction of Protein-Protein Interaction Networks: Algo-rithms and Resources. *Current genomics* 14: 397–414.

Zhang, H. et al. 2018. A Plant Phytosulfokine Peptide Initiates Auxin-Dependent Immunity through Cytosolic Ca²⁺ Signaling in Tomato. *Plant Cell*. 30: 652–667.

Zhang, L., Shi, X., Zhang, Y., Wang, J., Yang, J., Ishida, T., et al. 2019. CLE9 peptide-induced stomatal closure is mediated by abscisic acid, hydrogen peroxide, and nitric oxide in *Arabidopsis thaliana*. *Plant Cell Environ.* 42: 1033–1044.

Zhu, JK. 2002. Salt and drought stress signal transduction in plants. *Annu. Rev. Plant Biol.* 53: 247–273.

Zonia L., Munnik T. 2007. Life under pressure: Hydrostatic pressure in cell growth and function. *Trends Plant Sci.* 12: 90–97.

ACKNOWLEDGEMENTS

Foremost, I would like to express my sincere gratitude to **Prof. Dr. Margret Sauter** for the continuous support and guidance in all time of research and writing of this thesis. Thank you for your valuable discussions, insights, and motivation. All of this has helped me understand research better and I learnt a lot from you. I could not have asked for a better supervisor and mentor for my PhD study.

A special thanks to **Prof. Dr. Jennifer Selinski**, without whom completion of this thesis would have been impossible. I am extremely grateful for your timely rescue and valuable suggestions to improve this thesis. Investing time to read an entire thesis in such short time can be very tedious and thank you for doing it with such grace.

Next, I would like to extend my thanks to my wonderful group members. I can proudly say that I worked with the best people. My lab partners, **Lena Carstens** and **Timo Staffel** are an amazing company to do science with. They have given me wonderful memories. I enjoyed sharing my workspace with them and are more friends to me than colleagues. They always had my back and stayed with me through thick and thin. **Jay Jethva**, my fellow Indian friend, was willing to lend an ear to my problems at all times and offered advice that made me stay calm. **Tanja Rehders** was extremely kind to me by being my advisor, translator, and a delightful social room partner from whom I also learnt German traditions. **Michael Motzkus** assisted and guided me on protein experiments. It was super fun to be around you, and I will for sure miss my favorite cake from you. **Emese Eysholdt-Derzsó**, who I will remember for being cheerful is a wonderful lunch partner and I enjoyed our conversations. **Christine Kaufmann** guided me during my initial days on research and I admired her explaining skills. **Maxim Faroux**, you made the last few months livelier. I had fun listening to your science talks and singing.

Massive credit to my mother, **Jeyanthi** and my sister, **Roshini**, who are my lifelines. Thank you for supporting my dreams and encouraging me to pursue it. Without you two nothing would be possible, and I am forever indebted for everything you have given me. I'd also like to extend my gratitude to my uncles, **Ramamoorthy**, **Rutharamoorthy** and Aunt **Saroja**, which is long due, they always motivated me to study and believed that I would make them proud some day. Thanks for being there for my family in our difficult times.

Special mention to **Dinesh Subramanian** for being a supportive and concerned roommate. Huge thanks for all the encouraging talks, cooking, hangouts, fun and laughter. You made this journey relatively easy.

Last and definitely not the least, my friends, my saviours. **Praveen**, my constant. You are my family away home. Thank you for being in my life and making everything easy. **Shailja**, of all the things Kiel gave me, you are the most important that I cherish. Thanks for comforting me throughout, for believing in my abilities and never letting me down for once. **Ashwin**, I really don't know what I would've done without you. The amount of time you invested to keep my sanity is beyond thanking you. Without you the last two years would be unimaginable. **Arun**, you are truly a science enthusiast, and I learned a lot from you. Thanks for backing me up and making life in Kiel more enjoyable. **Deepika**, you were the reason for me to take up postgraduate studies and I cannot tell you how that one step changed my life. Thank you for continuously lifting my spirits for more than a decade. **Dinesh R**, I consider myself lucky enough to find you who always had high hopes for me. Thank you for trusting me and praying for my well-being.

DECLARATION

I hereby declare,

- That this doctoral thesis, apart from the advice from my supervisors Prof. Dr. Margret Sauter and Prof. Dr. Jennifer Selinski, in terms of content and design is my own work.
- That the thesis has not been submitted in whole or in part to the CAU Kiel or to another examining body as part of an examination procedure. Apart from the included submitted paper no other part of the thesis has been published or submitted for publishing.
- That the thesis has been prepared subject to the Rules of Good Scientific Practice of the German Research Foundation (DFG).
- That I have not attempted and failed to obtain a doctoral degree prior to this thesis.

Komathy Rajamanickam